ON THE NATURE AND ORIGINS OF BIOLOGICAL DIELECTROPHORESIS

By

CHI-SHIH CHEN

Bachelor of Science
Chung-Yuan College of Science and Engineering
Chung-Li, Taiwan
1964

Master of Science
University of Oregon
Eugene, Oregon
1968

Submitted to the Faculty of the Graduate College
of the Oklahoma State University
in partial fulfillment of the requirements
for the Degree of
DOCTOR OF PHILOSOPHY
May, 1973

ON THE NATURE AND ORIGINS OF BIOLOGICAL DIELECTROPHORESIS

Thesis Approved:

Thesis Adviser

Dean of the Graduate College

ACKNOWLEDGMENTS

The author is sincerely grateful to Professor H. A. Pohl, Thesis Committee Chairman, for his patient guidance, encouragement, assistance and warmest friendship throughout the course of this study. The author also wishes to express his gratitude to the Thesis Committee members, Professor E. E. Kohnke, Professor L. L. Gee and Professor N. N. Durham, for their interest and assistance.

Special thanks are also given to Dr. N. N. Durham, Dr. Chi-Sin Chen, Dr. W. Flory and Mrs. J. F. Ding for their generously supplied and prepared the cells used in this study, and to Mrs. Janet Sallee for her typing of the manuscript.

Finally, to his wife, Ruth Min-Hwa, goes his deepest appreciation for her untiring support, patience and understanding.

TABLE OF CONTENTS

Chapter		Page
I.	INTRODUCTION.	1
II.	THEORETICAL DISCUSSION.	10
III.	EXPERIMENTAL METHODS.	22
IV.	EXPERIMENTAL RESULTS.	39
V.	MISCELLANEOUS EFFECTS	84
VI.	DIELECTROPHORETIC PROPERTIES OF INANIMATE SUSPENSIONS . .	102
VII.	DIELECTROPHORETIC PROPERTIES OF CELLULAR SUSPENSIONS. . .	120
VIII.	SUMMARY AND SUGGESTIONS FOR FUTURE STUDY.	129
BIBLIOGRAPHY.		133
APPENDIX. DIELECTROPHORETIC PRECIPITATION OF SILVER BROMIDE SUSPENSIONS.		141

LIST OF TABLES

Table		Page
I.	The Values of Drift Velocity and Drift Distance at Various Frequencies.	89
II.	The Values of $\varepsilon_\infty - \varepsilon_o$ of the Electrophoretic Dispersion Effect at Various Frequencies.	92
III.	Possible Mechanisms of Dielectric Dispersion	105

LIST OF FIGURES

Figure		Page
1.	Diagram Comparing Behaviors of Neutral and Charged Bodies in a Nonuniform Electric Field	3
2.	A Schematic Graphic Representation of Double-Layer Relationships	19
3.	Diagrammatic Representation of the Effect of Ions on the Zeta Potential	21
4.	Exploded View of Cell Chamber	24
5.	Detailed Views of Assembled Cell	25
6.	Schematic for 2.55 MHz Oscillator	26
7.	Circuit Diagram of Oscillator	28
8.	Relating Cell (Yeast) Concentration to Optical Density	31
9.	The Change of Conductivity by Time	37
10.	Yield Spectra of AgBr With Different Resistivity	40
11.	Effects of Cations on Yield Spectra of SiO_2 Gel	41
12.	Effects of Anions on Yield Spectra of SiO_2 Gel	43
13.	Concentration Dependence on Yield Spectra of SiO_2 Gel	44
14.	Variation of Yield Spectra of SiO_2 With Electrodes and Voltages	45
15.	Effects of Cations on Yield Spectra of Ion Exchange Resin.	46
16.	Effects of Hydrogen Ions on Yield Spectra of Ion Exchange Resin (Acidic)	47
17.	Effects of Anions on Yield Spectra of Ion Exchange Resin (Acidic)	48
18.	Effects of Cations on Yield Spectra of Ion Exchange Resin (Basic)	49

LIST OF FIGURES (Continued)

Figure		Page
19.	Effects of Anions on Yield Spectra of Ion Exchange Resin (Basic)	50
20.	Yield Spectra of Rat Liver Mitochondria	51
21.	Yield Spectra of Rat Liver Mitochondria	52
22.	Yield Spectra of Rat Liver Mitochondria	53
23.	Variation of Yield Spectra (Mitochondria) With Length of Time After Isolated	55
24.	Yield Spectra of Pseudomona aeruginosa 1 (15-hr-old Cultures)	56
25.	Yield Spectra of Pseudomona aeruginosa 1 (30-hr-old Cultures)	57
26.	Yield Spectra of PA1 Debris With Different Resistivity	58
27.	Yield Spectra of PA1 and Cell Debris	59
28.	Yield Spectra of Cg1 and Cell Debris	60
29.	Yield Spectra of Cg2 and Cell Debris	61
30.	Yield Spectra of Pseudomona aeruginosa - Cg1 (11-hr-old Culture)	62
31.	Variation of Yield Spectra of E. coli With Resistivity (12-hr-old Culture)	63
32.	Variation of Yield Spectra of E. coli With Resistivity (15-hr-old Culture)	64
33.	Variation of Yield Spectra of E. coli With Resistivity (24-hr-old Culture)	65
34.	Variation of Yield Spectra of E. coli With Resistivity (69-hr-old Culture)	66
35.	Yield Spectra of Bacillus cereus	67
36.	Variation of Yield Spectra of B. cereus With Resistivity (10-hr-old Culture)	68
37.	Variation of Yield Spectra of B. cereus With Resistivity (24-hr-old Culture)	69

LIST OF FIGURES (Continued)

Figure		Page
38.	Yield Spectra of B. megaterium	71
39.	Concentration Dependence on Yield Spectra of Yeasts	72
40.	Yield Spectra of Yeasts After Treated With Chloroform	73
41.	Yield Spectra of Yeasts After Treated With Chloroform and Ethyl Alcohol	74
42.	Yield Spectra of Yeasts With Congo-Red Stained	75
43.	Single Cell Nonuniform Field Effects	76
44.	Single Cell Nonuniform Field Effects	77
45.	Single Cell Nonuniform Field Effects	78
46.	Single Cell Nonuniform Field Effects	79
47.	Single Cell Nonuniform Field Effects	80
48.	Single Cell Nonuniform Field Effects	81
49.	Yield Spectra of Zymosan	82
50.	The Plot of Equation (11)	87
51.	The Effect of Orientation on Yield Spectrum	95
52.	The Curves of Yield Vs. Time by Experiments and Equation (16)	115
53.	Yield Spectra of AgBr by Equation (18)	117
54.	Yield Spectra of SiO_2 by Equation (18)	118
55.	Ordering of Events Within the Cell Cycle of Saccharomyces cerevisiae	127

CHAPTER I

INTRODUCTION

For many years the behavior of biological cells and cellular components in applied electric fields has offered stimulating problems to physicists and electrical engineers. The object has been to determine structures, to identify molecular forces, and to characterize electrical processes. In recent years, many techniques developed in the physical sciences have been found applicable to problems of biological interest. One of these is dielectrophoresis. It has been found that through the application of alternating nonuniform electric fields, biological particles can be made to exhibit movement much like inanimate particles, which are dependent on their electrical characteristics. Since the polarizability of material bodies, especially living cells, varies strongly with the applied frequency, it is a relatively straightorward matter to obtain a "spectrum" for the dielectrophoretic responses of cellular suspensions. It is observed that different species show distinct "spectra" with up to three characteristic peaks or "relaxation times". The present study has the aim of explaining the mechanism of those peaks.

Nonuniform Field Effects

It is a familiar fact that in a uniform electric field, a force is exerted upon a charged object. If the field is made nonuniform, that type of force persists, and a new type of force arises because of polar-

ization effects. In the latter case of nonuniform fields, even neutral objects become subject to a force proportional to their polarizability. The two effects are shown diagramatically in Figure 1(A), positively charged body moves towards negative electrode. The neutral body is equal in amounts positive and negative of charge, but the force is proportional to the local field, a net force towards the region of more intense field results. In Figure 1(B), the postively charged body moves toward the negative electrode. Again, the neutral body is polarized, but does not reverse direction although the field is reversed. It still moves towards the region of highest field intensity. The two phenomena are distinguished by the terms "electrophoresis" for charged objects; and "dielectrophoresis" (1) for neutral objects being pulled along by a nonuniform field. In an ac field, the charged body would tend to merely "shudder" about the original location, while the neutral body would tend to drift rather steadily towards the region of highest field intensity. Strictly speaking, the charged body is actually gently repelled from the more intense ac field. More discussion is given in a later chapter. The effects of nonuniform fields were first noted, although probably not appreciated, by Gilbert (2) when he observed the deformation of a water droplet when rubbed amber was brought near it. The first useful dielectrophoretic technique was not developed until much later when Quincke (3) determined the permitivities of insulating liquids by measuring the height of the liquid between parallel plate electrodes as a function of the applied voltage. Similar measurements, differing only in minor details, have since been made by several investigators (4-9).

The use of nonuniform electric fields to produce particle motion was introduced by Soyenoff (10) when he observed the coalescence of coal

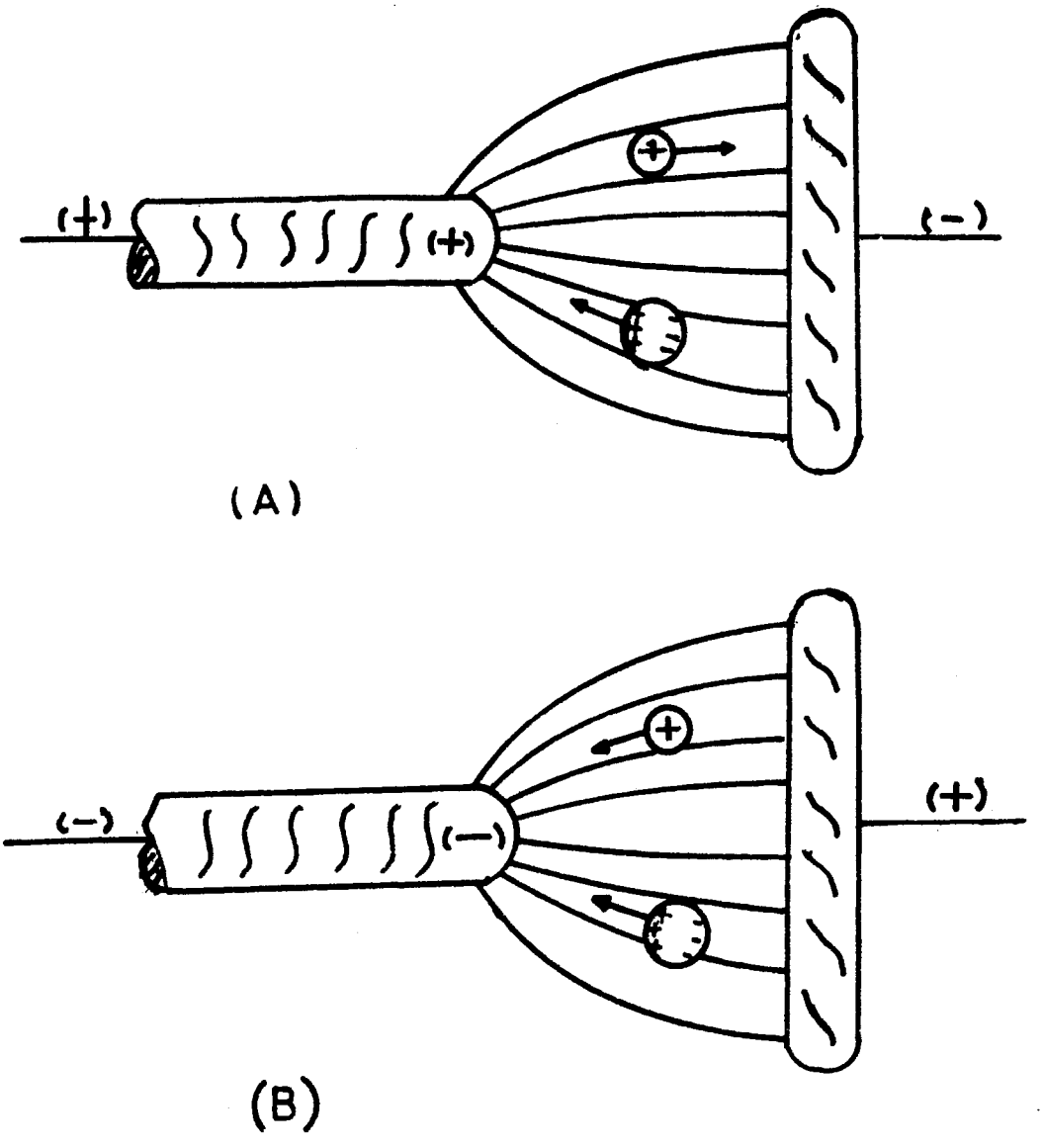

Figure 1. Diagram Comparing Behaviors of Neutral and Charge Bodies in a Nonuniform Electric Field

dust suspended in toluene. He was the first to note that a body of dielectric constant higher than the medium would move into the region of the strongest field. Similar results were obtained by Winslow (11) for silica gel in kerosene. Pohl (1) removed carbon black from a polyvinyl chloride-di-isopropyl ketone solution and defined the motion as dielectrophoresis. Later he studied the quantitative effects of the variation of several important parameters, including field strength, electrode size, and particle size (12), and developed the basic theory (13,14). Pohl and Plymale (15) were able to separate mixtures of minerals according to the dielectric constant using dielectrophoresis and to introduce a field shape which provides a constant dielectrophoretic force. Using a different apparatus, Verschure (16) was also able to separate mineral mixtures into their component parts according to the dielectric constant. Black and Hammond (17) applied dielectrophoresis to the isolation and purification of soybean phosphatides and bacterial spores (B. Megaterium). The study of particles in conducting liquids was initiated by Hawk (18) and continued by Feeley (19) and Chen (20), with the results that the dielectrophoresis was not only a function of the dielectric constant, but also depended on conductivities and frequency of the applied field.

Past work on the electrical character of cells goes back to the early studies of Muth (21), Liebesny (22), Heller (23), Schwan (24-27) and Pohl, et al. (28-30). It must be stressed, however, that prior to the work of Pohl and Hawk (28) no special consideration was given to the gathering, collecting, separating, or controlling of living organisms by the action of nonuniform electric fields acting upon them as neutral particles via their polarizabilities. Such motion produced by a nonuniform field acting on a polarizable neutral body is called dielectrophore-

sis, as described in the previous section. The reports by Schwan of extraordinarily high dielectric constants (10^2-10^4) for cell and tissue suspensions prompted Pohl and Hawk (28) to apply dielectrophoresis to such a suspension. Under the conditions of high frequency and low suspension conductivity, they obtained the separation of live and dead cells. Mason and Townsley (31) separated the cells in wort broth from cells grown in yeast nitrogen base of -1% glucose. They also demonstrated size difference in separated fractions from both batch and continuous separators.

Dielectric Behavior of Cells

The electrical properties of biological material have been studied almost continuously ever since suitable electrical techniques became available for this purpose. Earlier contributions did not help much toward an understanding of the factors responsible for the electrical properties of cells. This was due to inadequate theory and techniques. A very active period followed between 1925 and the Second World War when a number of biophysicists applied potential theory originally developed for dielectrics (32,33,34) to biological matter (blood, tissue, nerve cells). This effort led to an almost complete understanding of the anomalous dispersion at radio-frequency (β-dispersion). About 1935 investigations began of the electrical properties of protein molecules by application of the concept of polar molecules originated by Debye (35, 36). After 1940 techniques became available for investigation of the electrical properties at ultra-high and low frequencies. The frequency range so far explored extends from 5 cps up to 30000 Mc (i.e., almost 10 decades instead of the 4 decades (1 Kc to 10 Mc) available before the

Second World War). This resulted in the discovery of dispersion of both low and high frequencies (α- and β-dispersion).

The studies of Cole, Fricke, Curtis, and co-workers in their analysis of suspensions and tissues still provide the conceptual foundation for current work. According to this early work, whole cells generally display three major dispersion regions. The "α-region" occurs in the audio range (0.1 to 10 KHz) and is probably due to current shunted through the surrounding electrolyte medium or to charge near the cell surface "β-dispersion" is in the radio-frequency range (1 to 10 MHz) and primarily describes cell membrane properties. Finally, "γ-dispersion" appears at very high frequencies ($\lesssim$ 1000 MHz) and may be caused by internal subcellular components and molecules. Even cell water shows dispersion in this region.

In addition to the excellent book by Cole (37), several reviews of dielectric behavior of biological materials exist. The article "Determination of Biological Impedances" by Schwan (38) deals specifically with techniques appropriate to dielectric measurements in these applications. A short entry, "Bioelectricity: Alternating current: Admittance of Cells and Tissues" by Schwan and Cole in Medical Physics (39) gives a brief but thorough summary of the dielectric dispersion of whole cells. "Electrical Properties of Tissue and Cell Suspension" by Schwan (26) describes dielectric theories used in analyzing biological materials as well as presenting an extensive summary of data on tissues, cells, cell membranes, and macromolecules over the full frequency range.

The textbook Biophysical Chemistry by Edsall and Wyman (40) has chapter on "Electrostatics" and "Dielectric Constants and Their Significance" stated in the context of biological problems. The book Solid

State Biophysics edited by Wyarn (41) has a chapter on "The Study of Biological Molecules by Dielectric Methods" by Grant. In that chapter an attempt has been made to explain the nature of dielectric parameters, how they can be measured, and what kind of information at a molecular level can be obtained from their interpretation.

There are two collections of original papers from symposia which provide a good idea of recent work. A supplement honoring K. S. Cole was published in the Journal of Cellular and Comparative Physiology in 1965 (42) containing pertinent contributions by friends and collaborators. A meeting in Belgium in 1966 devoted an entire session to dispersion phenomena in solutions of macromolecules and is presented in Volume 13 of Protides of the Biological Fluids (43). The chapter "Dielectric Aspects of Biological Materials" of Digest of Literature on Dielectrics (44) also gives an excellent review.

Rather little experimental work extending over a sufficiently wide frequency range to be of interest has been carried out with suspensions of bacteria. Earlier measurements at low frequencies established that bacteria are poor conductors (45, 46). More recently, a study of the electrical properties of Escherischia coli extending from 0.1 KHz to 200 MHz has been published (47). The analysis of these measurements reveals again the α- and β-dispersions typical for other biological material. The β-dispersion is characterized by several relaxation times.

The data at low frequencies indicate a wide spectrum of relaxation times since the dielectric constant continues to increase over almost the total low frequency range. Measurement with another strain of E. Coli (48), however, shows a low frequency behavior more characteristic of a small spectrum of relaxation times. It is therefore concluded that

variations of preparation and type of bacteria have a strong influence on the α-dispersion.

Pauly (49) demonstrated with protoplasts of Micrococcus Lysodeikticus that the radio frequency dispersion of this organism arises from the presence of the cytoplasmic membrane rather than the cell wall. Studies by Carstensen, et al. (50-54) on bacteria (Micrococcus lysodeikticus, Mycoplasma laidlawii and Mycoplasma gallisepticum) has illustrated that the bacterial cell wall is responsible for the high dielectric constant at low frequencies. The dielectric constant of the protoplast is nearly two orders of magnitude lower than that of the intact cell over most of the frequency range below 100 KHz. The protoplast itself has an α-dispersion which may possibly be explained by the theory of Schwarz (55) for the low frequency dielectric dispersion of colloidal particles. Both M. laiddlawii and M. gallisepticum display the expected β-dispersion.

Scope of This Study

The present study extends the work of Pohl, Hawk, and Crane in that it investigates in detail the response of biological cells to a nonuniform electric field and attempts to explore the mechanisms that are responsible for the characteristic peaks in the dielectrophoretic "spectrum". The problem can be broken into five major parts:

1. Development of the necessary equipment and procedures to insure meaningful results.

2. Studies of the dielectrophoretic properties of AgBr, silica gel, cation exchange resin, and anion exchange resin used as models for the cells.

3. Studies of the dielectrophoretic properties of cells (Rat Liver Mitochondria, Bacteria, Yeasts, Zymosan).

4. Investigations of the effects such as (1) AC electrophoresis, (2) orientation of non-spherical particles, and (3) pearl-chain formation, (4) stirring, repulsion and rotation, and (5) heat effect that might effect the dielectrophoresis.

5. Physical, theoretical analyses of the yield spectrum, which are presented and discussed later in connection with experimental results.

CHAPTER II

THEORETICAL DISCUSSION

An adequate introduction to this study requires consideration of three more or less distinct but interrelated topics. These are dielectrophoresis, dielectric dispersion in heterogeneous systems, and the double layer structure of the solid/aqueous electrolyte interface. We proceed to each topic in turn.

Dielectrophoresis

The motion of electrically polarized but neutral matter induced by the action of a nonuniform electric field is called "dielectrophoresis" (1) as mentioned before. In practice, the study of the effects of nonuniform fields is made complex by the presence of both dielectrophoresis as well as by conduction, thermal convection, diffusion, electrode polarization, and the effects resulting from the sequence of charging and electrostatic repulsion.

We shall be concerned here principally with dielectrophoresis, especially that aspect in which polarization effects in nonuniform fields cause the most polar material to move toward the place of highest field intensity. For a perfectly insulating sphere of radius a, having dielectric constant or relative permittivity ε_2, and immersed in a perfectly insulating medium of dielectric constant ε_1, the dielectrophoretic force has been shown (13) to be given by

$$F = 2\pi a^3 \varepsilon_o \left[\frac{\varepsilon_1(\varepsilon_2 - \varepsilon_1)}{\varepsilon_2 + 2\varepsilon_1}\right] (\nabla|E|^2) \qquad (1)$$

where $|E|$ is the magnitude of the dc or root mean square ac electric field at any point in the suspending medium, and ε_o is the permittivity of free space.

The calculation of the force on a lossy dielectric sphere in a lossy dielectric medium is a matter of some difficulty. The usual starting point for calculations of this type is the Poynting vector theorem. But the Poynting vector is itself beset with deep problems of interpretation, some of philosophical character, and its use has recently come into question (56-58). Another problem arises in the proper treatment of complex quantities in the nonlinear algebra. Still another stems from determining the mechanical force resulting from the total averaged energy in a lossy dielectric subject to a time-varying field. Recently, Neufeld has challenged the usual theoretical basis for treating lossy media (58) and treats heat losses as a source of "extraneous" force.

The force on a loss-free dielectric sphere in a weakly varying but static field in a loss-free liquid is given by Equation (1). Crane (89) and Sher (59, 60) have suggested that for the case of a lossy sphere in a lossy liquid in a time varying field one may merely replace the static dielectric constants by their complex quantities (i.e., replace ε_2 by $\varepsilon_2^* = \varepsilon_2 - i\sigma_2/\omega$, etc., where σ is the specific conductivity, ω is the angular frequency, and $i = \sqrt{-1}$) in Equation (1) and then take the real part of the subsequent expression. This gives

$$\vec{F} = 2\pi a^3 \varepsilon_o \left(\frac{1}{4}\right) \mathrm{Re}\left\{\frac{\varepsilon_1^*(\varepsilon_2^* - \varepsilon_1^*)}{\varepsilon_2^* + 2\varepsilon_1^*}\right\} \vec{\nabla}|E|^2 \qquad (2)$$

which may be seen to reduce to Equation (1) in the simple case of ideal dielectrics. Though this result must be generalized to describe real systems accurately, it nevertheless illustrates the following essential points:

1) The force is proportional to the gradient of the mean electrical energy density or to the product of the electric field gradient and the field itself. Thus, the force does not change sign upon reversal of the field direction, and will therefore maintain a time averaged unidirectional value different from zero when a nonuniform ac field is present. The same force will act when the polarizable particle carries a net charge. In this case an additional periodic electrophoretic displacement of the particle will occur. Such electrophoretic effects will be discussed later.

2) The magnitude of the dielectrophoretic force acting upon a suspended particle is proportional to its volume. Therefore, if the particles are too small, the operation of diffusional forces will overshadow the dielectrophoretic force so that effects due to the latter will not be observed (61). These considerations set a lower limit on particle size for dielectrophoretic studies (61) in the range 0.01 - 0.1 μm. This same size range generally delineates the boundary between suspensions and colloidal dispersions (62).

3) Dielectrophoretic deposition or precipitation of particles at convex electrode surfaces in the regions of highest mean electrical energy density requires that the dielectric constant of the particle exceeds that of the suspending medium. This is the case of greatest practical interest. At this point, however, it is necessary to consider generalizations of the dielectrophoretic force expression which are ap-

propriate when both the medium and the particle are composed of lossy dielectrics (63). Such considerations show that a comparison of static dielectric constants does not provide a reliable indication of whether dielectrophoretic precipitation will occur. They show that a high dielectric dispersion associated with the particle will generally facilitate its precipitation. Precipitation may in fact occur in a frequency range of high dispersion associated with the particle, even though the static dielectric constant of the particle material is lower than that of the suspending medium

Dielectric Dispersion in Heterogeneous Systems

In the preceding subsection the relevance of dielectric properties to dielectrophoresis was considered entirely within the context of the bulk dielectric properties of the two substances involved. It assumed further that both substances had zero conductivity. When the conductivities of the substances are introduced explicitly, it then becomes necessary to consider interfacial polarization effects of the Maxwell-Wagner type (64-66). If in a homogeneous medium there are electrons or ions capable of displacement over distances of macroscopic magnitude, then these charges cause a current to flow when the medium is subjected to an electric field. If, however, the medium consists of a number of separate phases, some conducting, some not, then the charges move through the conducting phases and build up on the surfaces between the conducting and non-conducting phase. Each conducting region is in effect an electric dipole whose moment can be added to the moments because of the polarization of the molecules. The build-up of charge takes a finite time. At low frequencies this build-up is possible, and the charges

are almost in static equilibrium with the field so that there are no relaxation effects and high values of the dielectric constant result. At high frequencies there is little time for the build-up of charge, and the moments are therefore small, corresponding to low dielectric constants. At intermediate frequencies the acquired moments lag behind the field, the lag depending on the particle shape but not the size. This phenomenon is known as interfacial polarization or the Maxwell-Wagner effect; the essential prerequisite is the existence of a boundary between media of different electrical properties. The theory of the Maxwell-Wagner effect has been fully reviewed by Van Beek (67). He shows that a Debye type dielectric dispersion with a characteristic relaxation time

$$\tau = \varepsilon_o \left(\frac{\varepsilon_2 + 2\varepsilon_1}{\sigma_2 + 2\sigma_1}\right) \tag{3}$$

will occur. Here σ_1 and σ_2 are the bulk conductivities of the suspending medium and of the particle, respectively. This result is valid for sphere particles in the limit of zero volume fraction. Another source of dielectric dispersion in heterogeneous systems will arise when the suspended particles are surrounded by electric double layers (67). Two different theoretical approaches to the problem have been taken. In the first approach a double layer is represented by a thin conducting shell which surrounds the suspended particle. The "conducting shell" model was first analyzed by Miles and Robertson (68). Later and more detailed developments have been given by O'Konski (69). In this theory the ideas incorporated in the Maxwell-Wagner (65, 66) and Debye-Falkenhagen (70) theories are used. O'Konski suggests that in addition to the charge build-up at the interfaces between media of different bulk conductivities,

as postulated by the Maxwell-Wagner theory, there is the effect of the mobility of the ions in the resultant ion atmosphere. The latter is the Debye-Falkenhagen contribution and may be expressed in terms of a surface conductivity. Thus, O'Konski recognizes that the Maxwell-Wagner and Debye-Falkenhagen treatments incorporate the same fundamental process--namely ion-transport--but by introducing a different set of boundary conditions a model is introduced in which the ionic mobilities enter naturally. In deriving expressions for the complex dielectric constant, the relaxation times, and the low and high-frequency dielectric increments, O'Konski uses the results of Polder and Van Santen (71) for spheres and of Fricke (72) for ellipsoids. He finds that the relaxation time of the surface charge density on removal of the polarizing field (i.e., the ionic relaxation time for the sphere) is given by

$$\tau_i = \frac{\varepsilon_o a (\varepsilon_2 + 2\varepsilon_1)}{2\sigma_s} \tag{4}$$

where σ_s is the surface conductivity. For randomly oriented ellipsoids

$$\tau_i = \frac{\varepsilon_o (\varepsilon_j + \varepsilon_1 X)}{\sigma_{sj} + \sigma_1 X)} \tag{5}$$

where

$$X = \varepsilon_2^2 + \varepsilon_1\varepsilon_2 - 2\varepsilon_1^2 + (\varepsilon_s'')^2 + \varepsilon_1'' \varepsilon_s'' - 2(\varepsilon_1'')^2 \tag{6}$$

ε_j is the dielectric constant of the solute along the j axis $\sigma_{sj} = \sigma_j + \sigma_j'$ in which σ_j' is the surface contribution to the effective conductivity σ_{sj}.

In the second theoretical approach to the problem of double layer

dispersion, exemplified by the work of Schwarz (73), the migration of charge in the double layer is presumed to be diffusion controlled. Under this condition the relaxation time should be of the order

$$\tau \sim a^2/D \sim \frac{a^2}{ukT} \qquad (6)$$

where D is the microscopic diffusion coefficient of the mobile charge carriers in the double layer, u is the mechanical mobility equal to velocity per unit force, K is the Boltzmann constant, and T is the absolute temperature. Note that the mechanical mobility u is equal to μ/q, where μ is the electrical mobility and q is the magnitude of the charge on the migrating entity, (e.g., ion or crystal lattice defect). Equation (6) follows directly from the solution of the one-dimensional random walk problem and the Nernst-Einstein relation (74). Schwarz considered the polarization to be caused by field-induced migration of counterions over the surface of a charged particle to which they were strongly bound.

An attempt to generalize the Schwarz theory to the more realistic case where there is a diffuse atmosphere beside the bound ions, was undertaken by Schurr (75). However, in this work, the drop of the polarization potential across the oscillating diffuse layer was not taken into account either. Alwitt modestly extended the Schwarz theory, utilizing a relaxation spectrum of ionic mobilities derived from properties of the classical diffuse double layer. This results in dispersion and absorption curves for colloidal suspensions that are broader and flatter than Debye-type curves that were expected in the Schwarz theory and are a function of ζ potential. Dukhin, et al. (76-80) developed the theory of polarization of the diffuse part of a thin double layer of spherical

or elongated colloidal particles in an alternating electric field. He claimed that the observed low-frequency dispersion of the dielectric constant is due not to deformation of the layer of bound ions but to polarization of the diffuse atmosphere, the ions of which exchange freely with the bulk electrolyte. He showed that τ differs from that of Schwarz by a factor 1/m where

$$M = 1 + Z^+Z^- (Z^+ + Z^-) \chi \sigma_o/C_o$$

or

$$\tau = \frac{a^2}{2D} \frac{1}{1 + Z^+Z^- (Z^+ + Z^-) \chi \sigma_o/C_o} \tag{7}$$

where $Z^{\pm}$ is the valence of cation and anion, x is the reciprocal thickness of the diffuse layer, σ_o is the density of fixed surface charge, and C_o is the concentration of the ions at an appreciable distance from the particle.

An alternative approach by Mandel (81) gave similar results, but was based upon assumed rod-like molecules with discrete binding sites. In his theory, however, no reasonable relation was given between the degree of association and the concentration of counter-ions, and all bound ions were supposed to contribute to polarization. The other expressions which are derived by Oosawa (82-84) for the dielectric increment and the relaxation time were obtained by expanding the fluctuation of bound counterions in a fourier series along the polyion of length L as follows:

$$\tau = \frac{\zeta}{kT} (\ell/2\pi K)^2 \frac{1}{1 + \theta_+ \omega_k} \tag{8}$$

where $\theta_+ = n_e^2/\varepsilon_o kT\ell$ is the reduced charge density of the polyion, $e^2\omega_K/\varepsilon_o$ the Kth Fourier component of interaction energy between counterions, ζ the friction constant of counterions, N the number of polyions per unit volume, and n the number of charged sites of a single polyion.

In this enumeration of dielectric dispersion mechanisms in heterogeneous systems, we have sought only to expose the underlying physical basis of those mechanisms which are most likely to be operative in our system. The cited literature should be consulted for more rigorous treatments.

Double Layer Structure of the Solid/Aqueous Electrolyte Interface

It was suggested by H. Von Helmholtz that an electrical double layer is generally formed at the separation of two phases. He treated the problem mathematically by assuming the double layer to be virtually an electrical condenser with two parallel plates separated by not more than a molecular distance. The first quantitative description of the space charge distribution arising at the boundary between a liquid and a solid was given independently by Gouy (85) and Chapman (86). They proposed that the charge density had a maximum at the interface and fell off exponentially into the liquid. Stern (87) modified their treatment by pointing out that ions in solution could not approach closer than their radius to the solid phase. This led to the distinction between the diffuse double layer (Gouy and Chapman) and the compact double layer (Stern). Figure 2 shows the schematic graphic representation of double layer relationships according to the theory of Stern.

A refinement of the Stern model has been proposed by Grahame (88) who distinguishes between an "outer Helmholtz plane" to indicate the

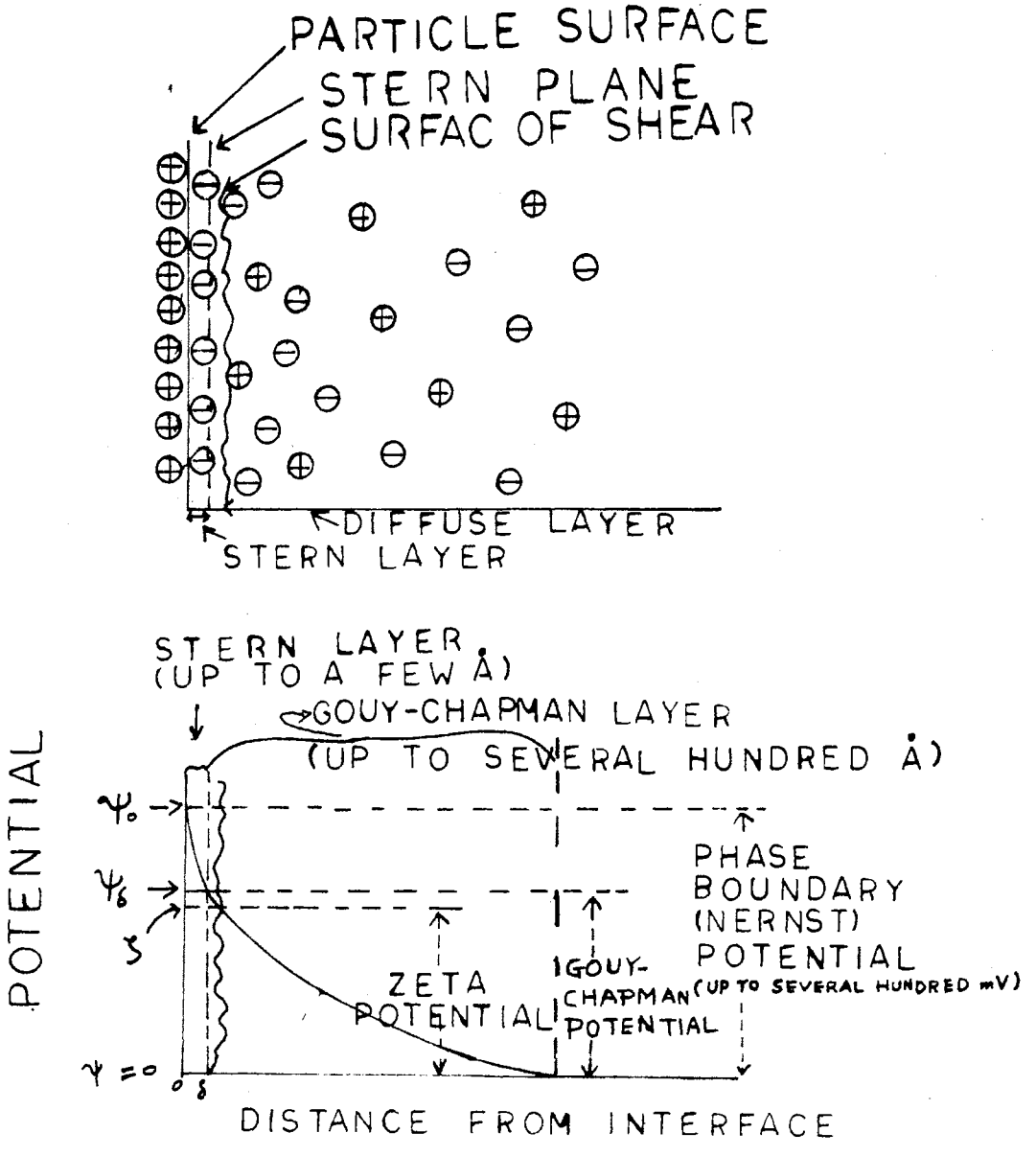

Figure 2. A Schematic Graphic Representation of Double-Layer Relationships

closest distance of approach of hydrated ions and an "inner Helmholtz plane" to indicate the centres of ions, particularly anions, which are dehydrated (at least in the direction of the surface) on adsorption.

Substances which do not ionize in water are usually found to be negatively charged in contact with water, and the addition of small amounts of univalent electrolyte tends to increase this charge. In the cases of negative zeta-potential, it is believed that hydroxyl ions from water and possibly also anions from the electrolyte are attached to the solid. An equal number of positive ions will remain in the liquid, some closely held in the fixed part of the double layer and the rest in the diffused portion. The fall of potential from the solid to the bulk of the solution is shown diagramatically in Figure 3, Curve I.

If the concentration of the electrolyte is increased, there will be a tendency for the cations to accumulate on the solution side of the fixed double layer, (i.e., in the vicinity of the dotted line XY in Figure 3). At one time, it was thought that the sole effect of this accumulation was a decrease of the charge density σ, but now it seems to be established that the thickness d of the double layer is decreased simultaneously. This will result in a decrease of Zeta-potential, as depicted in Figure 3, II. The higher the valence of the cation, the lower the concentration of the solution required to bring about sufficient change in the adsorption layer to produce a given effect. If one increases the positive ion concentration, the sign of the electrokinetic potential may eventually be reversed; this is due to the neutralization of the charge on the particle or perhaps to the decrease of the thickness of the double layer to such an extent that it collapses and the double layer is reformed with the charges reversed (see Figure 3, III).

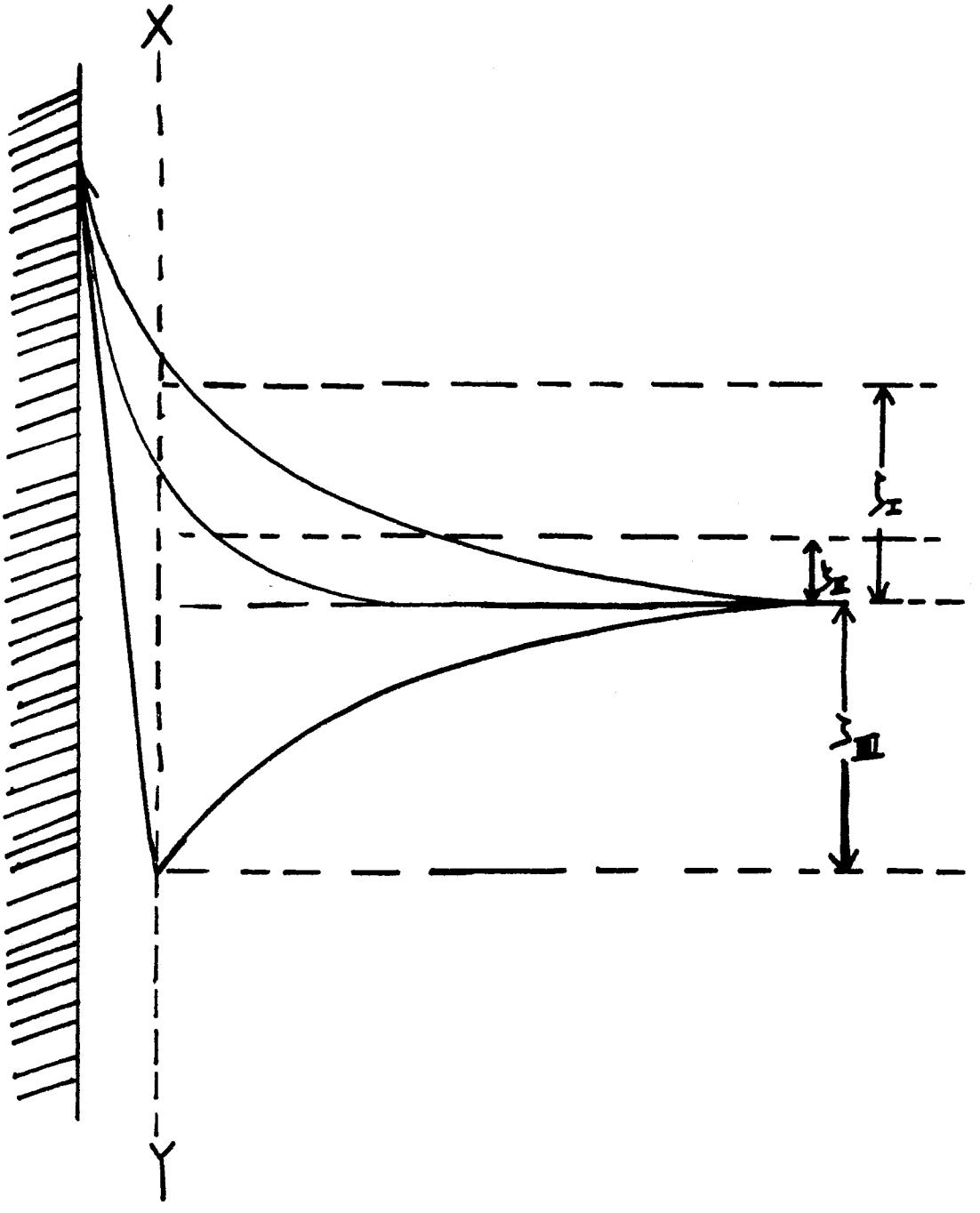

Figure 3. Diagrammatic Representation of the Effect of Ions on the Zeta Potential

CHAPTER III

EXPERIMENTAL METHODS

Choice and Description of Chamber

There were many constraints, often conflicting, on the choice of a chamber to contain the cell suspension. But the consideration of most importance was good microscopic viewability. The chamber thus had to be small enough to fit on the stage of the Bausch and Lomb microscope; the thickness of the liquid layer had to be small enough so that particle concentration of a few percent would not interfere with proper substage illumination; the liquid could not have contact with free air or else evaporation would disturb the microscopic scene; the chamber had to have working distance to permit the use of the objective lens desired; an electric field had to be applied to the suspension, so-contained; and the metal body of the objective lens obviously had to be kept out of the field.

These consideration eventually led to a successful design for an expendable chamber which could easily be built from commercially available components. A pin-plate design was used by Pohl and Hawk (28), but Crane (89) replaced it with a pin-pin arrangement which produces exactly the same field. The rounded pin tips act essentially as two separated spheres. Near the tips, this field can be shown to be approximately equivalent to that produced by concentric spheres. In practice the accepted measure of the dielectrophoretic effect is the "yield" or linear

extent of growth perpendicular to an electrode surface of a layer of precipitating particles. The yield is measured directly under the microscope as the total growth observed at a prescribed time or time intervals after the onset of precipitation. The wire-wire design which I have chosen offered a better judgment of yield than the pin-plate or pin-pin type. This wire-wire design, shown in Figures 4 and 5, uses a proprietary product, glass, in an essential way.

Equipment

Voltage Supplies

One of the keys to successful studies with dielectrophoresis is the availability of moderate voltage over a wide range of frequencies. Electrical excitation from low frequencies to 600 KHz was provided by a Hewlett-Packard model 200 CD audio oscillator. Its output level was increased to 120 volts peak to peak by a simple triode amplifier, then applied to the electrodes. A crystal driven oscillator which produced a 2.55 MHz signal at up to 200 volts was designed and built by the O.S.U. Electrical Engineering Department. A schematic of the electrical circuitry appears in Figure 6. It requires +300 volts and -150 volts from a power supply. In our case two lambda C-280 M power supplies were used. Higher frequencies were supplied by a Heathkit DX-60B transmitter using a 7.334 MHz crystal. The harmonics available were 14.7, 22.0, and 29.4 MHz, and the maximum voltage obtainable ranged from 30 volts at 29.4 MHz to 50 volts at 7.33 MHz. In order to dissipate the power generated by the transmitters, it was necessary to connect the test cell in parallel with a Heathkit Cantenna 50 ohms dummy load. An oscillator designed by Dr. Bennett L. Basore (Electrical Engineering Department,

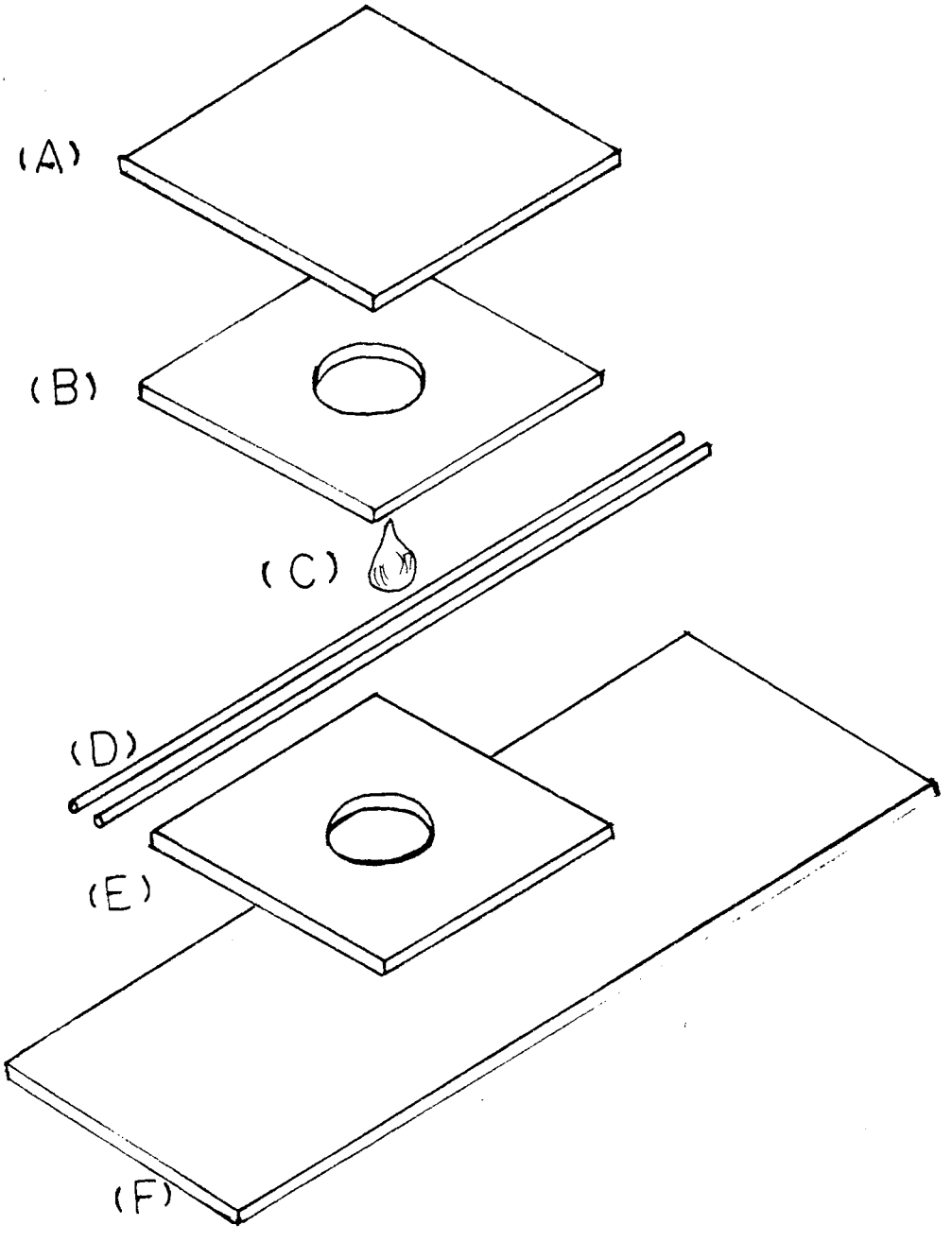

Figure 4. Exploded View of Cell. Not to scale. (A) Cover glass 22 x 22 x 0.22 mm, (B) and (E) cover glass as in (A) but with a 5 mm diameter hole for sample. (C) Sample fluid introduced with a dropping pipette. (D) Two parallel platinum wires, 0.0254 mm diam. (F) Microscope slides 77 x 26 x 0.95 mm

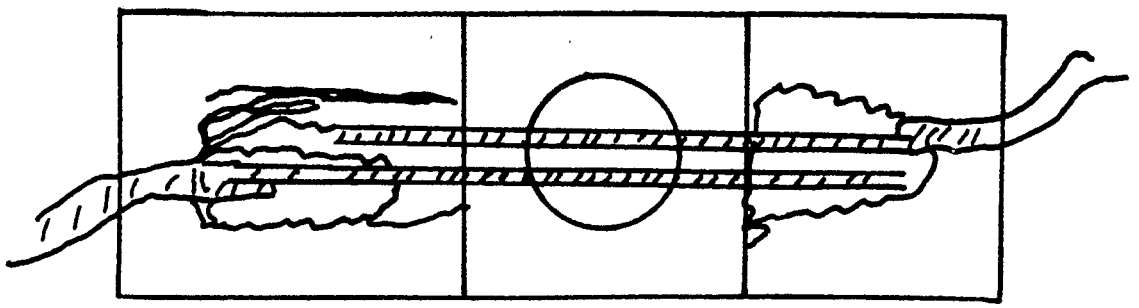

(A) TOP VIEW

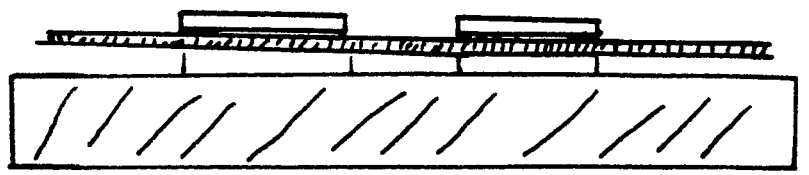

(B) SIDE VIEW

Figure 5. Detailed Views of Assembled Cell

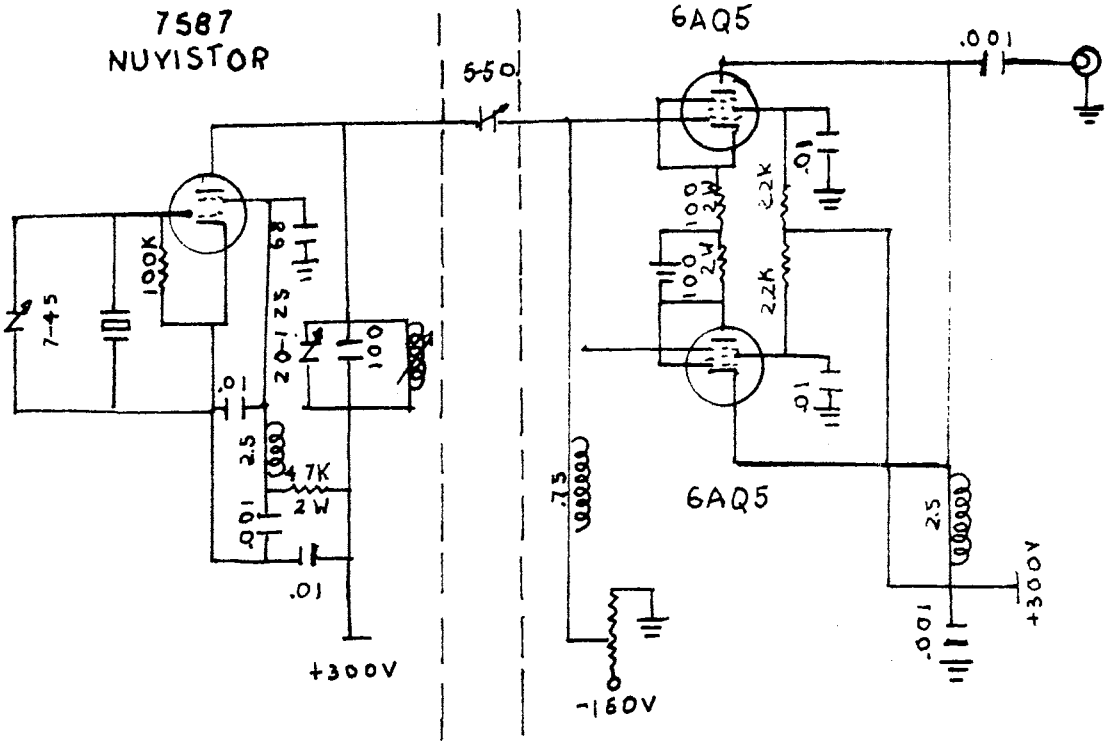

Figure 6. Schematic for 2.55 MHz Oscillator

O.S.U.) was used sometimes. The oscillator provided enough voltage for frequencies up to 16 MHz. A circuit diagram is provided in Figure 7. A Tektronix 533A oscilloscope was used to monitor the frequency of the applied signal and to check whether the signal is truly sinusoidal or not. The Hewlett-Packard 410B vacuum tube voltmeter was used for voltage measurement. It was accurate to ± 3% at frequencies below 400 MHz and gave relative indications up to 1 GHz; the a.c. voltage limit was 300 volts.

pAg, Conductivity and Concentration Measurement

pAg

Solution pAg was measured potentiometrically using a silver wire electrode. A Beckman reference electrode (calomel in saturated KCl solution) was used. The reference electrode was connected to the Ag^+ ion bearing solution via a Beckman salt bridge containing 0.1M KNO_3. Electrode emf was measured with a Beckman Model ss-2 PH meter. The system was standardized by using a 10^{-4}M $AgNO_3$ solution prepared volumetrically.

Direct measurement of the pAg of the suspensions by immersion of the electrodes described above was found to be unsatisfactory because of persistent variation with time of the recorded potential. This is thought to have been caused by an accumulation of particles at the electrodes. This difficulty was encountered both in the precipitated and fully dispersed suspensions, indicating that colloidal particles remained in suspension in the former case. This difficulty was circumvented by preparing a series of dilute colloid-free solutions of $AgNO_3$ with pAg values between 4 and 5, and of KBr with pAg values between 7.4 and 8.4. In both cases the corresponding concentrations lie between 10^{-5} and

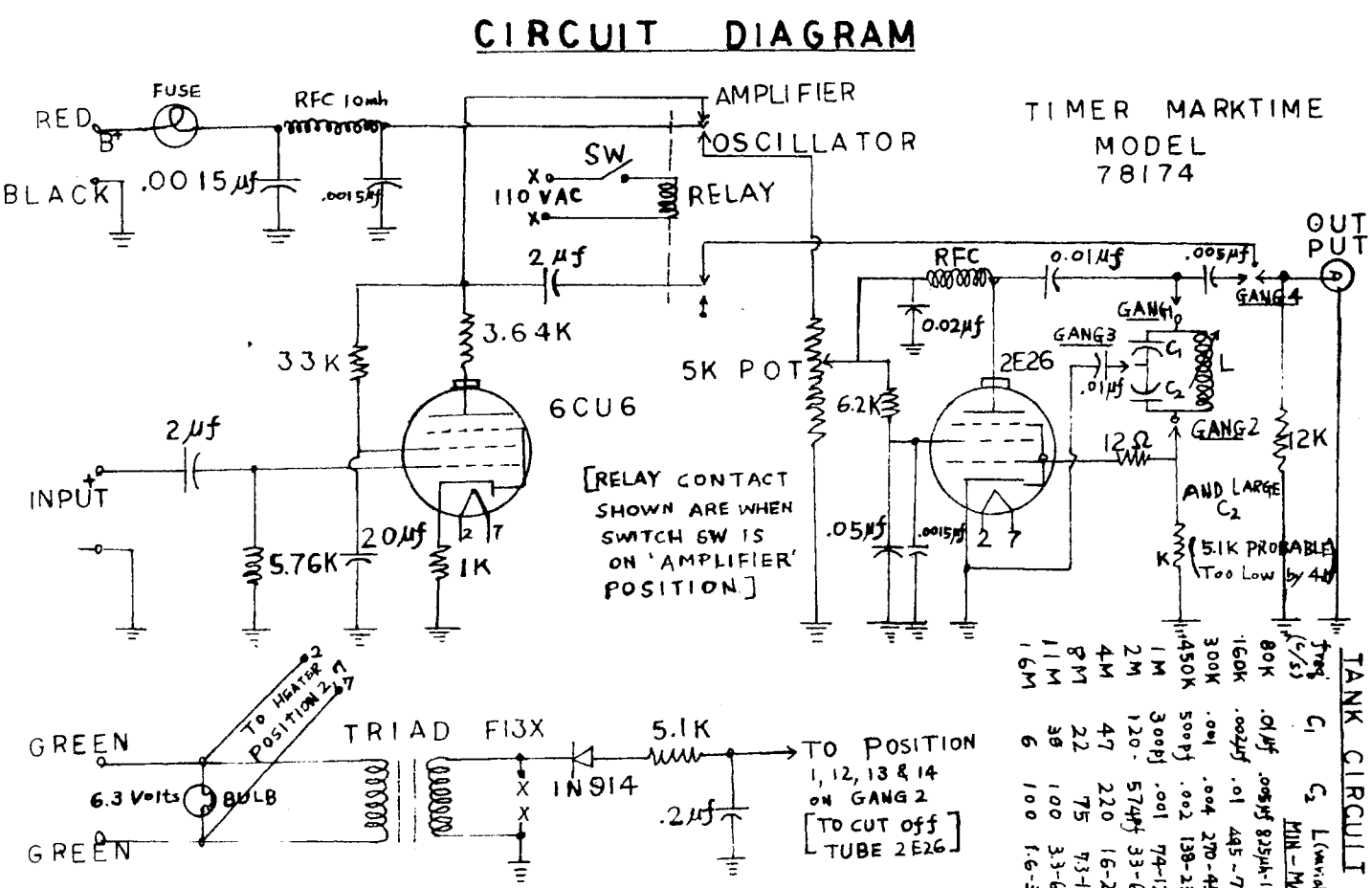

Figure 7. Circuit Diagram of Oscillator

10^{-4}M. The pAg range between 5 and 7.4 was covered by mixing appropriate ratios of the two solutions at 10^{-5}M, thereby maintaining approximately constant ionicity over the range. Solutions so prepared in this pAg range were also found to be sufficiently free of colloidal particles to permit potentiometric pAg determinations without difficulty. Suspensions used for measurements were prepared by allowing 15 ml of the fully dispersed master suspension to precipitate in a Pyrex beaker. The supernatant was then removed, and the precipitate was resuspended in an equal volume of colloid-free solution having the desired pAg. The procedure was repeated, after which the pAg of the suspension was taken to be equal to that of the colloid-free solution used in its preparation.

It was found that suspensions of the concentration required could not be prepared in the pAg range from 4.8 to 5.6. In this range the particles coagulated and could not be resuspended. This is undoubtedly because of the close proximity to the point of zero charge at a pAg of 5.4.

Conductivity

It is observed that the conductivity of the cellular suspensions has considerable effect upon the dielectrophoretic response to a nonuniform electric field. Precise measurement of it is important. The bridge used here was a General Radio 1650B impedance bridge (General Radio Co.) with a resistance range of 10^{-7} ohms and an accuracy of 1% between frequencies of 20 Hz and 20 KHz. A dipping-type YSI (Yellow Springs Instrument Co.) 3400 series conductivity cell was used with Pt-black electrodes.

Concentration

Cell suspension concentrations were determined using an optical density apparatus (Lumetron Colorimeter Model 401) and calibrated independently by counting procedures. A conversion curve relating yeast cell concentration to optical density is shown in Figure 8.

Microscope

The microscopic observations were made with a Baush and Lomb phase contrast microscope. It was equipped with a 1x-2x zoom which, with the proper objectives and 10x wide field eye-pieces, permitted almost continuous variation of magnification from 35 to 1940. However, because of the physical size of the electrode cells and the small working distance of the high power objectives, the practical upper limit to the magnification was 860. This was with 43x objective, 10x eyepieces, and 2x zoom.

A 10 mm reticle marked into 100 divisions was mounted into one of the oculars. It was calibrated with the various objectives at several zoom settings using an Edscrop standard graduated slide. The calculated distances using the reticle were within three per cent of the actual distance for the 10x and 20x objectives when the zoom was either in the 1x or 2x position.

Materials

AgBr Sols

Suspensions were prepared by addition of 100 ml of 0.1M reagent grade $AgNO_3$ to a slightly larger volume of 0.1M reagent grade KBr. The

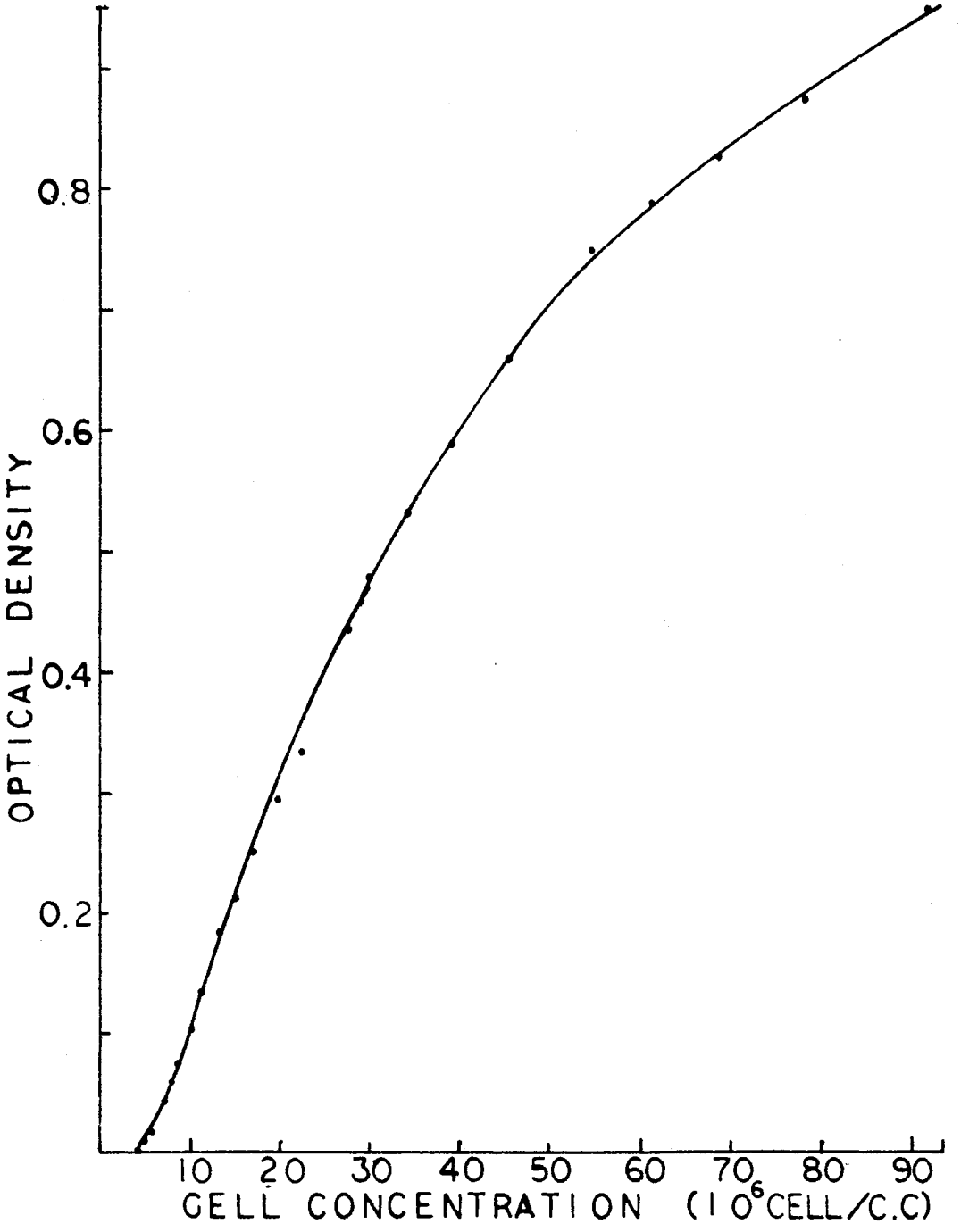

Figure 8. Relating Cells (Yeasts) Concentration to Optical Density

suspension was immediately diluted to less than 0.01 M with respect to the residual KNO_3. This reduction of ionicity was sufficient to prevent agglomeration of the AgBr particles. The suspension was permitted to stand overnight for precipitation in shallow Pyrex containers. The supernatant solution was then carefully removed by aspiration and replaced by distilled water. The precipitated AgBr particles were readily resuspended. This procedure was repeated twice, with the final addition of distilled water being of smaller quantity to obtain a more concentrated suspension. This "master suspension" served as the starting material for all experiments. Since the measurements to be made necessitated exposure of the suspensions to intense illumination, no effort was made to protect them from ambient light. By evaporating a known volume of the suspension and weighing the residue, it was established that the particle concentration was about one per cent by weight. Droplets of the suspension were dried on Formvar grids, and the AgBr particles were examined under the electron microscope. A particle size in the range 0.1 - 0.5U was observed. The particles were irregular in shape. No development of crystallographic faces was evident.

SiO_2 (Gel)

(1) SiO_2 gel (Ludox, Du Pont Co.) through ion exchange resin columr to deionize.

(2) Dry (200°C for 24 hrs.).

(3) Grind to pass 200 mesh (use mill).

(4) Select out particle size range desired by settling. This method is based on the fact that the sedimentation velocity of large and heavy particles is greater than that of small and light particles. Sup-

pose that in water are dispersed particles of radius r and density ρ. The sedimentation rate of particle is then determined by two forces: by the force of gravity which for small spheres will be $4/3\pi r^3 (\rho,\rho_o)$ g, ρ_o being the density of the medium (g is the gravitational constant), and by the force of friction, $6\pi\eta rv$, η being the viscosity of the medium and v the sedimentation rate. When the particle is falling with a constant velocity, both forces will be equal: $6\pi\eta rv = 4/3\ \pi r^3 (\rho-\rho_o)g$. This is the expression for the well-known law of Stokes. Since S(displacement) = vt (elapsed time), thus $S = \frac{2r^2(\rho-\rho_o)gt}{9\eta}$. For SiO_2, $\rho = 2.2$ and $\eta = 0.009358$ poise, at 23^oC, so $S = 2.7926 \times 10^4 r^2 t$.

The suspensions were poured into a petri dish of a certain height. By choosing the proper time to pour off the supernatant, we could select the particle size range desired. Sedimentation under gravity is very important in soil science and has been practices since the beginning of the nineteenth century. It is, however, useful only for particles larger than about 0.1μ. If the particles are too small and too light to be pulled down to the bottom by the gravitational force, their sedimentation rate in the nature field of gravity will be too slow. It would be greater if we could increase the force of gravity. This is realized in the centrifuge. Thus, for smaller particles we select out the particle size range by centrifuge. The range we used is 0.7 - 0.01μ.

Ion Exchange Resin

(1) Cation exchange resin (Dowex 50 x-x8, Baker Chemical Co., Phillipsburg, N.J.). Grind and then select out particle size desired (1μ - 0.063μ).

(2) Anion exchange resin (Dowex 1-x8, Baker Chemical Co., Phillips-

burg, N.J.). Grind and then select out particle size desired (1μ - 0.077μ).

Preparation of Rat Liver Mitochondria

i. Excise liver and place in 100 ml graduated cylinder containing 50 ml of sucrose solution--note volume displaced by liver.

ii. Pour contents into beaker and mince liver with scissors. Decant off sucrose solution with hair and other non-liver material. Add another 50 ml sucrose and mince again with scissors; decant off sucrose solution again.

iii. Add sucrose (9 vol. sucrose/vol. of liver) split into two homogenizing vessels; split liver between these two vessels. Homogenize with two passes with Potter-Elvehjem teflon pestle per vessel.

iv. Centrifuge in servall at 2,000 rpm for 8 to 10 minutes. (power state setting of 10 for servall in cold room.)

v. Decant supernatant and discard pellet. Centrifuge the supernatant at 8,500 rpm for eight to ten minutes (power state setting of 37).

vi. Decant supernatant off and save pellet. Resuspend pellet with rubber policeman using one-half as much sucrose solution as for original homogenization. Transfer mitochondria solution to homogenizer and lightly suspend mitochondria by hand homogenization.

vii. Centrifuge suspension at 8,500 rpm for eight to ten minutes (power state setting of 37). Pour off supernatant; pellet contains mitochondria.

viii. Resuspend mitochondria with small amount of sucrose using rubber policeman. Lightly hand homogenize to resuspend mitochondria. Should have about 5 ml of mitochondria from 10g liver.

Precautions:

1) Overall preparation should be done within one hour.

2) Do not attempt to get better than 30% yield on mitochondria. On each resuspension of mitochondria by rubber policeman, remove mitochondria from around the center core of pellet. Do not resuspend whole pellet at either step.

3) All glassware must be washed with soap, rinsed 15 times with tap water, 10 times with deionized water, and 3 times with glass-distilled water.

Bacteria

The Pseudomonas aeruginosa strain 1 (designated hereafter as Pa-1) and its mutants cg 1. and cg 2. were obtained from the lab of Dr. Elizabeth Gaudy, Dept. of Microbiology, Oklahoma State University. Escherichia coli was obtained from Dr. Norman Durham, and the Bacillus cereus, and Bacillus megaterium were obtained from Research Station, Continental Oil Co., Ponca City, Oklahoma.

Stock cultures were maintained on nutrient agar slants by periodic transfer; the cultures were stored at $4^{\circ}C$ after growth. All cultures were incubated at $30^{\circ}C$ on nutrient agar (Difco).

Yeast (Saccharomyces cerevisiae)

The original stock was obtained from commercial dry yeast by growing it on peptone-dextrose agar. Pure cultures were growth at room temperature on peptone-dextrose agar (Difco).

Zymosan

The term "Zymosan" refers to crude yeast cell wall preparations consisting chiefly of protein-carbohydrate complexes (73,74). This material was obtained from Mann Research Laboratories, Division of Becton, Dickinson and Co., N.Y., N.Y. It is a light gray powder. It is practically insoluble in water, but readily disperses to give a homogeneous suspension.

A Typical Run

First the cells (yeasts) are suspended in deionized water. The suspension was centrifuged until the cells were packed at the bottom of the centrifuge tube, and the liquid was poured off. They were then resuspended and centrifuged. This procedure was repeated until the conductivity of the suspension, as measured with the Y.S.I. probe and impedance bridge, was at or below the desired value. In between measurements the probe was kept in a test tube of deionized water to prevent contamination by the probe. If the suspension conductivity became too low, it could be increased by the addition of dilute KCl solution. With the cell concentration adjusted to the proper value, these suspensions should be kept for thirty minutes, as we can see from Figure 9. The conductivity changes rapidly within thirty minutes, and the change of conductivity affects the yield. Usually, the cells were kept at $0^{\circ}C$.

Before the electrode chamber can be used, it must be rinsed several times with deionized water. Spraying with a water jet obtained from a squeeze bottle is the simplest and surest way to rinse the electrode. The chamber is then dried using an air jet from a squeeze bottle. This drying is necessary to prevent a dilution of the suspension when it is

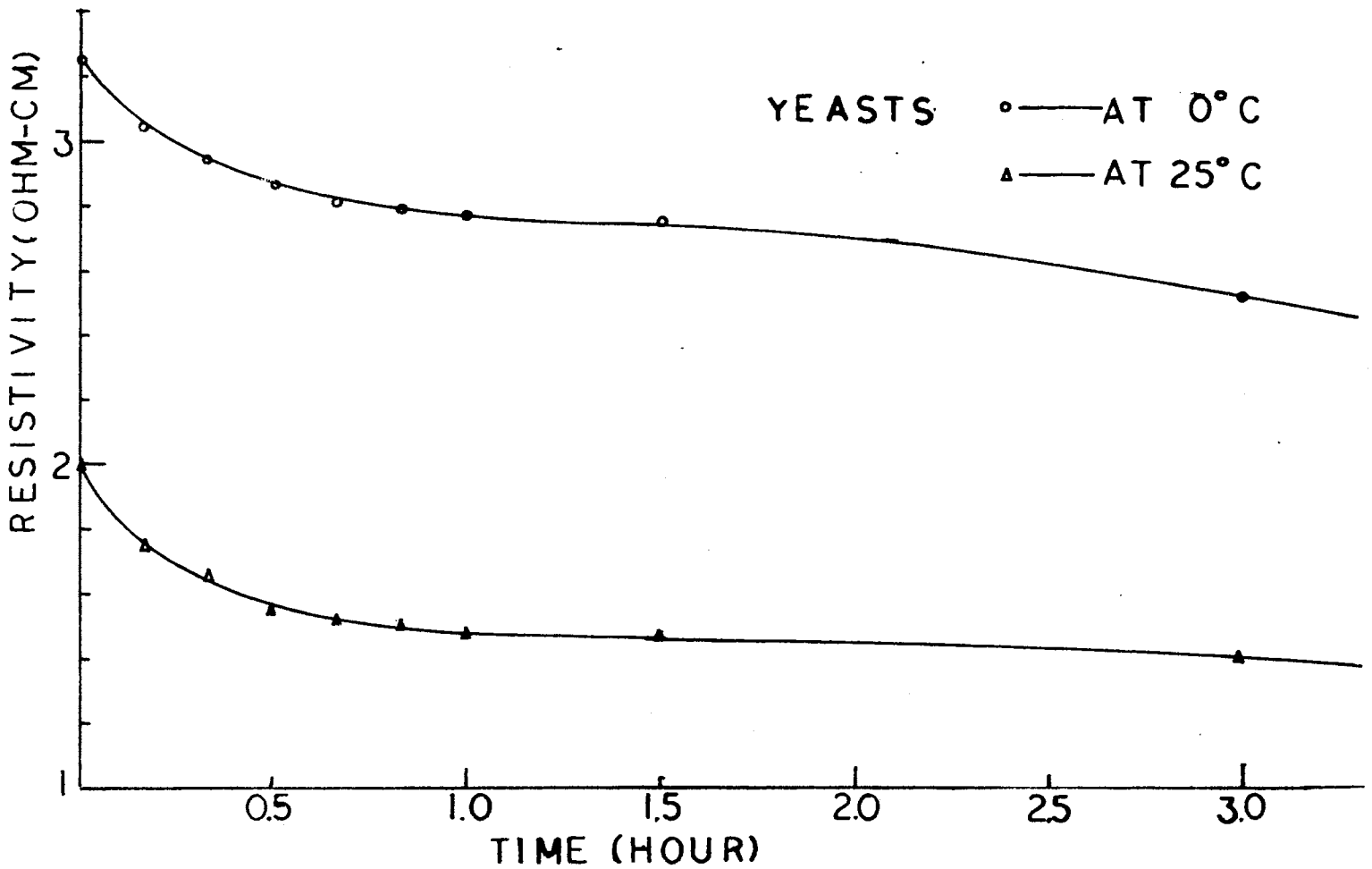

Figure 9. The Change of Conductivity by Time; Optical Density = 0.24 (of 2) at 550, Total Volume 16 ml

placed in the chamber. Each time before the well is filled, the suspension should be thoroughly mixed to counteract any settling which might have occurred.

After the chamber has been filled, it was covered with cover glass and mounted on the microscope stage, and electrical leads connected. The frequency and voltage of the applied signal were selected, and the cells in suspension were still; then the connecting switch was thrown, applying the voltage across the electrodes. It was observed that while the field is on, the cells generally migrate to the electrode. They attached themselves there, in chain-like formations commonly called pearl-chains, parallel to the field lines. The average length of these chains after a given time was designated as the yield and was measured using the reticle in the microscope. For this particular run the lengths would be measured at the end of two minutes and the field would be shut off.

Once the measurement was complete, the chamber was removed from the microscope stage, rinsed with the deionized water jet, and dried with the air jets. Actually not all of the cells are removed from the electrode by this process. A gentle brushing with a soft pipe cleaner is sometimes necessary, after which the chamber is rinsed and dried. It is then filled with more solution; a new frequency is selected; and the procedure is repeated. This is continued for all of the desired frequencies. At the end of the experiment, the conductivity of the system should be checked.

CHAPTER IV

EXPERIMENTAL RESULTS

AgBr Sols

The results of the dielectrophoretic yield as a function of frequency for aqueous suspensions at three different values of pAg, the variation of ν_p, the frequency of peak yield with pAg, and the dielectrophoretic yield for suspending media consisting of dioxane and four different dioxane/water mixtures are shown in Appendix A. Figure 10 illustrates the dependence of the yield upon the resistivity for the frequencies ranging from 1 KHz to 7.3 MHz. The most striking feature of these results is the yield peak depending upon the resistivity. As resistivity decreases, the yield peak decreases and moves to a higher frequency. The resistivity was changed by adding KBr.

SiO_2 (Gel) Suspensions

The experimental results for SiO_2 have been obtained under a 420x phase microscope. Figure 11 illustrates, for aqueous suspensions at three different cation valences (Na^+, Ca^{++}, La^{+++}) in two concentrations (0.5 mM and 0.05 mM), the dependence of the yield upon the frequency of the applied ac potential. The most striking feature of these results is the yield peak, which occurs at frequencies ranging from 250 KHz to 2 MHz, depending upon the resistivity and the valence of the solution. For

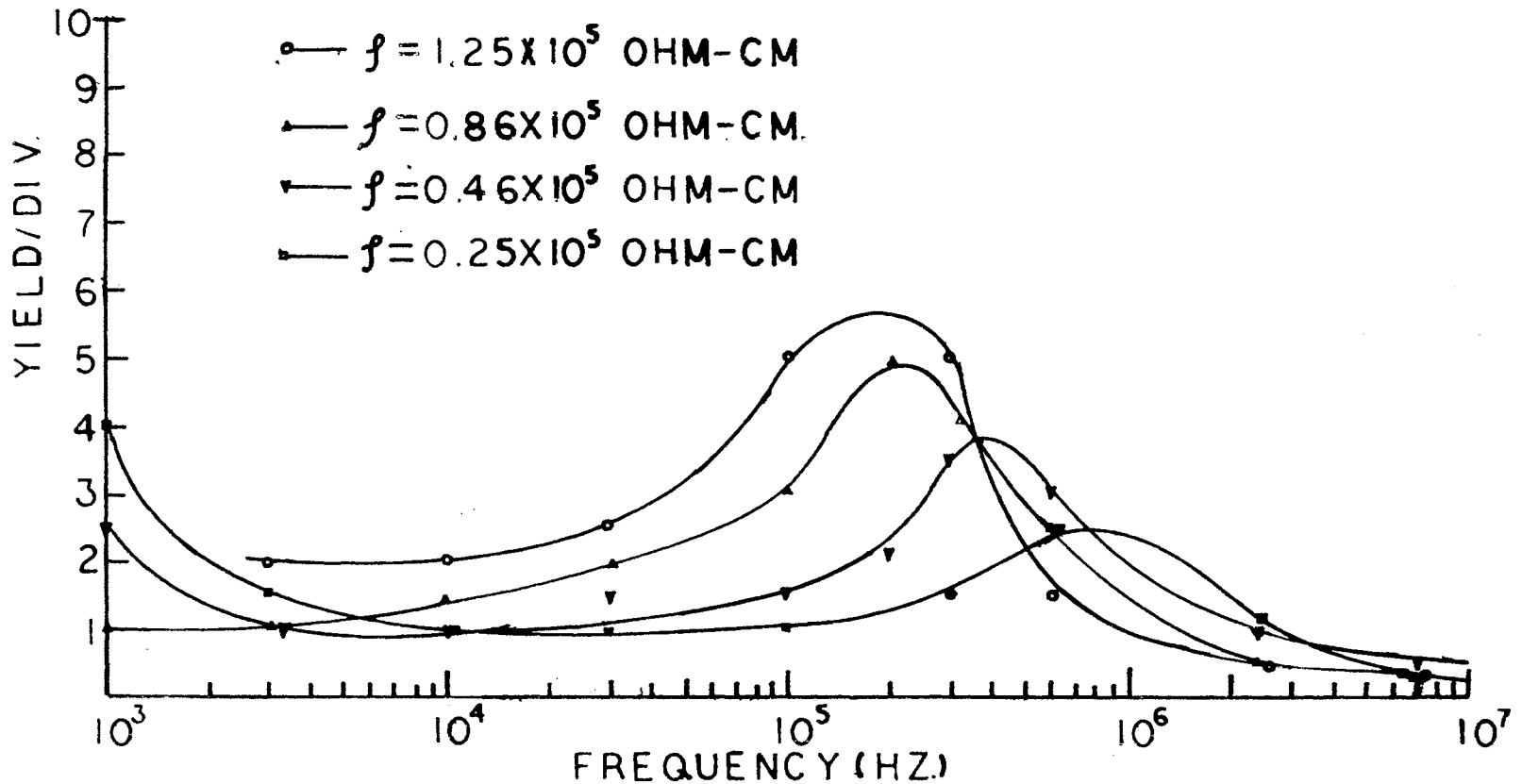

Figure 10. Variation of Yield Spectra of AgBr With Resistivity W-W: 0.025 - 0.95 mm (Diam. 0.025 mm, Space. 0.95 mm) 24 Volts, Collected in 2 Min, 420X

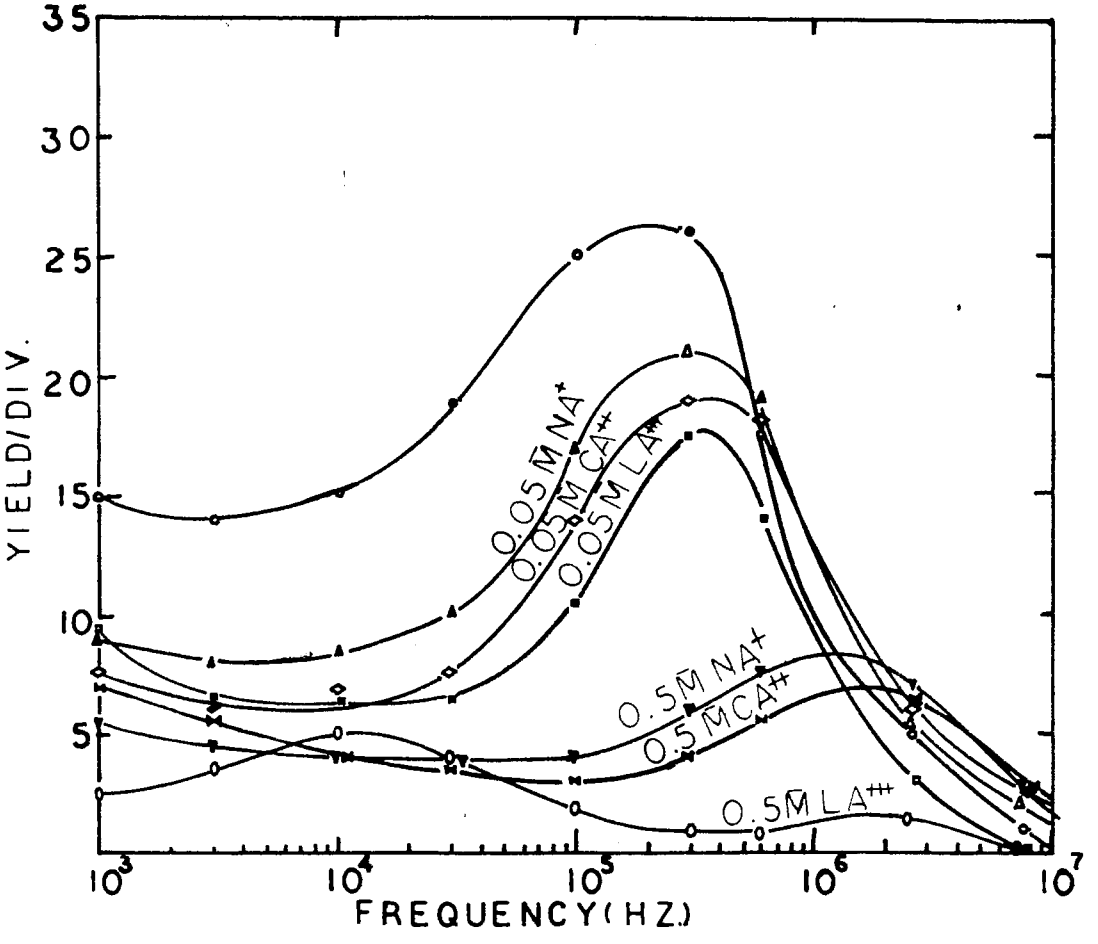

Figure 11. Effects of Cations on Yield Spectra of SiO_2 Gel; w-w; 0.025 - 0.97 mm, O.D. (Optical Density) = 0.6 at 550, 24 Volts, Collected in 12 Min., 420x; $\rho = 1.2 \times 10^5$ ohm-cm, (Δ) $\rho = 7 \times 10^4$ ohm-cm, (∇) $\rho = 1.9 \times 10^4$ ohm-cm (0.5 mM $NaNO_3$), ($\diamond$) $\rho = 4.1 \times 10^4$ ohm-cm (0.05 mM $Ca(NO_3)_2$), ($\bowtie$) $\rho = 0.91 \times 10^4$ ohm-cm (0.5 mM $Ca(NO_3)_2$), ($\square$) $\rho = 5.15 \times 10^4$ ohm-cm (0.05 mM $La(NO_3)_3$), (O) $\rho = 0.61 \times 10^4$ ohm-cm (0.5 mM $La(NO_3)_3$)

the effects of anion valence ($SO_4^{=}$ and $C_6O_5H_7^{-}$) of the yield upon the frequency of the applied ac potential, see Figure 12. The variation with the concentration, the electrode size, and the distance between electrodes of the spectra is illustrated in Figures 13 and 14.

The enhanced yield occurring at low frequencies ($\nu < 1$ KHz) and not be studied extensively because of the difficulty of complete elimination of the electrode impurity and polarization. In addition, the form of the low frequency collection was qualitatively different, with clump-like aggregation of the particles instead of as chain form on the electrode being observed.

Ion Exchange Resin

Figures 15, 16 and 17 illustrate, for cation exchange resin suspensions at different anion and cation valence (H^+, Na^+, Ca^{++}, La^{+++}, NO_3^-, $SO_4^{=}$ and $C_6O_5H_7^{-}$) in two concentrations (0.5 mM and 0.05 mM), the dependence of the yield upon the frequency of the applied ac potential. The anion exchange resin suspensions are illustrated in Figures 18 and 19. The most striking feature of these results is the high yield at low frequency ($\simeq$ 1 KHz) for cation exchange resin. On low frequency ($\lesssim$ 1 KHz), the anomalous growth of pearl chains from the end that was closest to the electrode was observed.

Rat Liver Mitochondria

The yield spectra have been shown on Figures 20, 21, and 22. In Figures 20 and 21, the mitochondria have good biological activity as measured by Dr. W. Flory, Biochemistry, O.S.U.

In Figure 22 the mitochondria have low biological activity. The

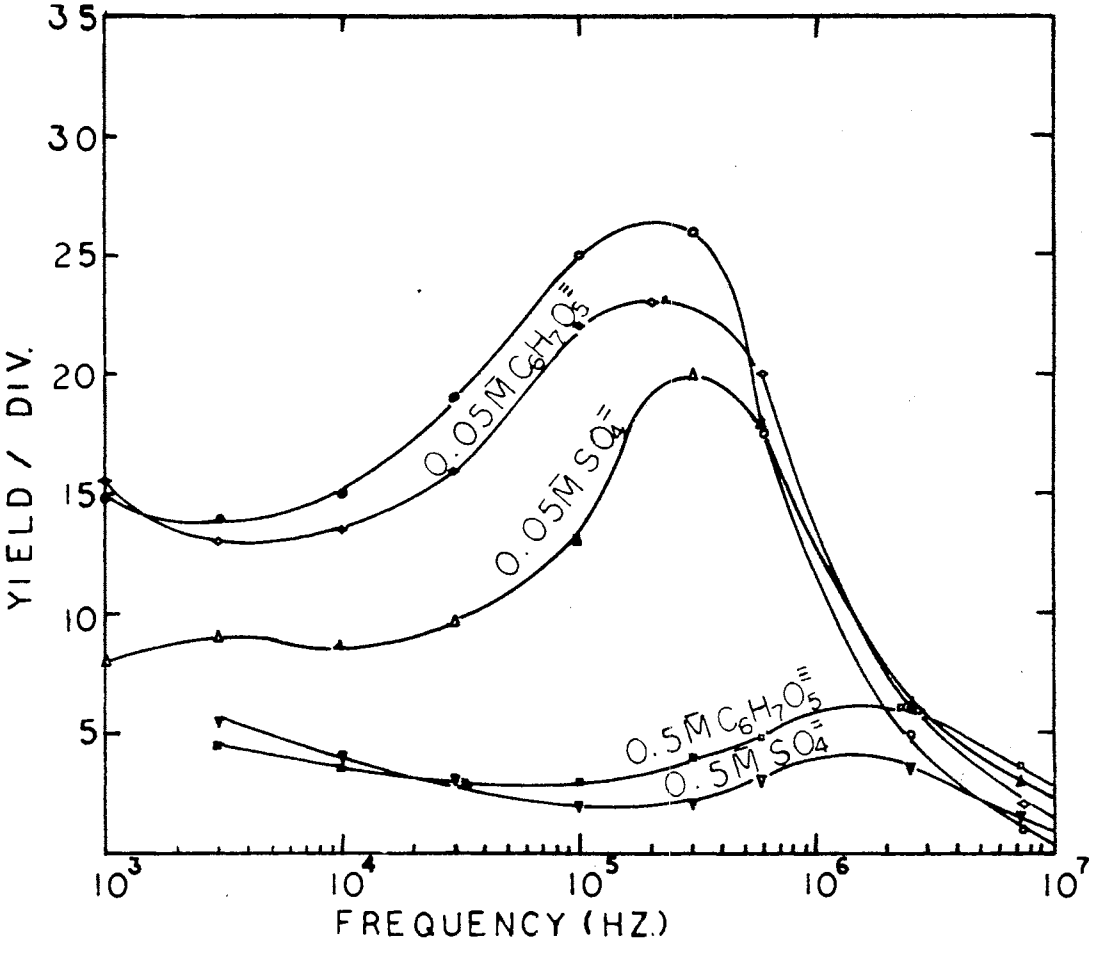

Figure 12. Effects of Anions on Yield Spectra of SiO_2 Gel; w-w: 0.025 - 0.97 mm, 24 Volts, Collected in 2 Min, 420x, O.D. = 0.6 at 550; (O) $\rho = 1.2 \times 10^5$ ohm-cm, (Δ) $\rho = 4.1 \times 10^4$ ohm-cm (0.05 mM Na_2SO_4), (▽) $\rho = 0.85 \times 10^4$ ohm-cm (0.5 mM Na_2SO_4), (◇) $\rho = 7.7 \times 10^4$ ohm-cm (0.05 mM $Na_3C_6O_5H_7$), (▭) $\rho = 0.94 \times 10^4$ ohm-cm (0.5 mM $Na_3C_6O_5H_7$)

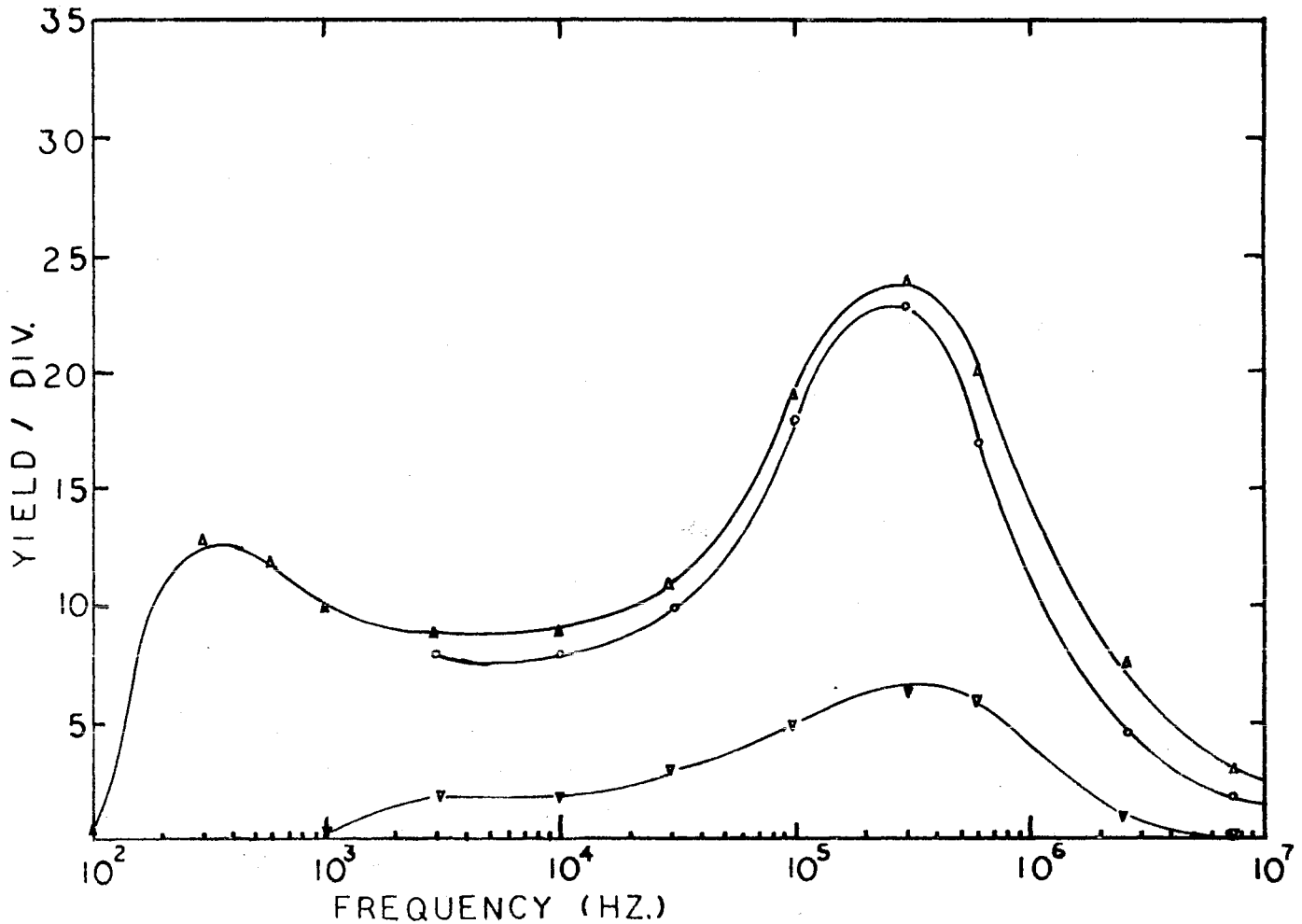

Figure 13. Concentration Dependence on Yield Spectra of SiO_2 Gel: w-w: 0.025 - 1.06 mm, 24 Volts, Collected in 2 Min, 420x, (O) $\rho = 0.8 \times 10^5$ ohm-cm (O.D. = 0.63 at 550), (Δ) $\rho = 0.62 \times 10^5$ ohm-cm (O.D. = 0.92 at 550), (∇) $\rho = 0.6 \times 10^5$ ohm-cm (O.D. = 0.05 at 550)

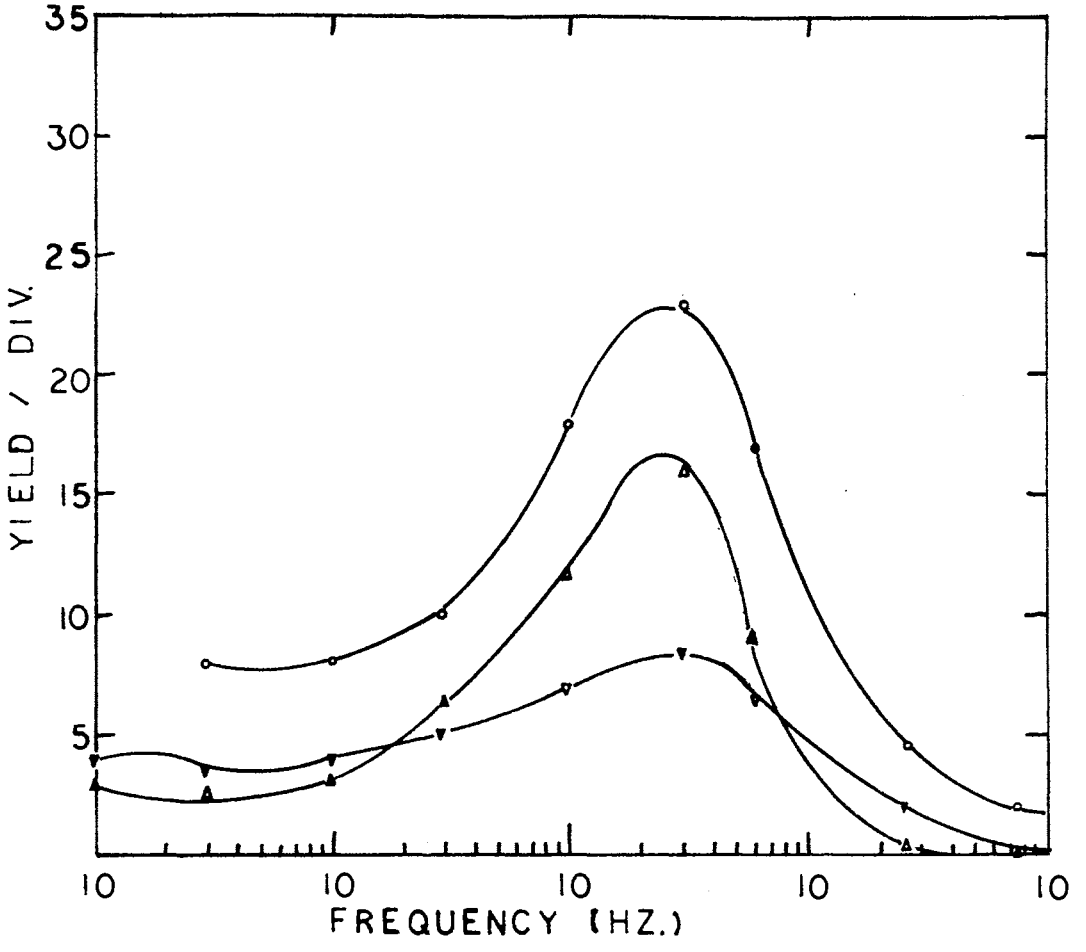

Figure 14. Variation of Yield Spectra (SiO_2) With Electrodes and Voltages; $\rho = 0.8 \times 10^5$ ohm-cm, 420x, O.D. = 0.63 at 550; (O) w-w: 0.025 - 1.06 (24v), (Δ) w-w: 0.25 - 1.04 (24v), (▽) w-w: 0.025 - 1.06 (10v)

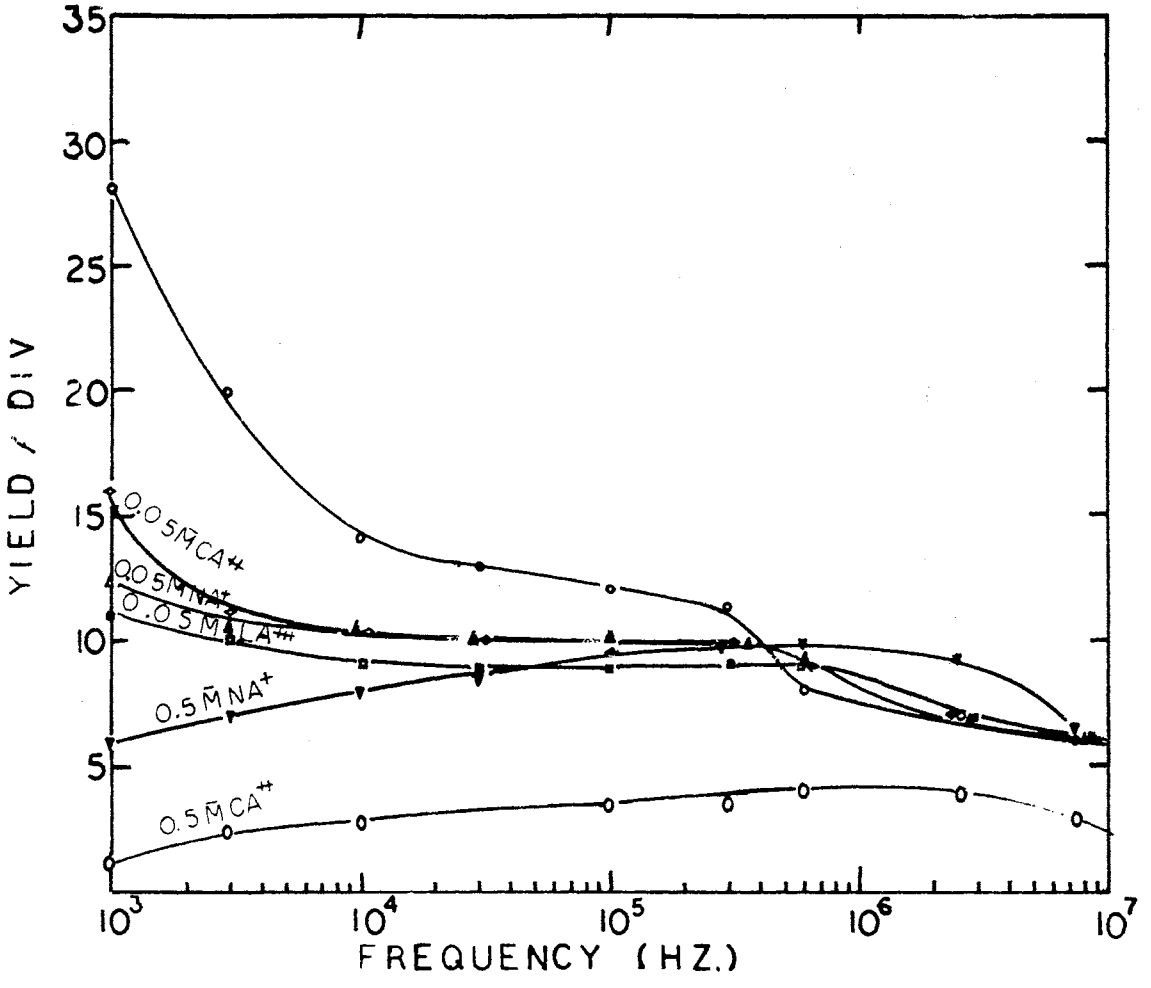

Figure 15. Effects of Cations on Yield Spectra of Ion Exchange Resin (Acidic); w-w: 0.025 - 0.97 mm, O.D. = 0.4 at 550, 5 Volt, Collected in 2 Min, 420x; (O) $\rho = 8.8 \times 10^4$ ohm-cm, (Δ) $\rho = 3.85 \times 10^4$ ohm-cm (0.05 mM $NaNO_3$), (∇) $\rho = 0.71 \times 10^4$ ohm-cm (0.5 mM $NaNO_3$), ($\diamond$) $\rho = 2.7 \times 10^4$ ohm-cm (0.05 mM $Ca(NO_3)_2$), (O) $\rho = 0.32 \times 10^4$ ohm-cm (0.5 mM $Ca(NO_3)_2$), ($\boxplus$) $\rho = 1.87 \times 10^4$ ohm-cm (0.05 mM $La(NO_3)_3$)

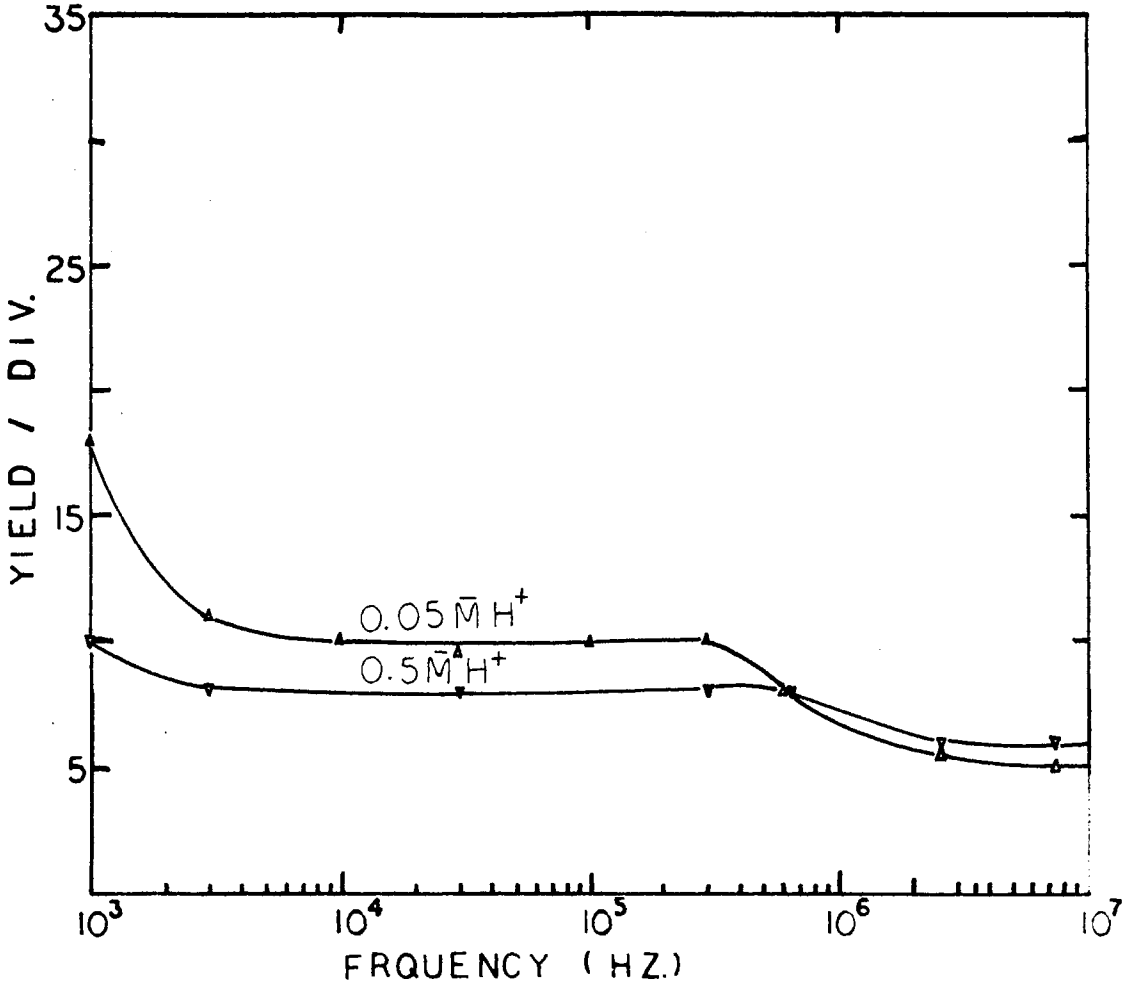

Figure 16. Effects of Hydrogen Ions on Yield Spectra of Ion Exchange Resin (Acidic); w-w: 0.025 - 0.97 mm, O.D. = 0.4 at 550, 5 Volts, Collected in 2 Min, 420x; (Δ) $\rho = 5.4 \times 10^4$ ohm-cm (0.05 mM HNO_3), (▽) $\rho = 1.3 \times 10^4$ ohm-cm (0.5 mM HNO_3)

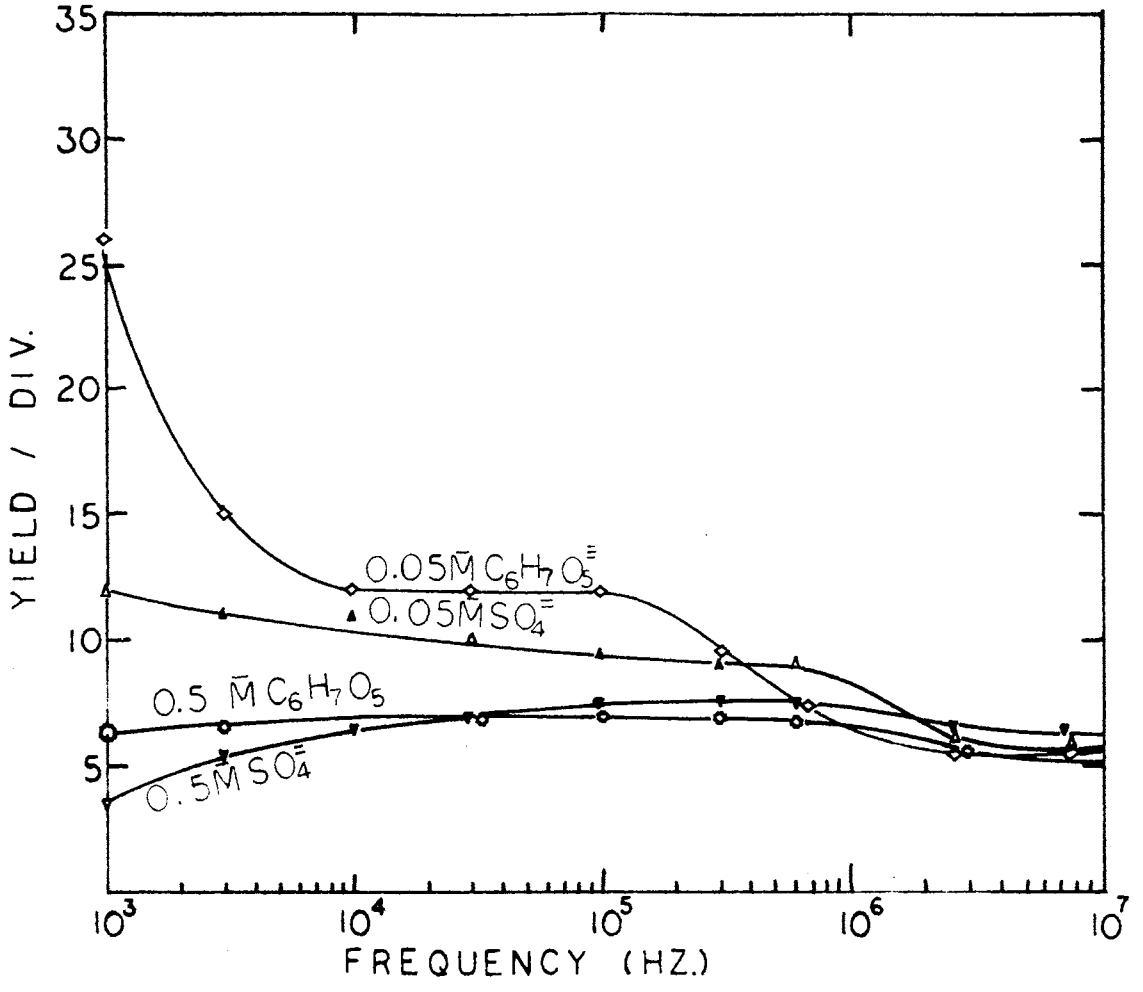

Figure 17. Effects of Anions on Yield Spectra of Ion Exchange Resin (Acidic); w-w: 0.025 - 0.97 mm, O.D. = 0.4 at 550, 5 Volts, Collected in 2 Min, 420x; (Δ) $\rho = 2.25 \times 10^4$ ohm-cm (0.05 mM Na_2SO_4), (▽) $\rho = 0.39 \times 10^4$ ohm-cm (0.5 mM Na_2SO_4), (◇) $\rho = 8.2 \times 10^4$ ohm-cm (0.05 mM $Na_3C_6O_5H_7$), (○) $\rho = 1.8 \times 10^4$ ohm-cm (0.5 mM $Na_3C_6O_5H_7$)

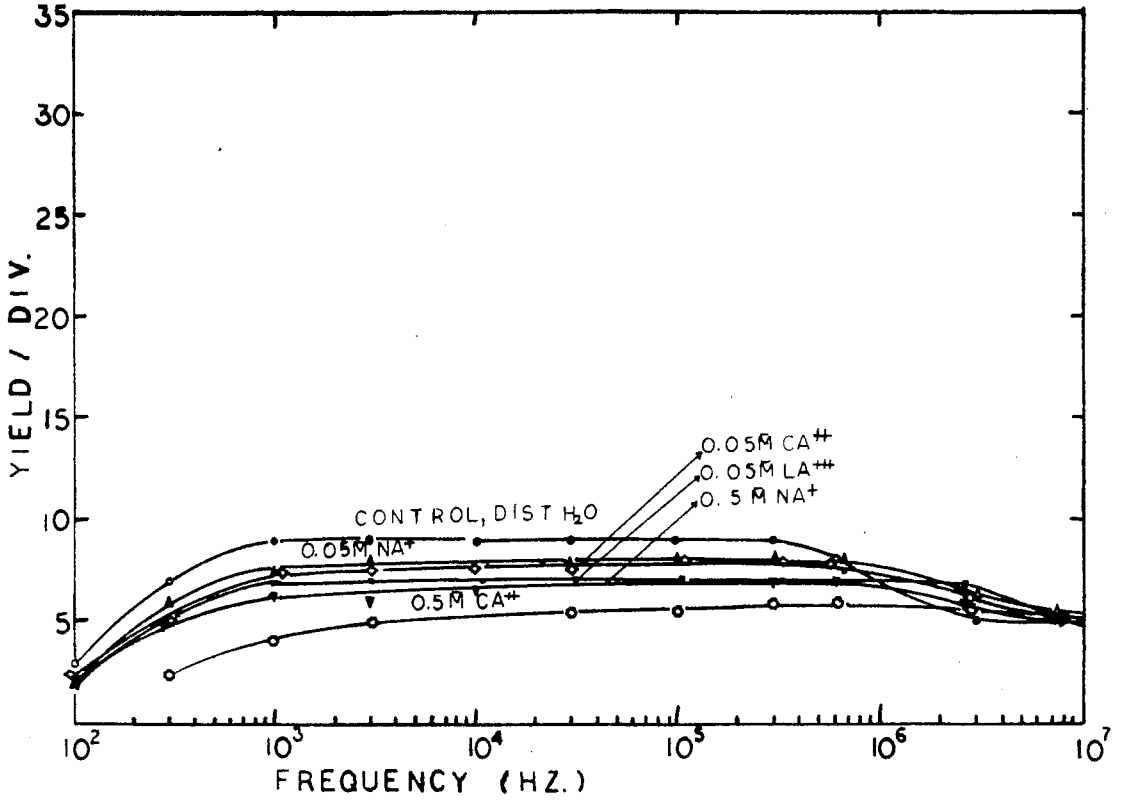

Figure 18. Effects of Cations on Yield Spectra of Ion Exchange Resin (Basic); w-w: 0.025 - 0.97 mm, O.D. = 0.6 at 550, 5 Volts, Collected in 2 Min, 420x; (O) $\rho = 1.5 \times 10^5$ ohm-cm, (Δ) $\rho = 5.9 \times 10^4$ ohm-cm (0.05 mM $NaNO_3$), (∇) $\rho = 1.85 \times 10^4$ ohm-cm (0.5 mM $NaNO_3$), ($\Diamond$) $\rho = 5.6 \times 10^4$ ohm-cm (0.05 mM $Ca(NO_3)_2$), ($\square$) $\rho = 0.95 \times 10^4$ ohm-cm (0.5 mM $Ca(NO_3)_2$), ($\bullet$) $= 4.1 \times 10^4$ ohm-cm (0.05 mM $La(NO_3)_3$)

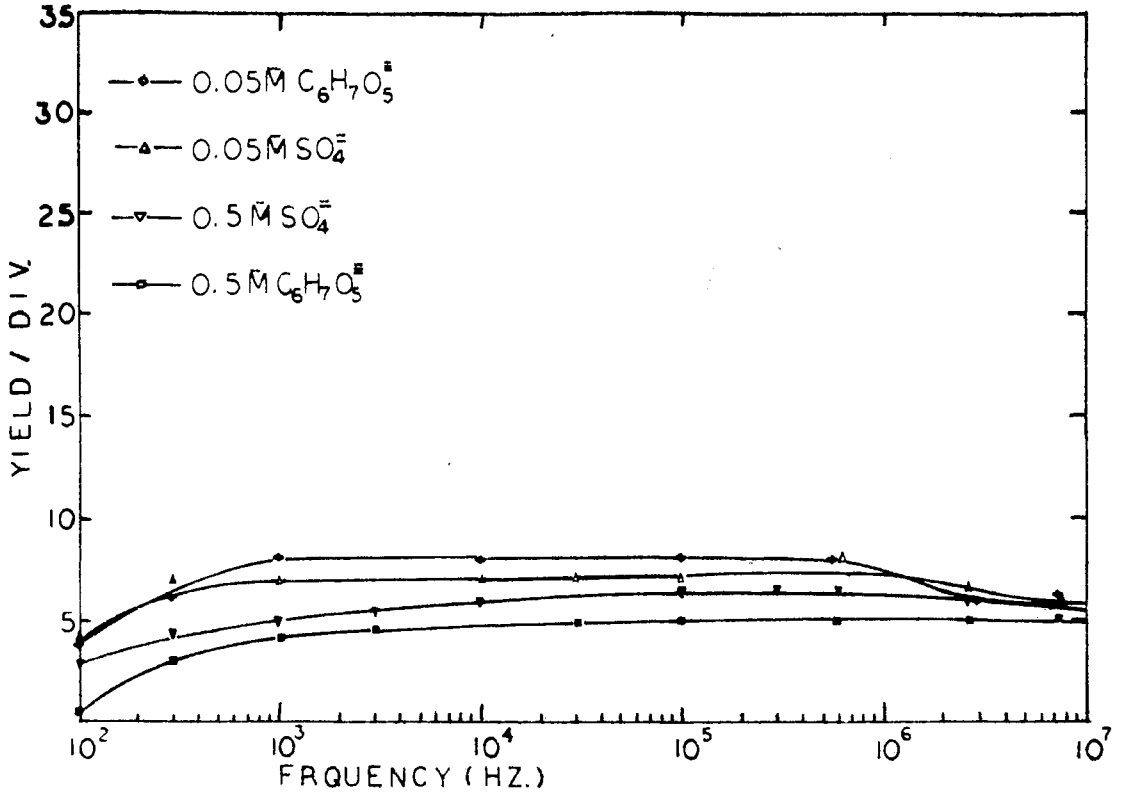

Figure 19. Effects of Anions on Yield Spectra of Ion Exchange Resin (Basic); w-w: 0.025 - 0.97 mm, O.D. = 0.6 at 550, 5 Volts, Collected in 2 Min, 420x; (Δ) ρ = 3.5×10^4 ohm-cm (0.05 mM $NaSO_4$), (▽) ρ = 0.8×10^4 ohm-cm (0.5 mM Na_2SO_4), (◇) ρ = 4.6×10^4 ohm-cm (0.05 mM $Na_3C_6O_5H_7$), (○) ρ = 0.78×10^4 ohm-cm (0.5 mM $Na_3C_6O_5H_7$)

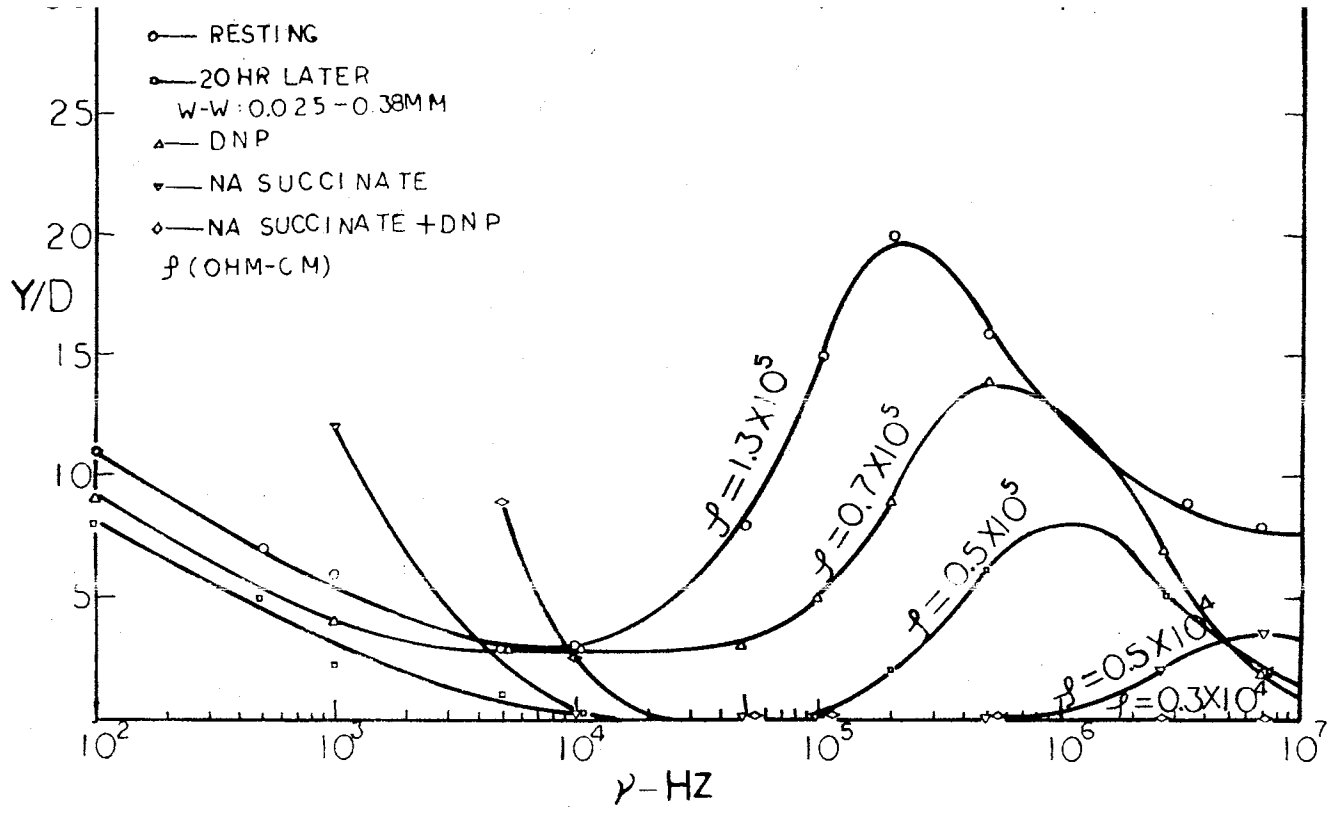

Figure 20. Yield Spectra of Rat Liver Mitochondrai w-w: 0.025 - 0.3 mm, 20 Volts, Collected in 2 Min, 820x, O.D. = 0.8

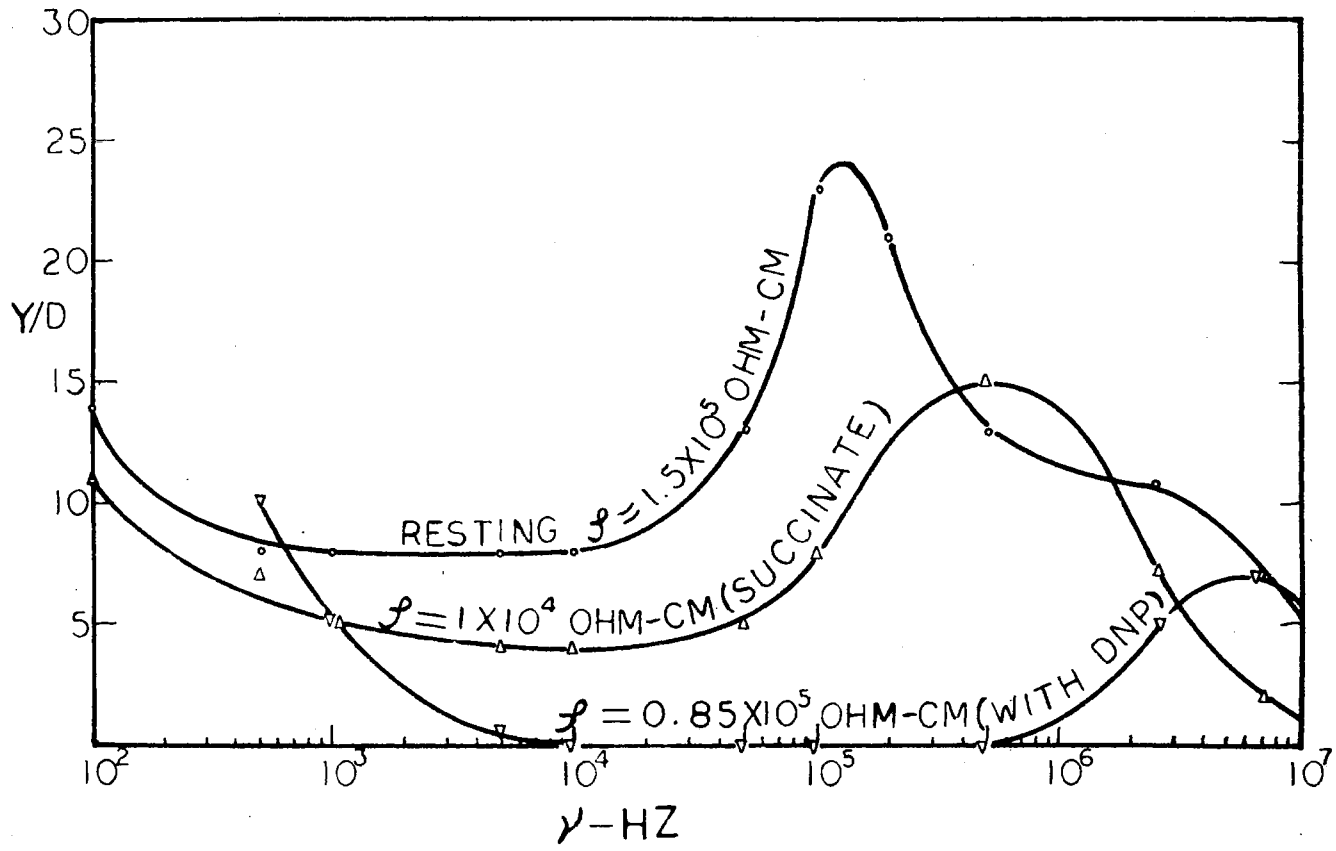

Figure 21. Yield Spectra of Rat Liver Mitochondria w-w: 0.025 - 0.3 mm, 820x, 20 Volts, Collected in 2 Min, O.D. = 0.8

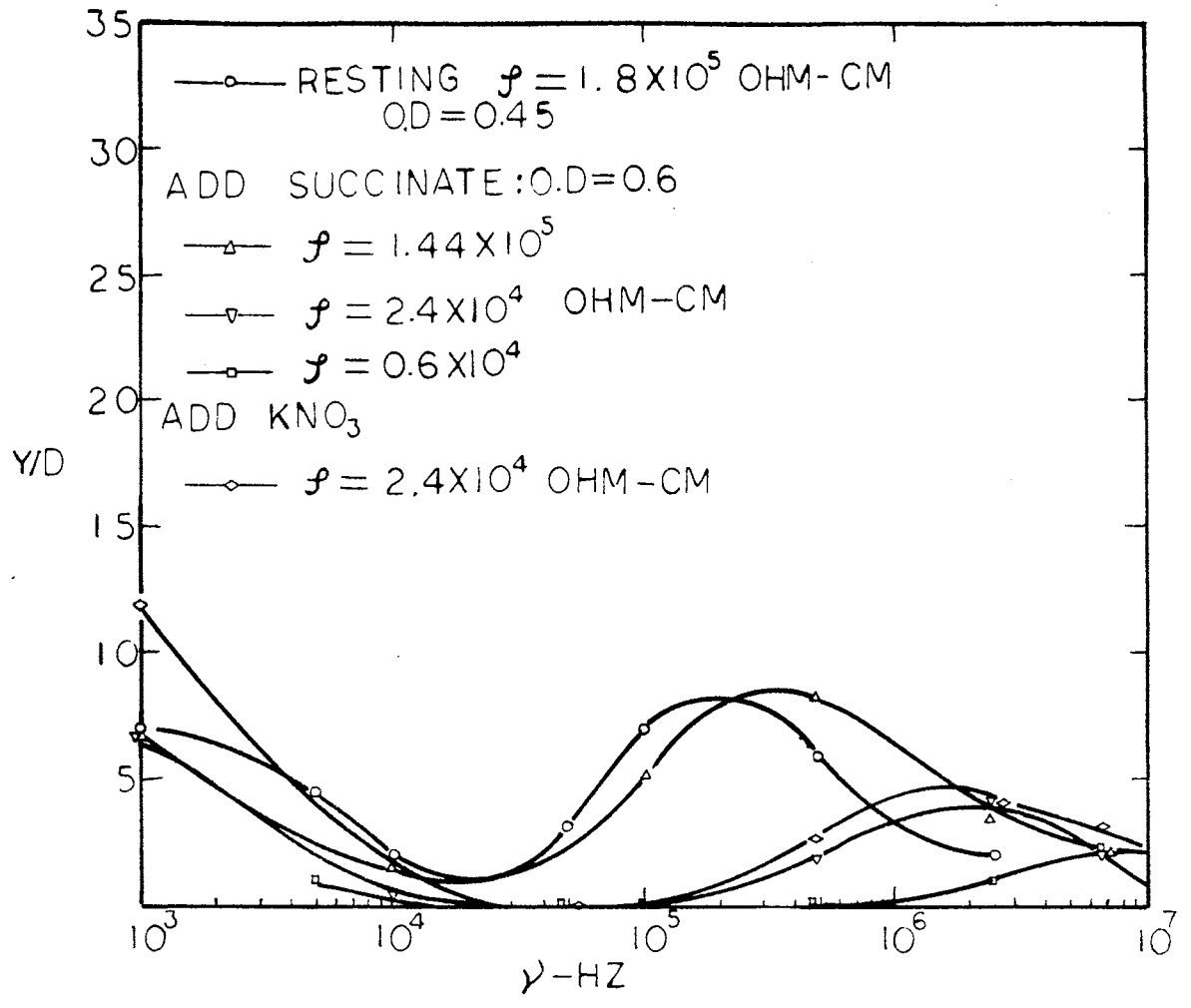

Figure 22. Yield Spectra of Rat Liver Mitochondria w-w: 0.025 - 0.3 mm, 820x, 20 Volts, Collected in 2 Min

results are similar to AgBr Sols and SiO_2(gel), except the subpeak appears on the 2.55 to 7.3 MHz. The spectra of active and poorly active mitochondria were quite different. The change of yield by the time is shown in Figure 23.

Bacteria

(1) Pseudomona aeruginosa (0.5 to 0.6 by 1.5μ) - Figures 24 and 25, show the yield spectra of 15 hr. and 30 hr. old PA1 (wild type) as affected by suspension resistivity. The yield spectra of PA1 cell debris (broken by ultrasonics) at different resistivities is illustrated in Figure 26. The resistivity was changed by KCl. The comparison of the whole cell with cell debris is shown in Figure 27 (for PA1), Figure 28 (for Cg1), and Figure 29 (for Cg2). The yield spectrum of the Ag 10 cell debris is also included in Figure 27. Figure 30 illustrates, for 11 hr. old Cg1 at four different resistivities, the dependence of the yield upon the frequency of the applied ac potential. These spectra are similar to the spectra of PA1.

(2) Escherichia coli (0.5 by 1.0 to 3.0 μ)--Figures 31 to 34 illustrate, for aqueous suspensions of E. coli with different ages, resistivities (change by KCl), and valence, the dependence of the yield upon the frequency of the applied ac potential.

(3) Bacillus cereus (1.0 to 1.2 by 3.0 to 5.0μ)--Figure 35 illustrates the difference in culture age of the yield spectrum. The dependence of the resistivity is illustrated in Figures 36 and 37. The most striking feature of these results in the yield peak, which occurs at frequencies ranging from 100K to 300 KHz, depending upon the age of the culture. The normal collection of the cell on the electrode is end

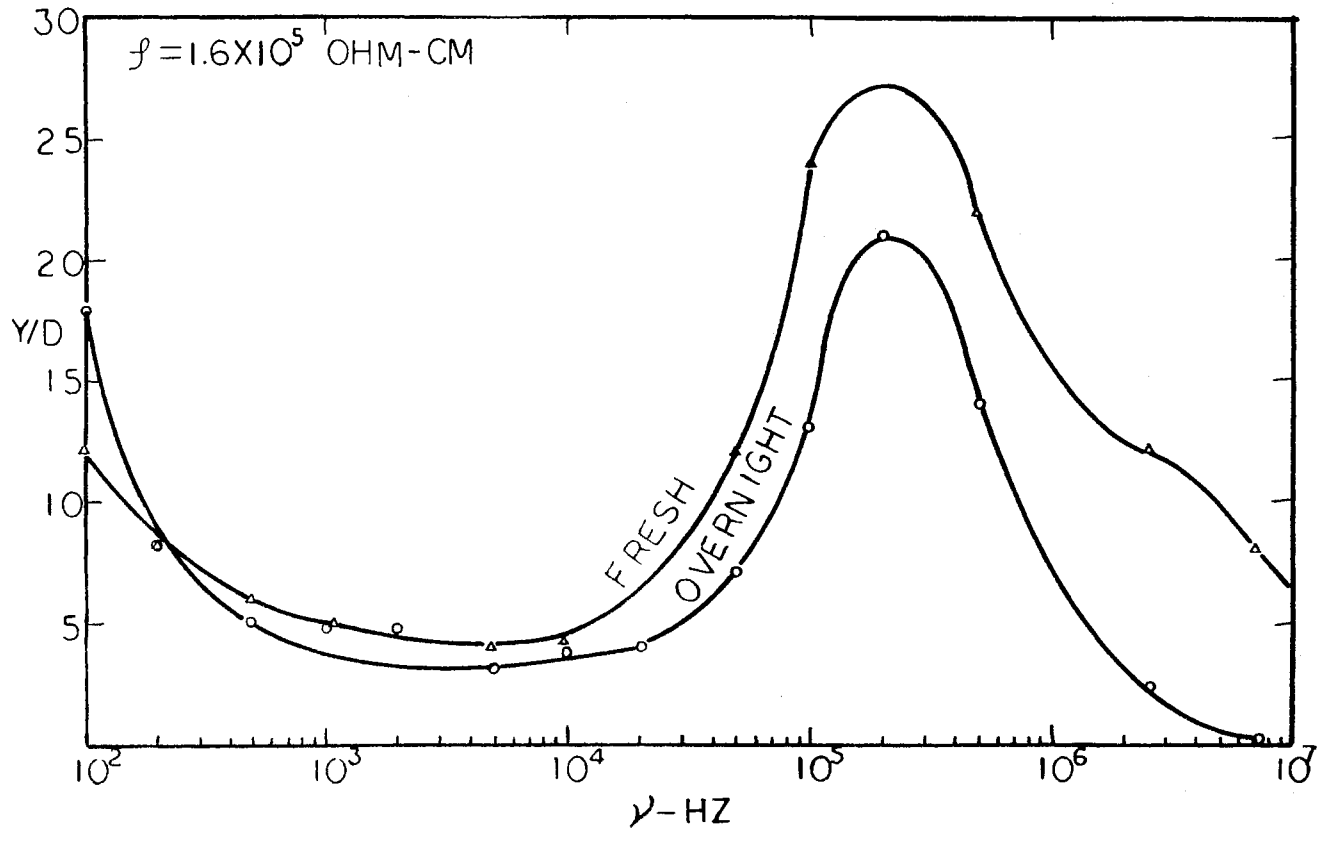

Figure 23. Variation of Yield Spectra (Mitochondria) With Length of Time After Isolated. w-w: 0.025 - 0.3 mm O.D. = 0.8, 24 Volts, Collected in 2 mm, 820x

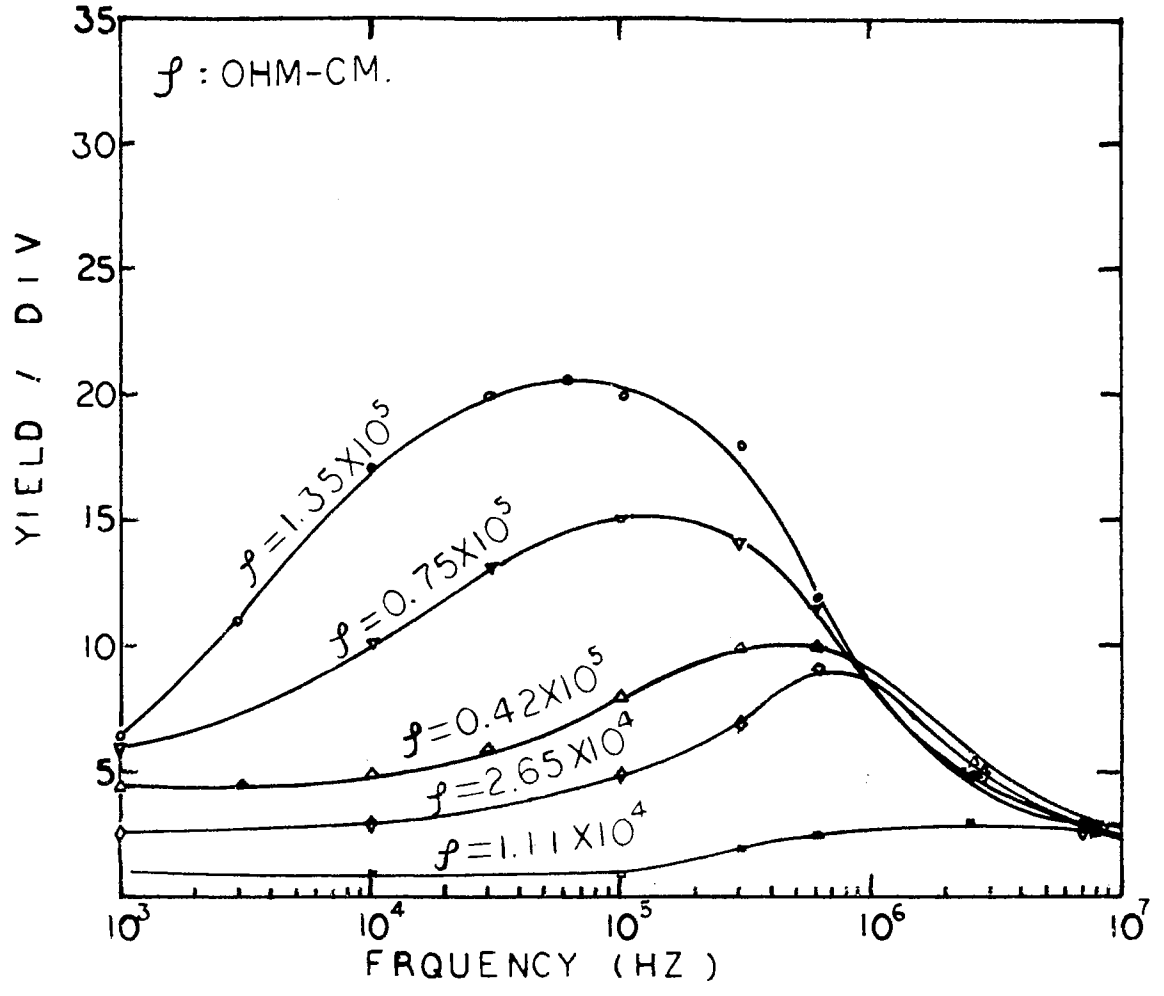

Figure 24. Yield Spectra of Pseudomona aeruginosa 1 (15-hr-old cultures). w-w: 0.025 - 0.586 mm, O.D. = 0.03, 24 Volts - 2 min, 210x

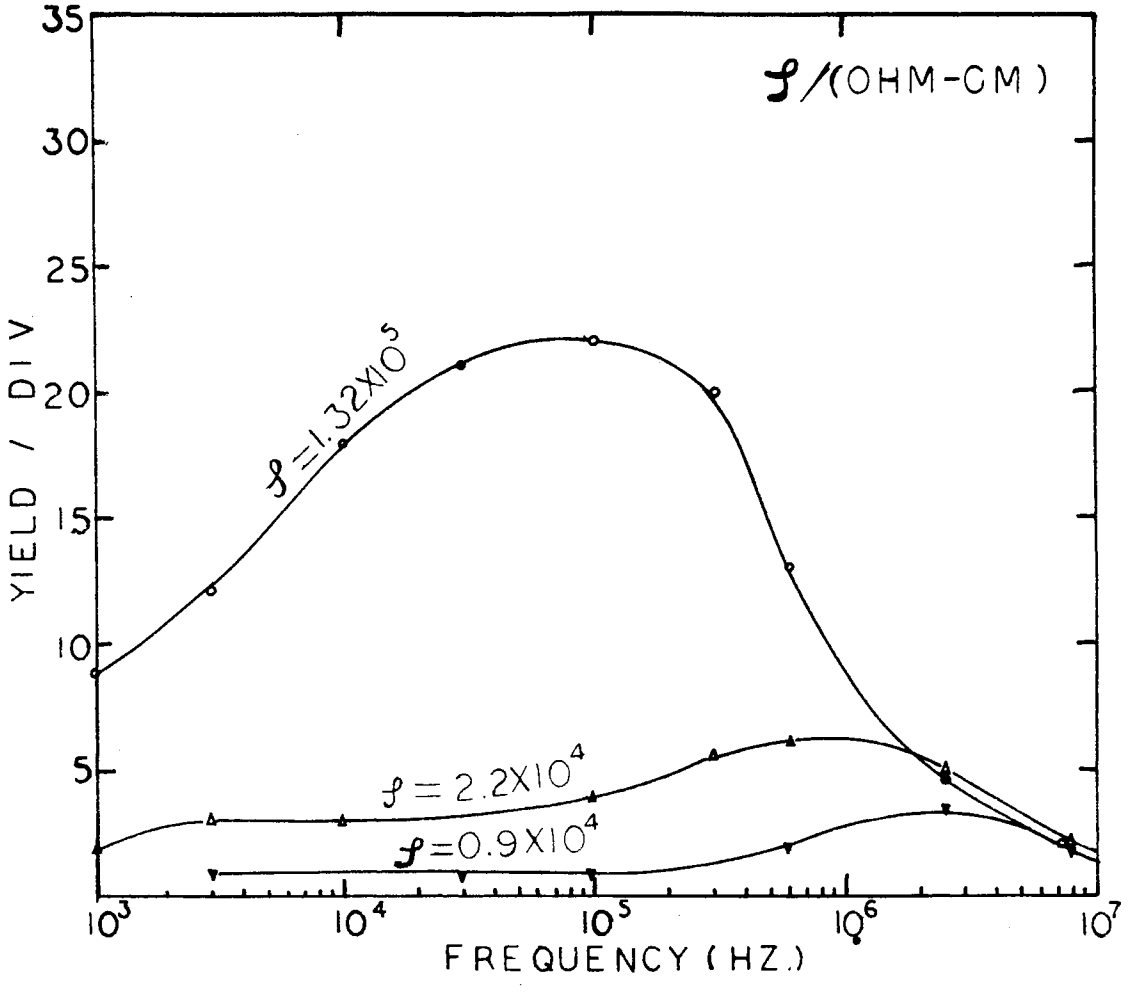

Figure 25. Yield Spectra of Pseudomona aeruginosa 1 (30-hr-old Cultures). w-w: 0.025 - 0.586 mm, 24 Volts, O.D. = 0.05, 210x

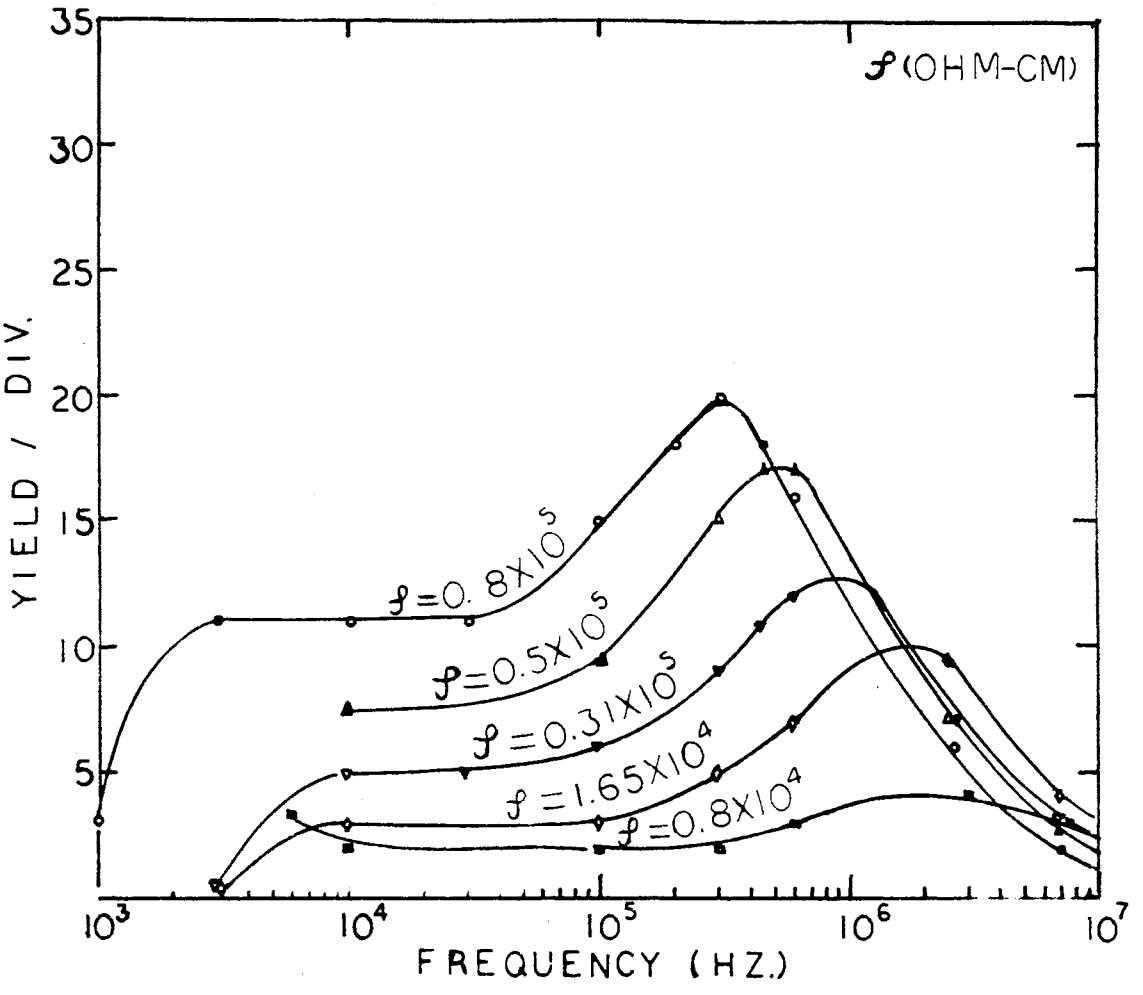

Figure 26. Yield Spectra of PAl Debris With Different Resistivity. w-w: 0.025 - 0.586 mm, 24 Volts, Collected in 2 Min, O.D. = 0.09, 420x

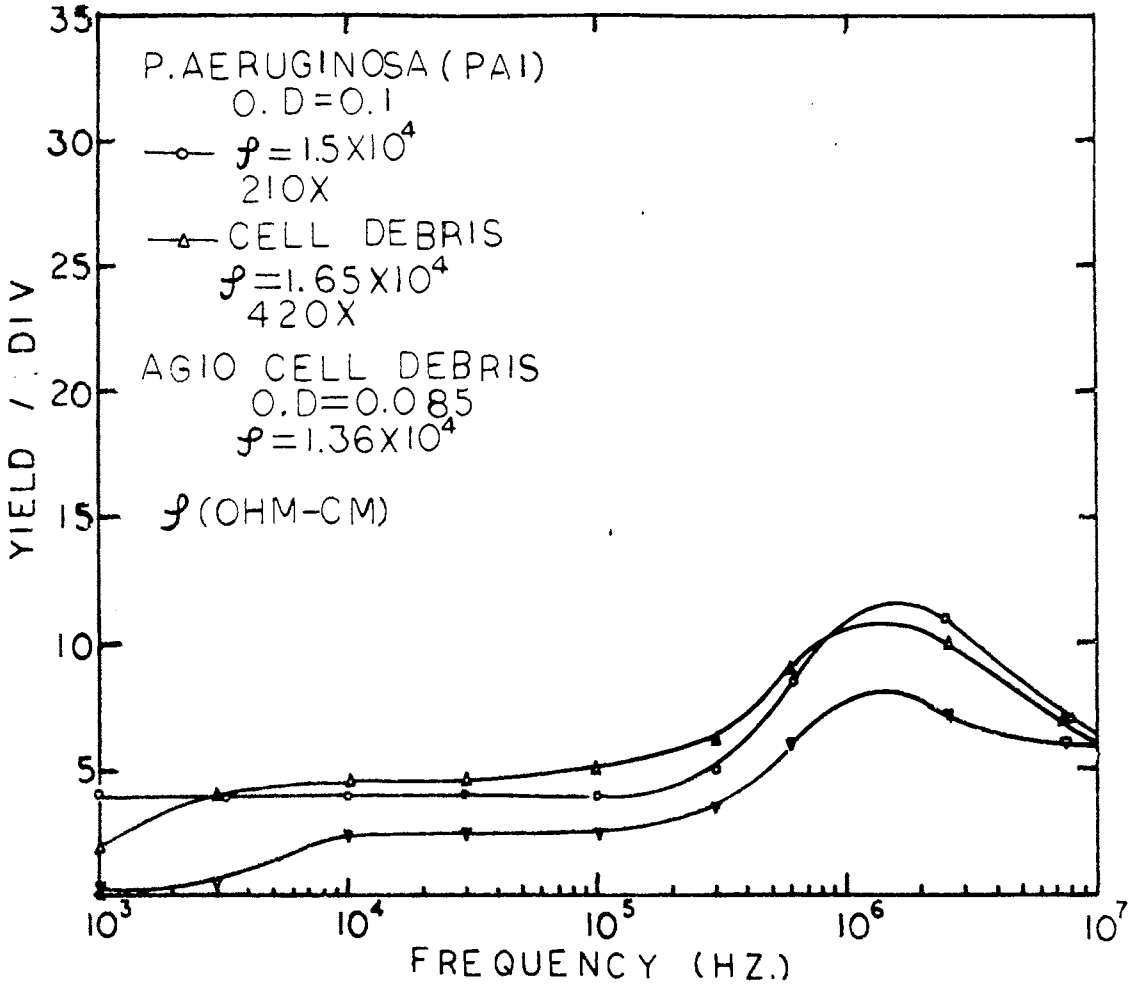

Figure 27. Yield Spectra of PAl and Cell Debris. w-w: 0.025 - 0.586 mm, 24 Volts, O.D. = 0.1, 420x

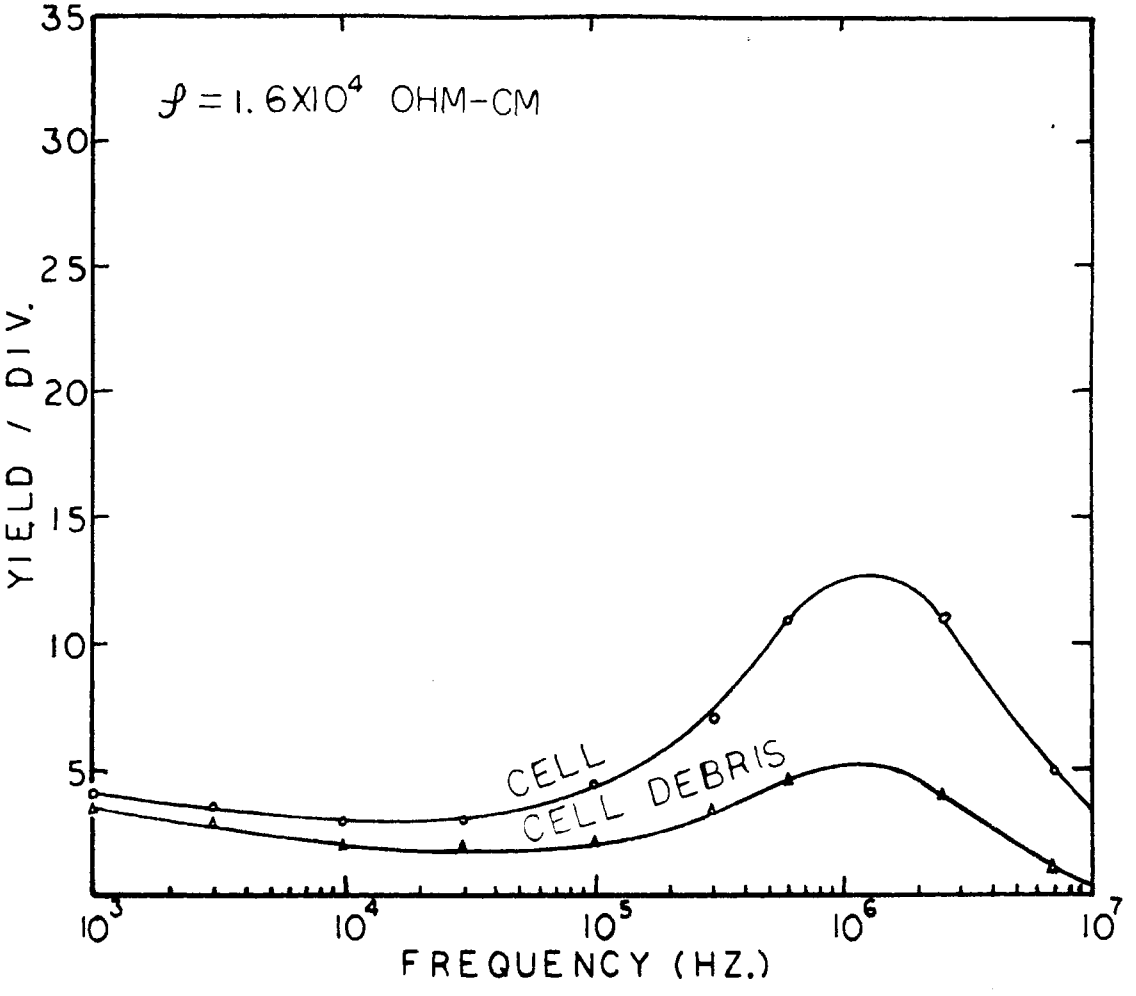

Figure 28. Yield Spectra of Cg 1 and Cell Debris. w-w: 0.025 - 0.586 mm, 24 Volts, O.D. = 0.08, 210x

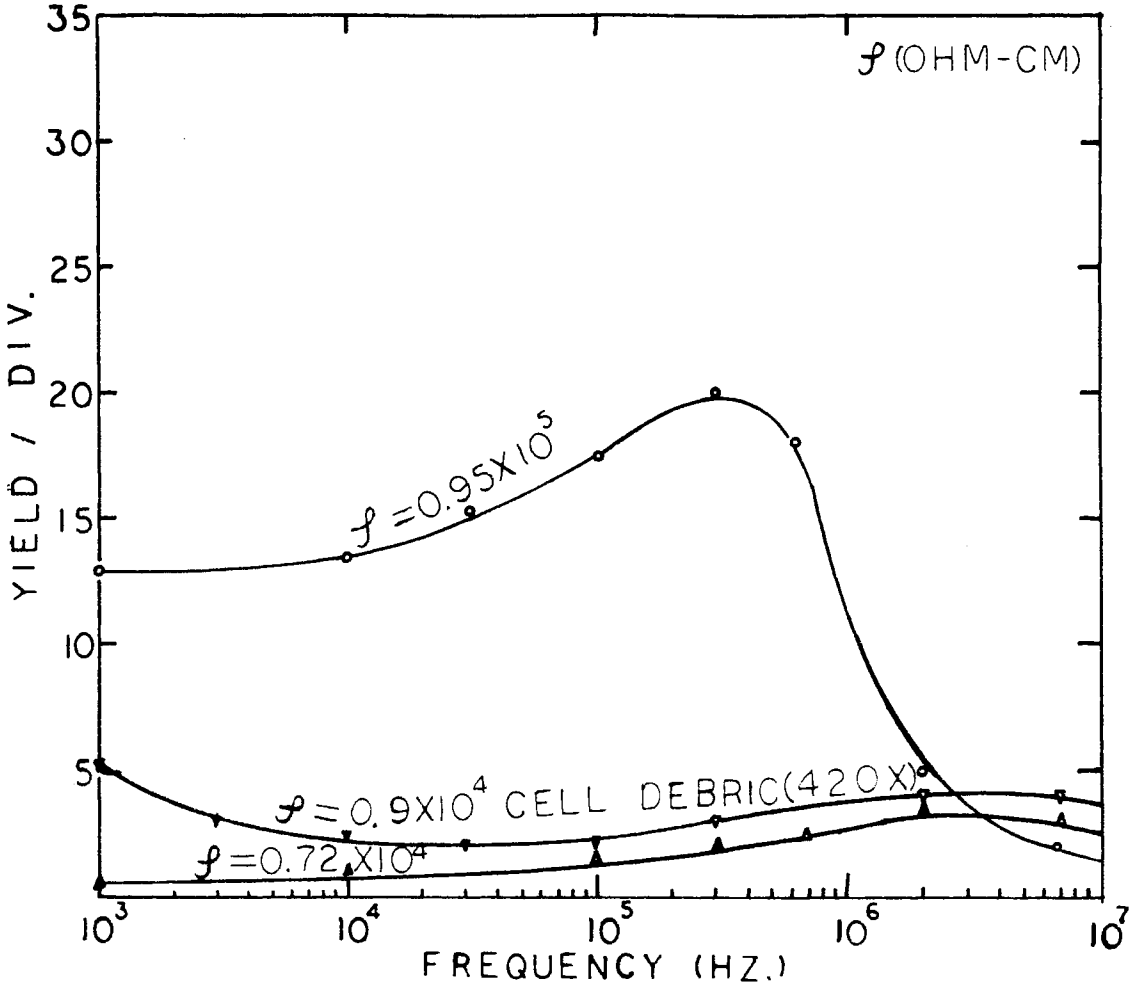

Figure 29. Yield Spectra of Cg 2 (Yeast Extract + Glycerol Medium) and Cell Debris. w-w: 0.025 - 0.586 mm, O.D. = 0.0125, 210x

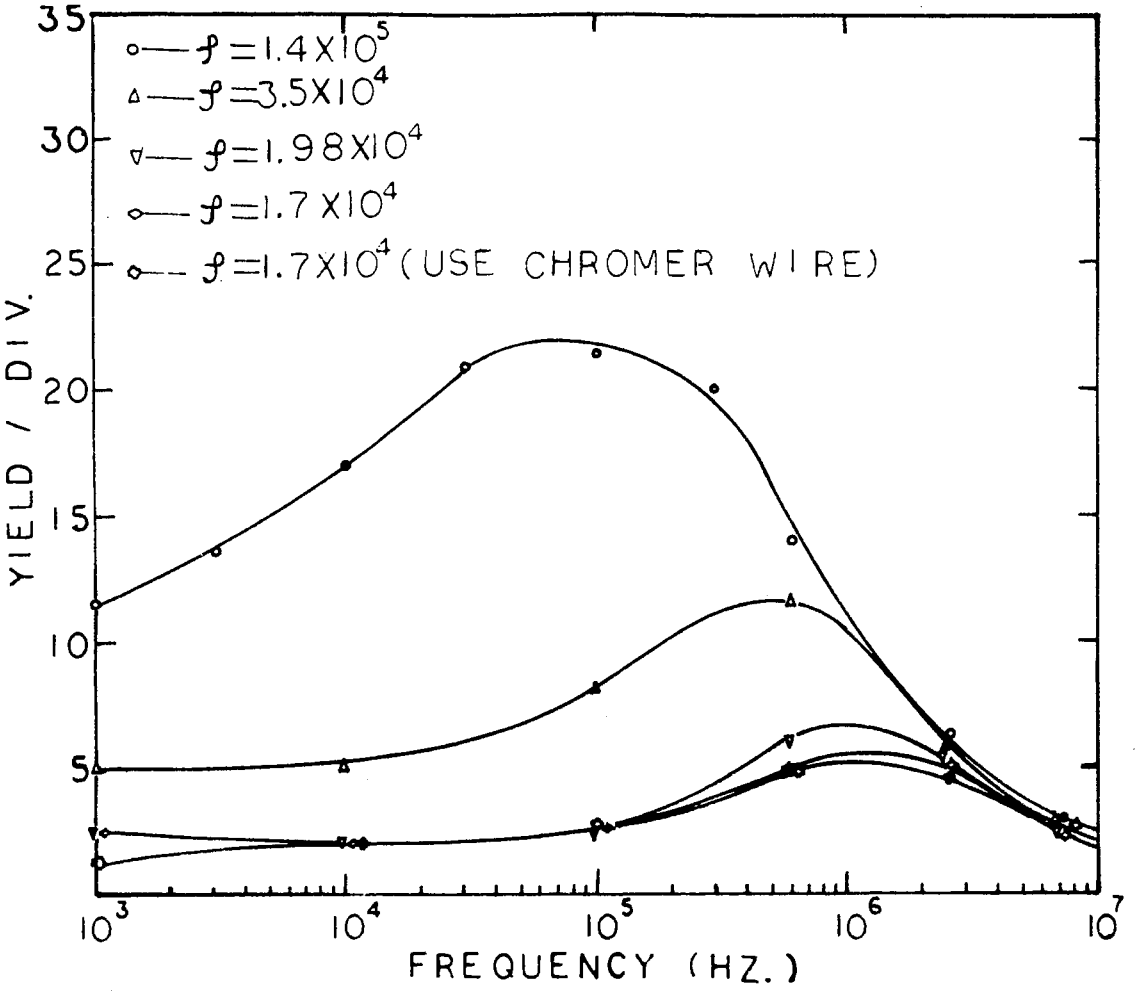

Figure 30. Yield Spectra of Pseudomona aeruginosa - Cg 1 (11-hr-old Cultures). w-w: 0.025 - 1.06 mm, O.D. = 0.02, 210x, 24 Volts

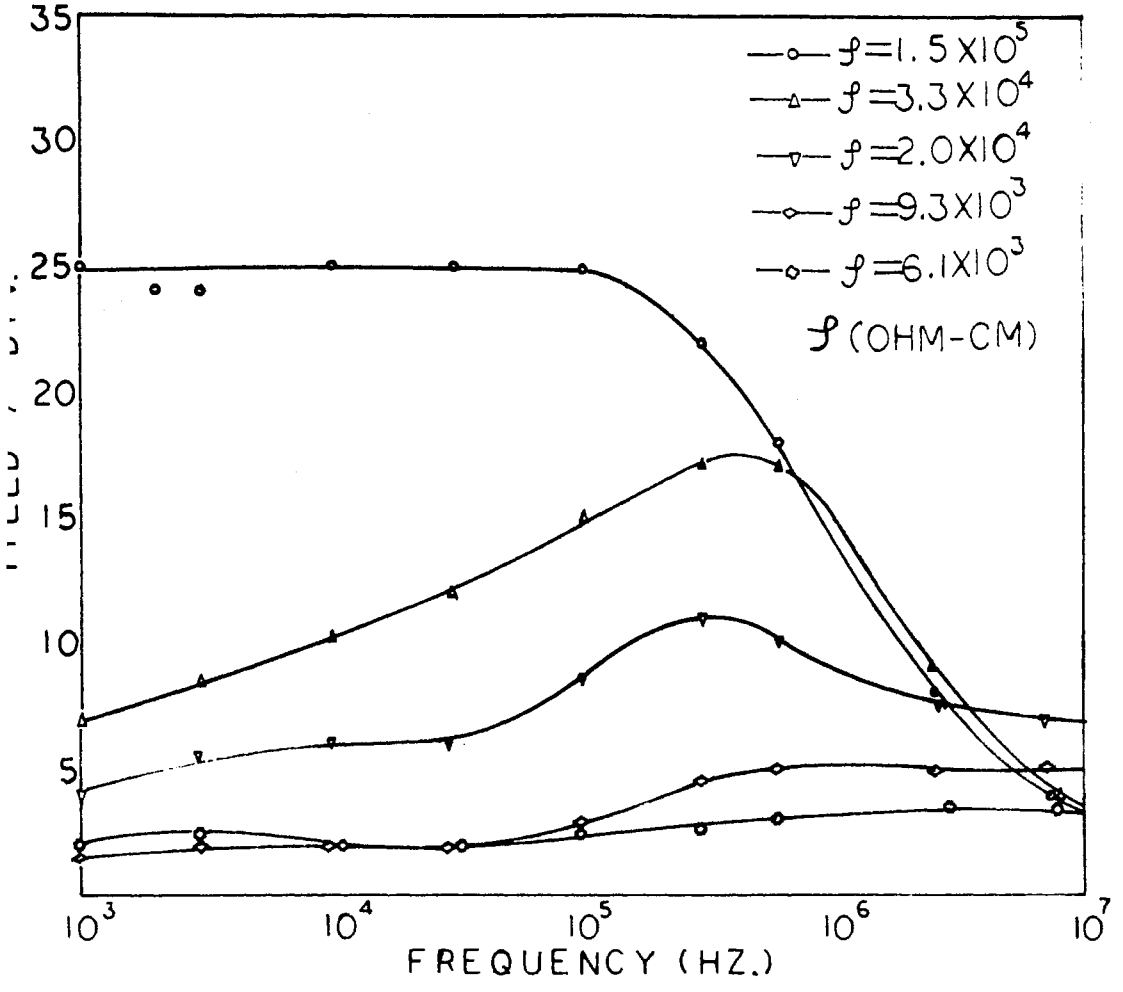

Figure 31. Variation of Yield Spectra of E. coli (12-hr-old Culture) With Resistivity. w-w: 0.025 - 0.586 mm, 24 Volts, 210x

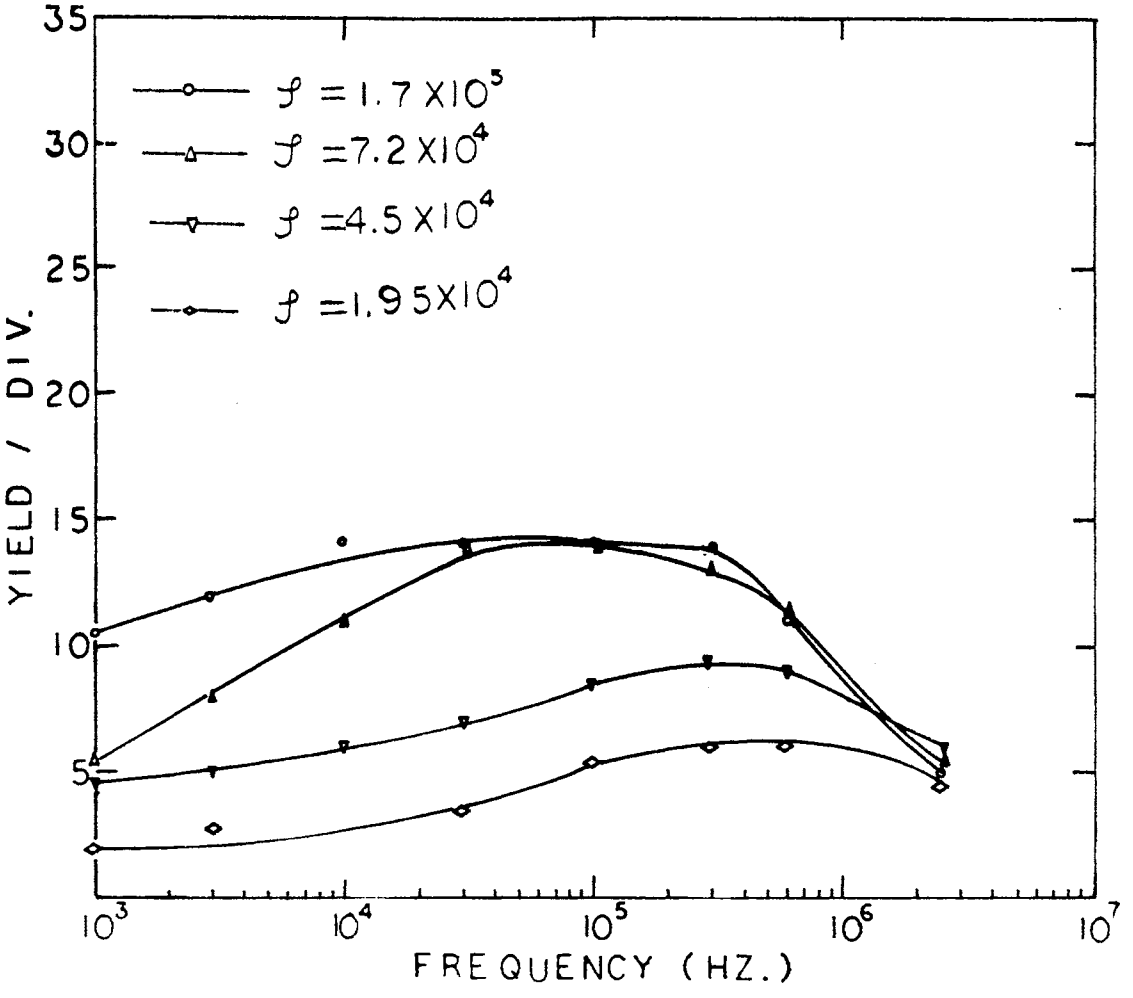

Figure 32. Variation of Yield Spectra of E. coli With Resistivity (15-hr-old Culture). w-w: 0.025 - 0.586 mm, 210x, O.D. = 0.05, 15 Volts

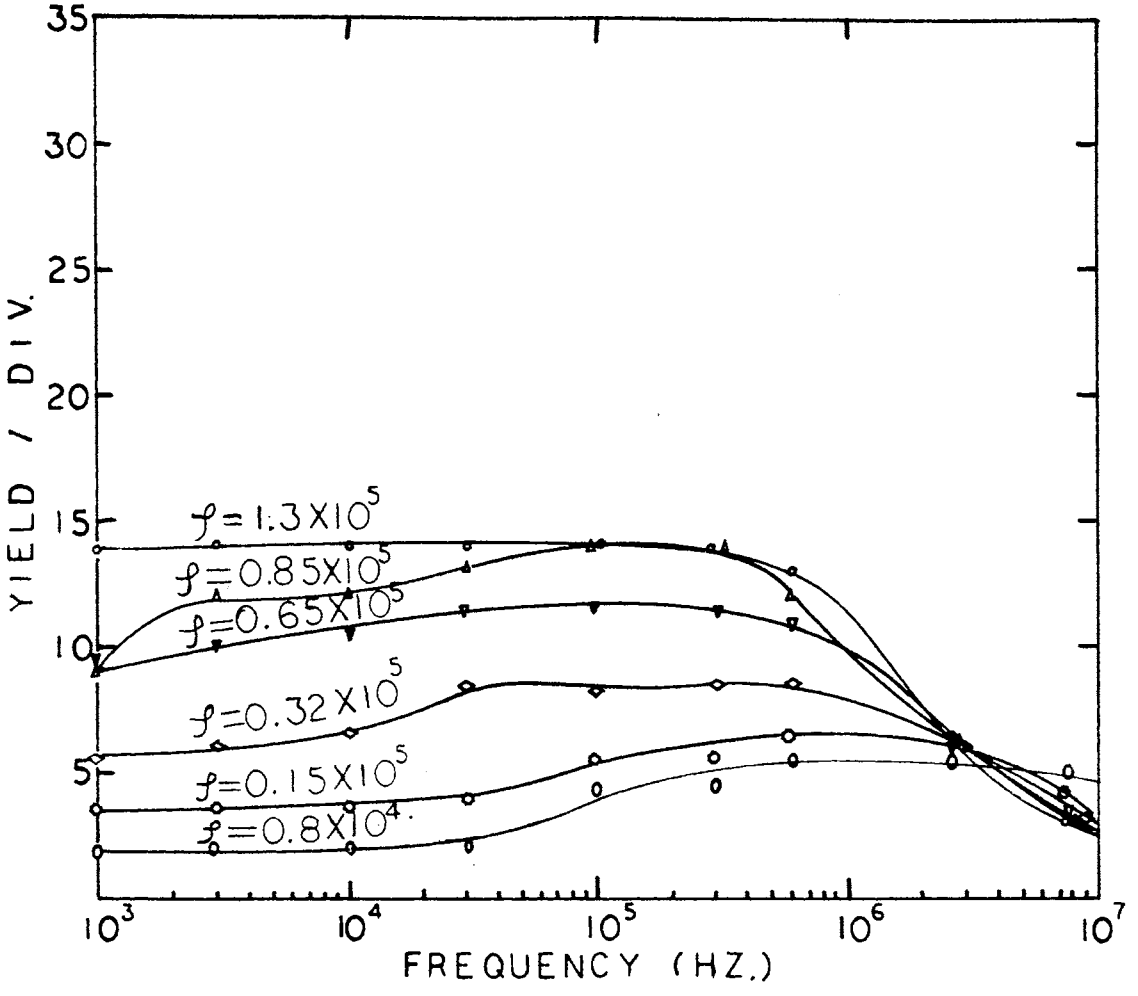

Figure 33. Variation of Yield Spectra of E. coli With Resistivity (24-hr-old Culture). w-w: 0.025 - 1.06 mm, 24 Volts, O.D. = 0.09 210x

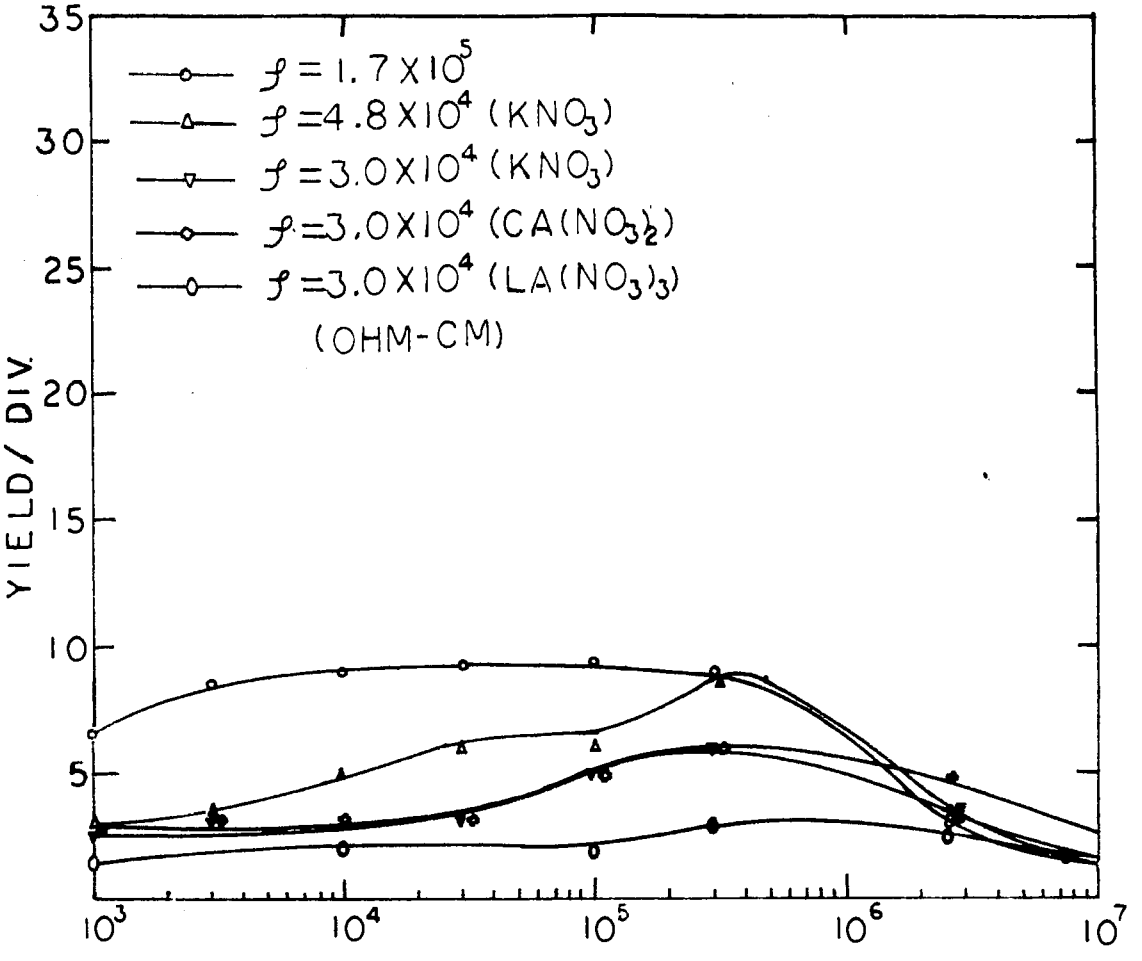

Figure 34. Variation of Yield Spectra of E. coli With Resistivity (69-hr-old Culture). w-w: 0.025 - 0.9 mm, 210x, 24 Volts, O.D. = 0.04

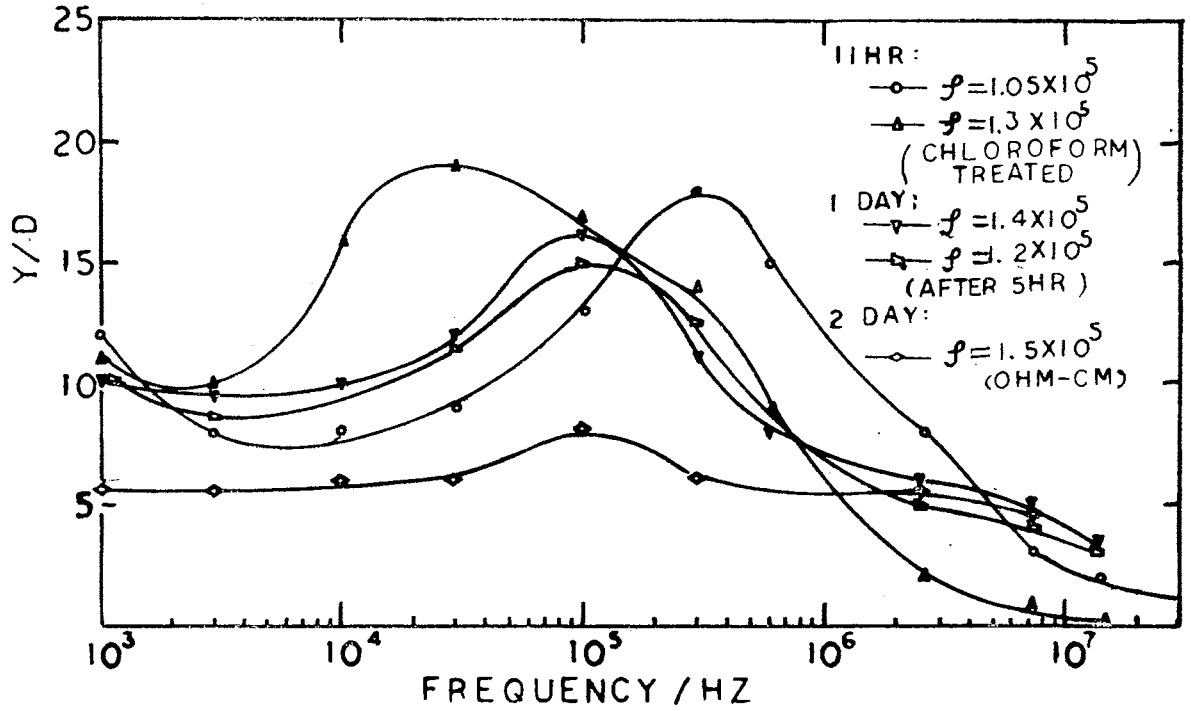

Figure 35. Yield Spectra of Bacillus cereus. w-w: 0.025 - 0.4 mm, 24 Volts, 210x, O.D. = 0.05

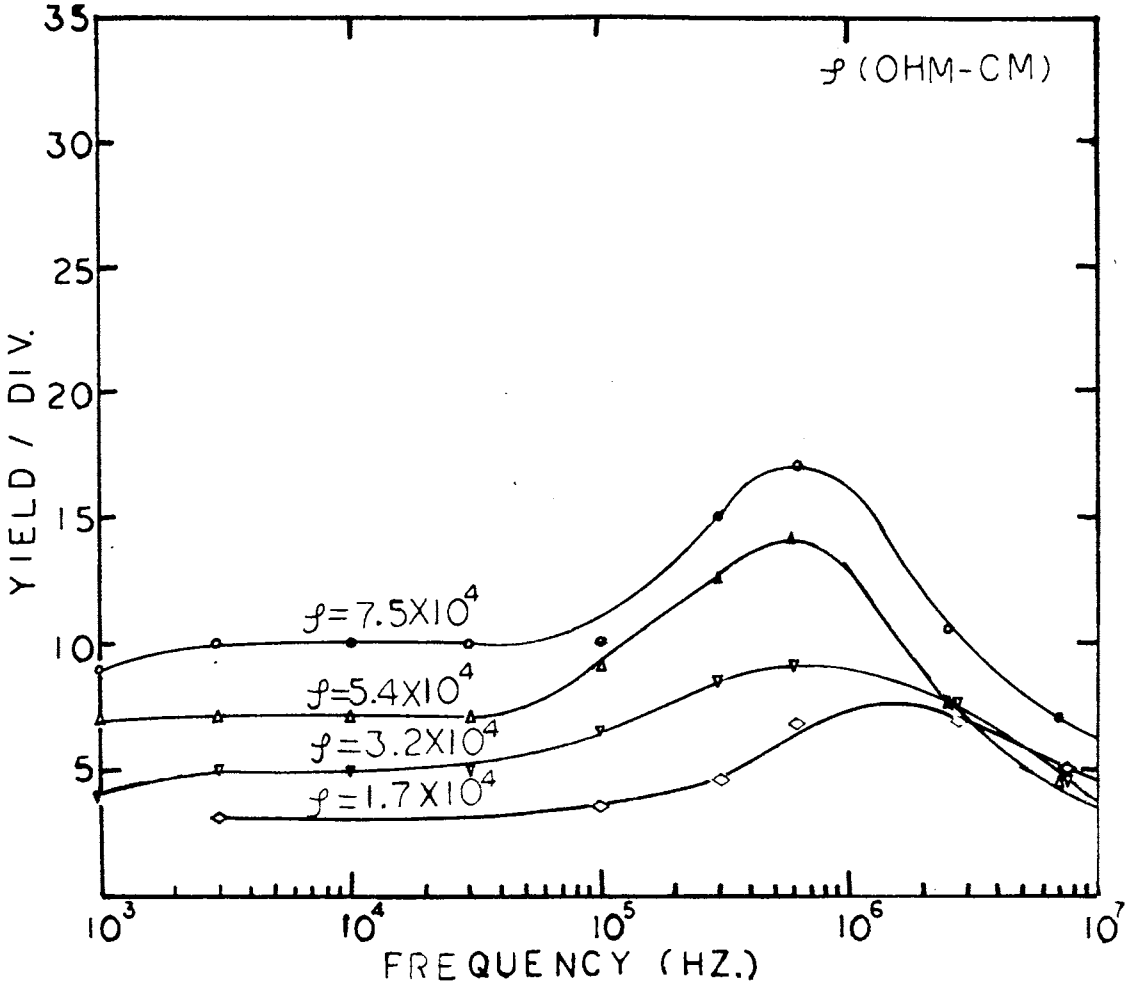

Figure 36. Variation of Yield Spectra of B. cereus With Resistivity (10-hr-old Culture). w-w: 0.025 - 1.06 mm, O.D. = 0.05, 24 Volts, 210x

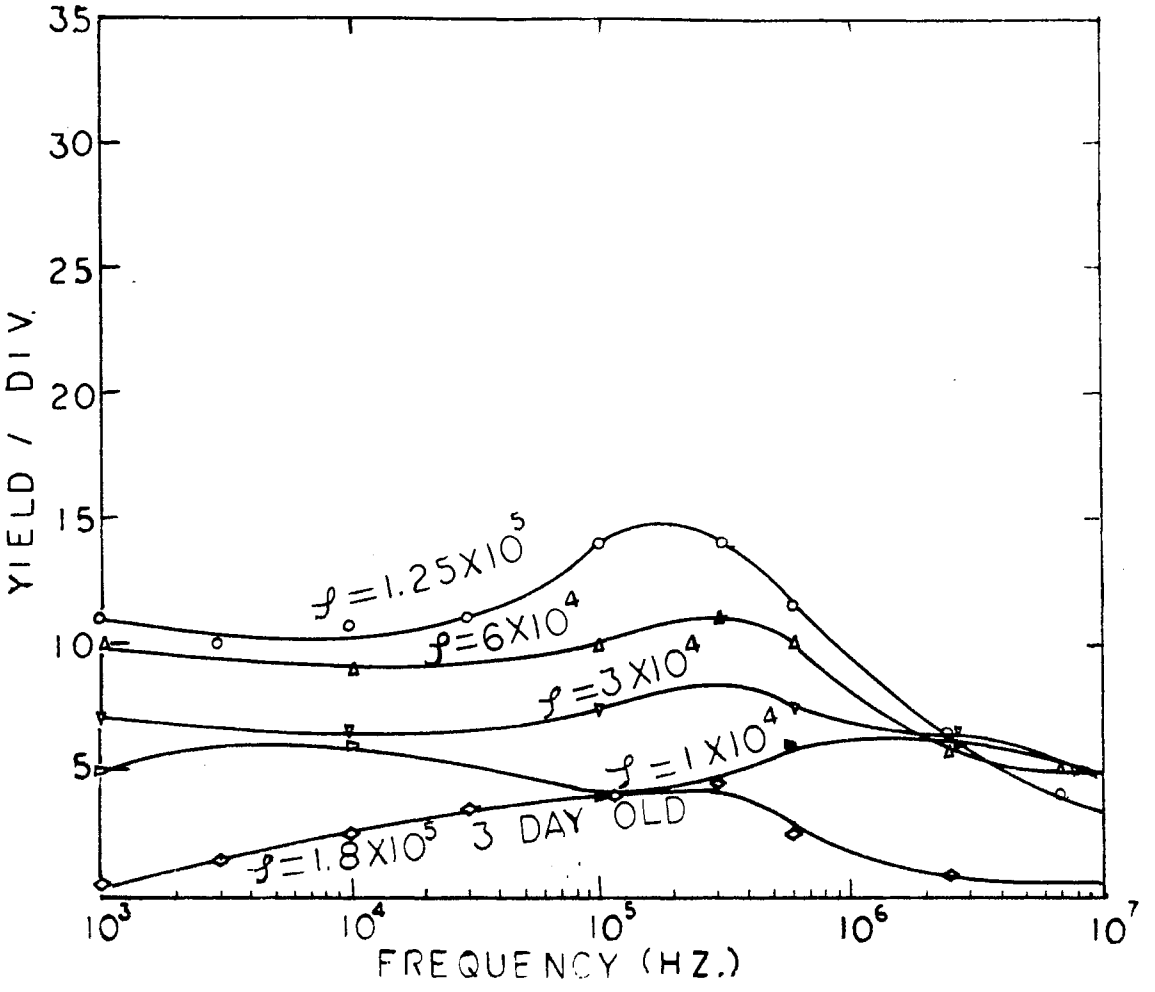

Figure 37. Variation of Yield Spectra of B. cereus With Resistivity (24-hr-old Culture). w-w: 0.025 - 0.586 mm, 210x, O.D. = 0.05, 24 Volts

on; that is, the cells are parallel to the electric field or perpendicular to the wire electrode. At high frequency (> 2.55 MHz), the B. cereus, coming by sideways, has been observed. Collected cells may by made alternately to stand up and lie down as the frequency is switched low and high. This might affect the yield spectrum quantitatively.

(4) Bacillus megaterium (1.2 to 1.5 by 2.0 to 4.0μ)--Figure 38 shows the yield spectra of B. megaterium of different ages.

Yeasts

Figure 39 illustrates the dependence of the concentration on yield spectra. For frequencies from 30 K to 2.55 MHz, the effects are large as compared with another frequency's range. Yeasts that were treated with chloroform or ethyl alcohol are quite different from the norm. This difference can be seen on Figures 40 and 41. After keeping the cells on 61° to 63°C for 10 minutes, half the suspension was stained by congo red (5% in distill water) for 1 hour. Both parts (stained and non-stained) were washed six times. Spectra of both parts are shown in Figures 42 to 48 illustrate the single-cell nonuniform field effect. The dielectrophoretic force is balanced by gravity. V_m is the critical voltage; at this voltage the cell would stay on the electrode. If we lower the voltage the cell would move away by gravitational force. The blank on lower frequency means the cell either moves away or moves aside; no balance could be made in this case.

Zymosan

Figure 49 shown the yield spectra of Zymosan and its effect by the chloroform or Ethyl Alcohol. The variation with resistivity (change by

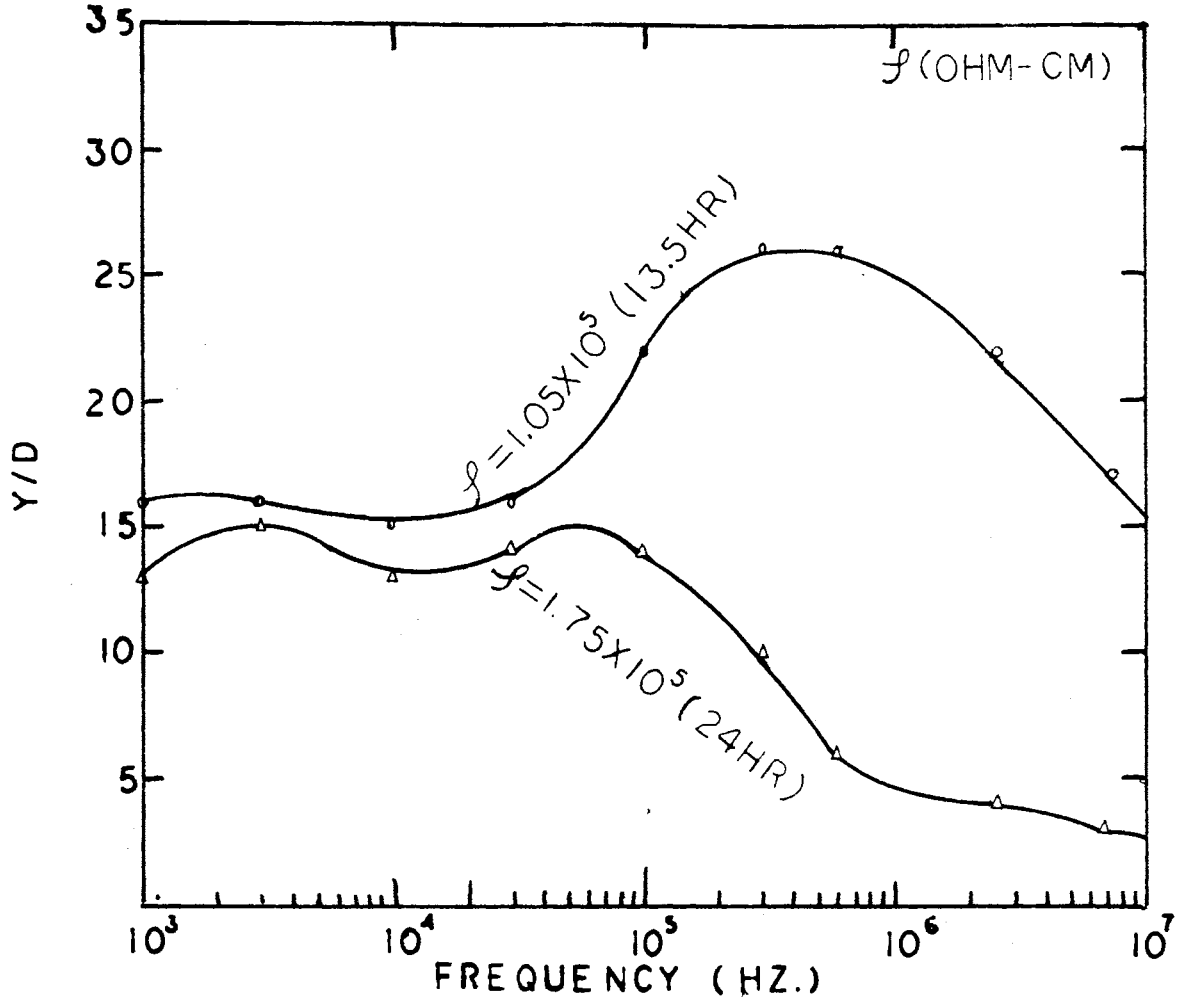

Figure 38. Yield Spectra of B. megaterium. w-w: 0.025 - 0.586 mm, 24 Volts, 210x, O.D. = 0.035

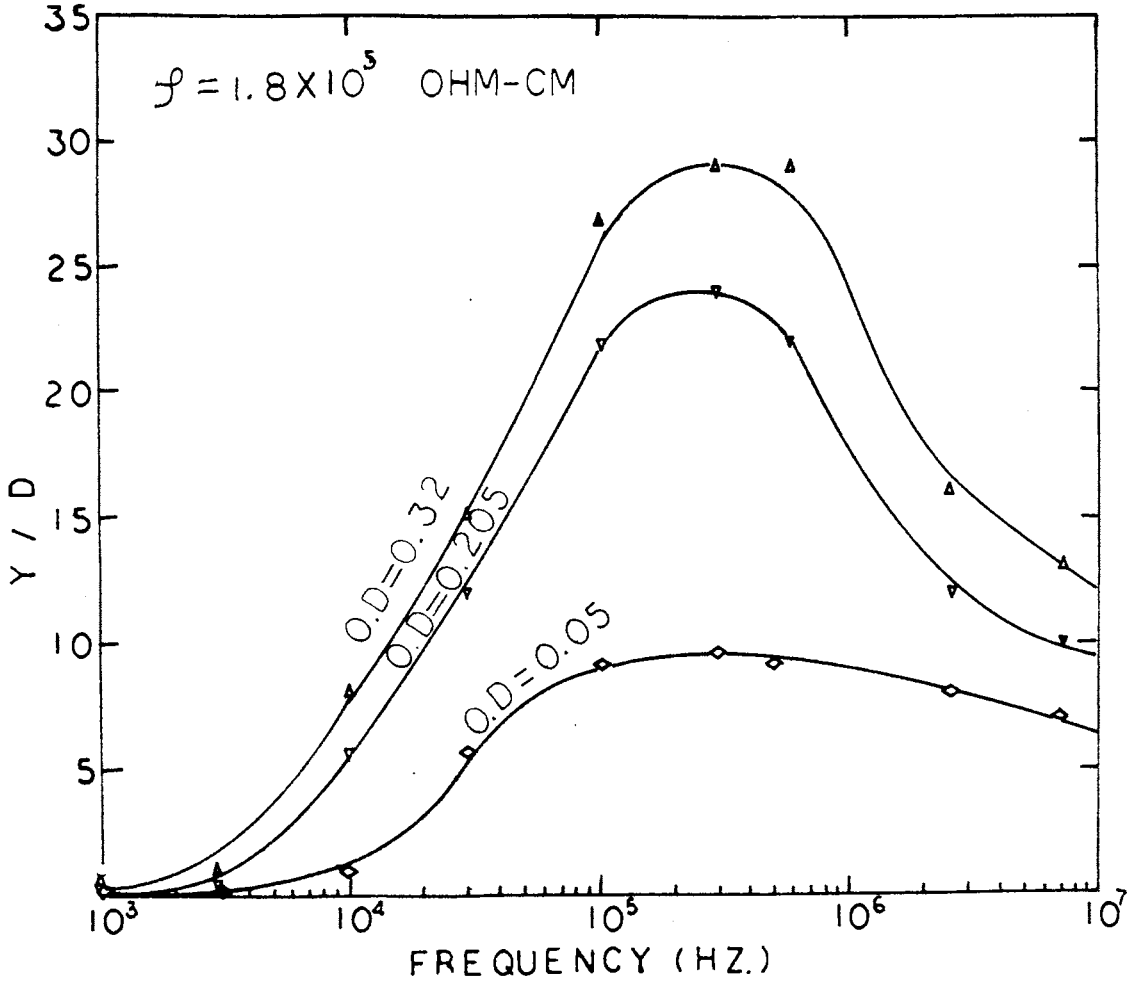

Figure 39. Concentration Dependence on Yield Spectra of Yeasts (18-hr-old Culture). w-w: 0.025 - 1.06 mm, 210x, 24 Volts

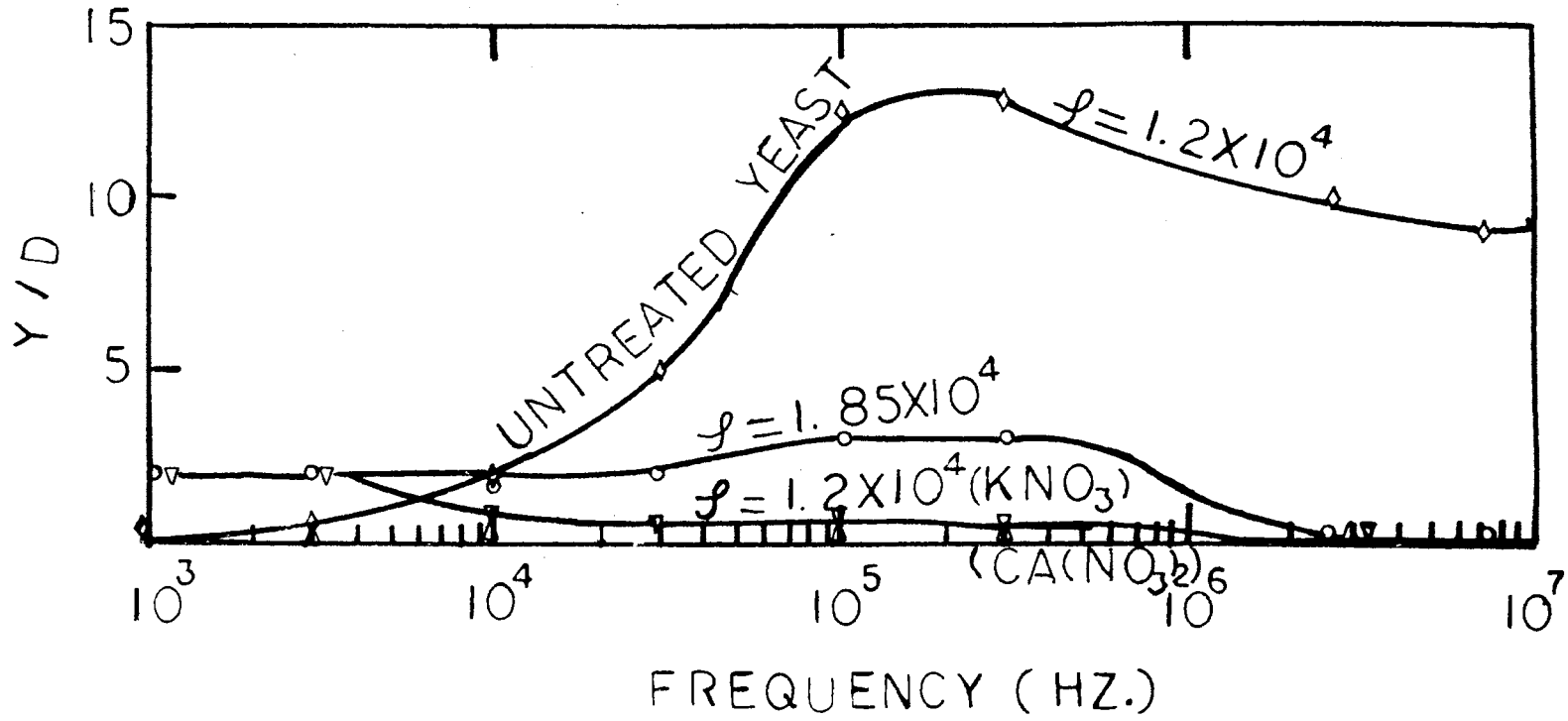

Figure 40. Yield Spectra of Yeasts After Treated With Chloroform (One Week Old Culture). O.D. = 0.05, 210x, 24 Volts, w-w: 0.025 - 0.46 mm

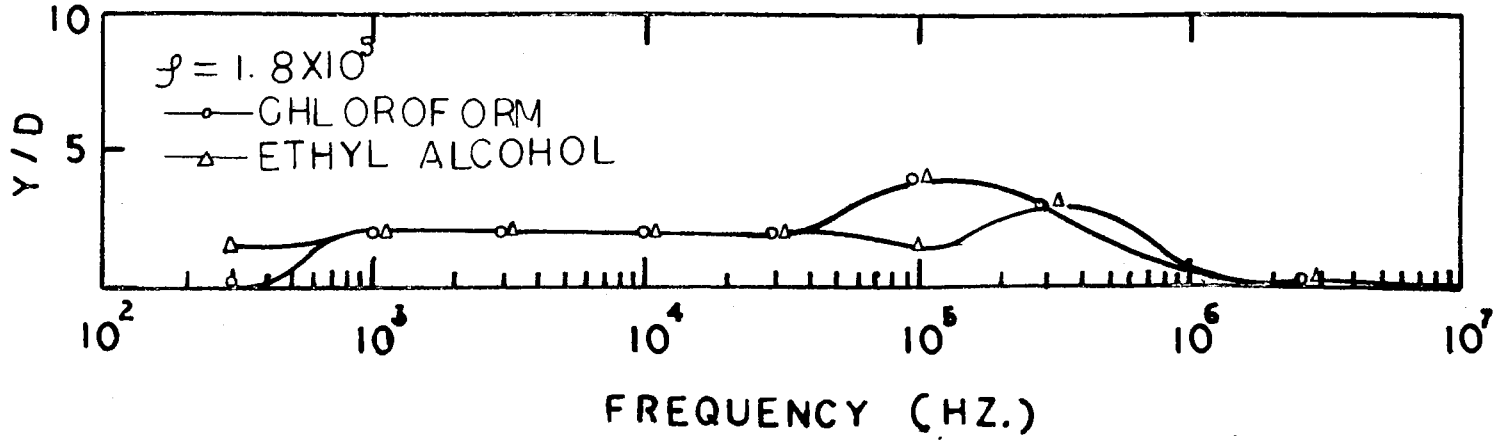

Figure 41. Yield Spectra of Yeasts After Treated With Chloroform (10 Min.) and Ethyl Alcohol (5 Min). w-w: 0.025 - 0.9 mm, O.D. = 0.1, 24 Volts, 210x

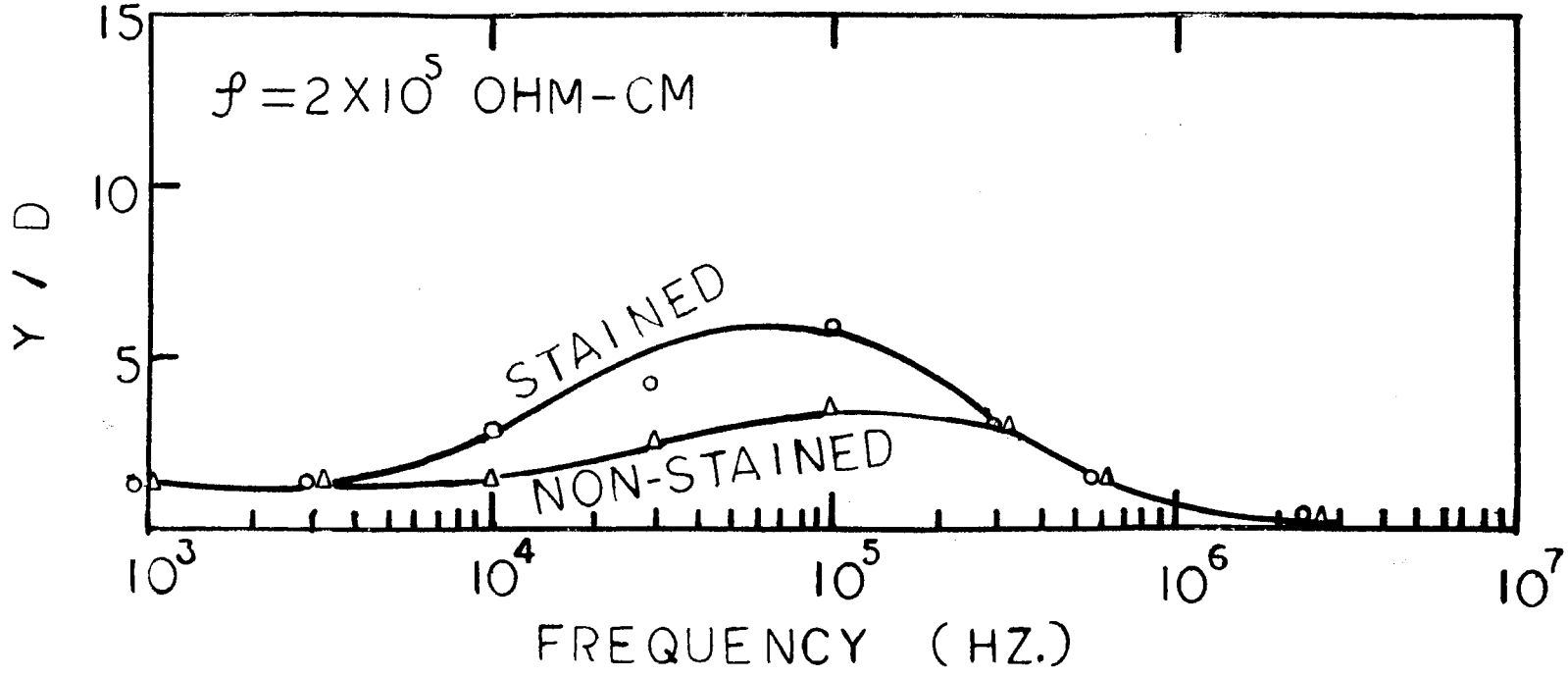

Figure 42. Yield Spectra of Yeasts With Congo-Red Stained. w-w: 0.025 - 0.586 mm, 24 Volts, 210x, O.D. = 0.1

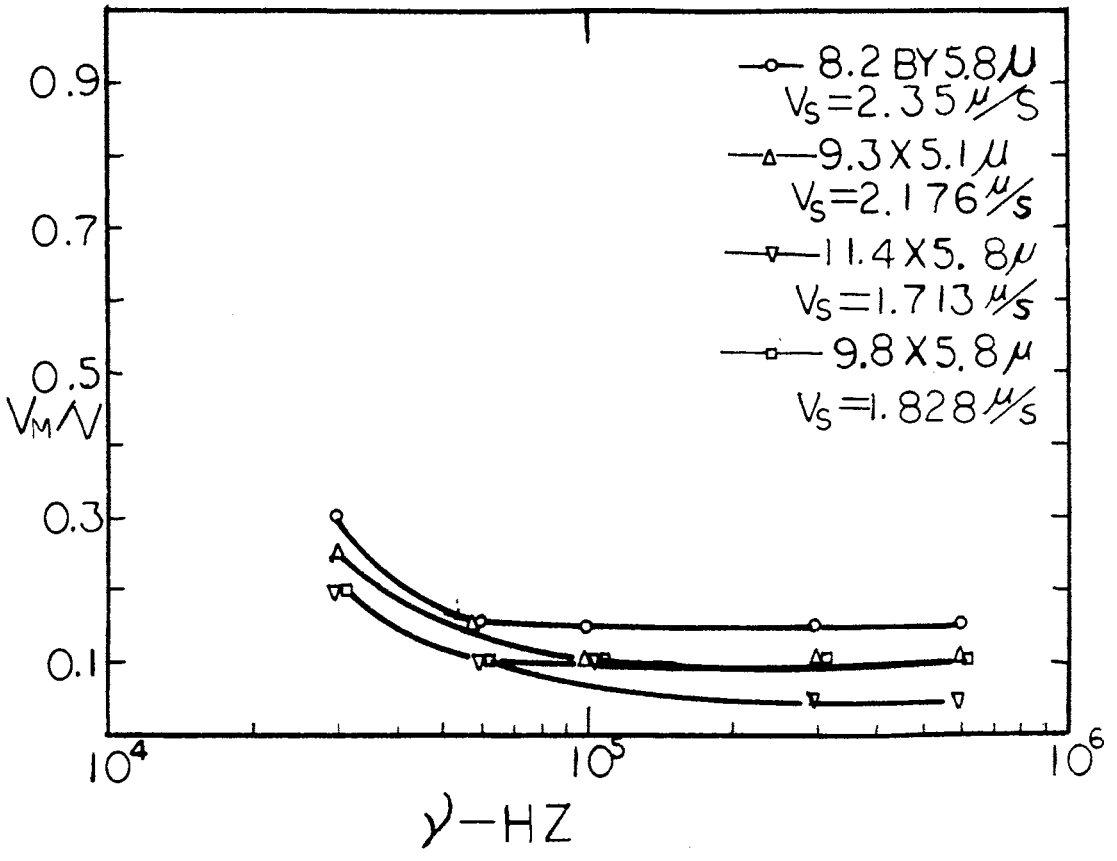

Figure 43. Single Cell Nonuniform Field Effects. w-w: 0.025 - 0.4 mm, 430x. $\rho = 1.5 \times 10^5$ ohm-cm (36.5-hr-old Culture)

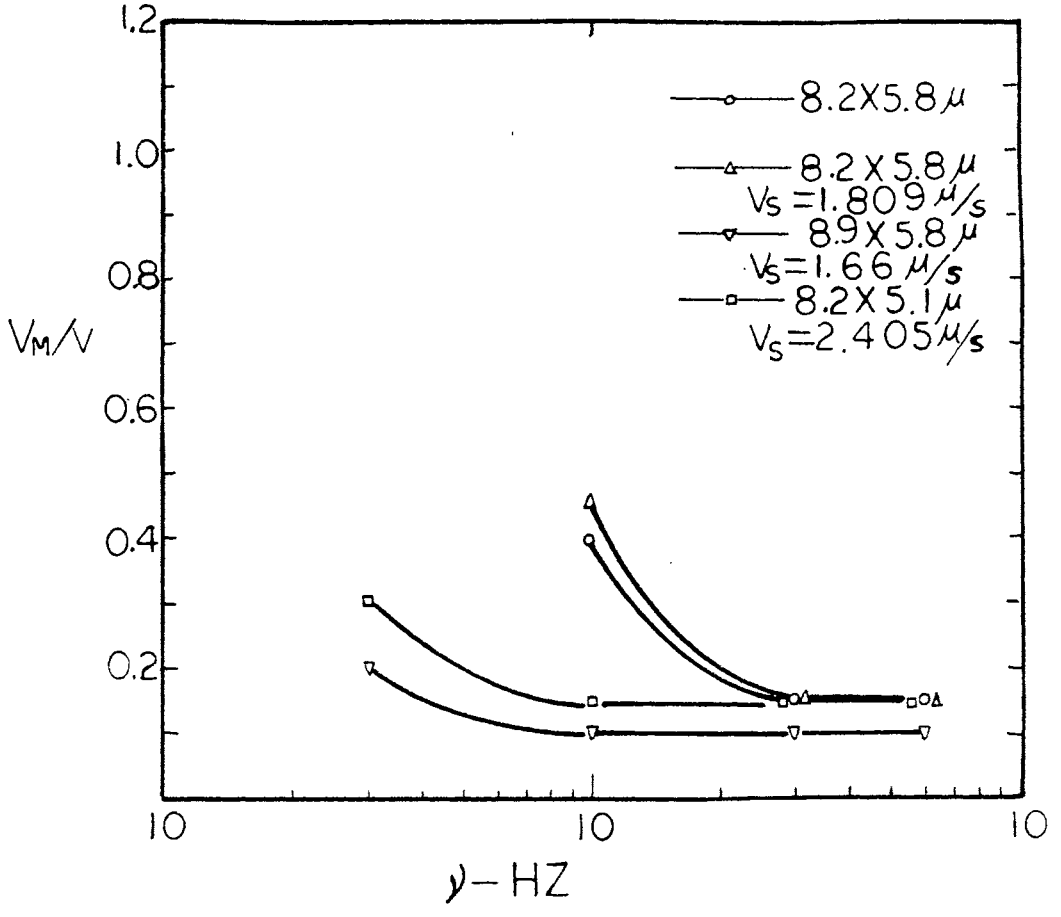

Figure 44. Single Cell Nonuniform Field Effect. w-w: 0.025 - 0.4 mm, 2.56×10^6 Cells/Ml., 430x (2 Days Old Culture)

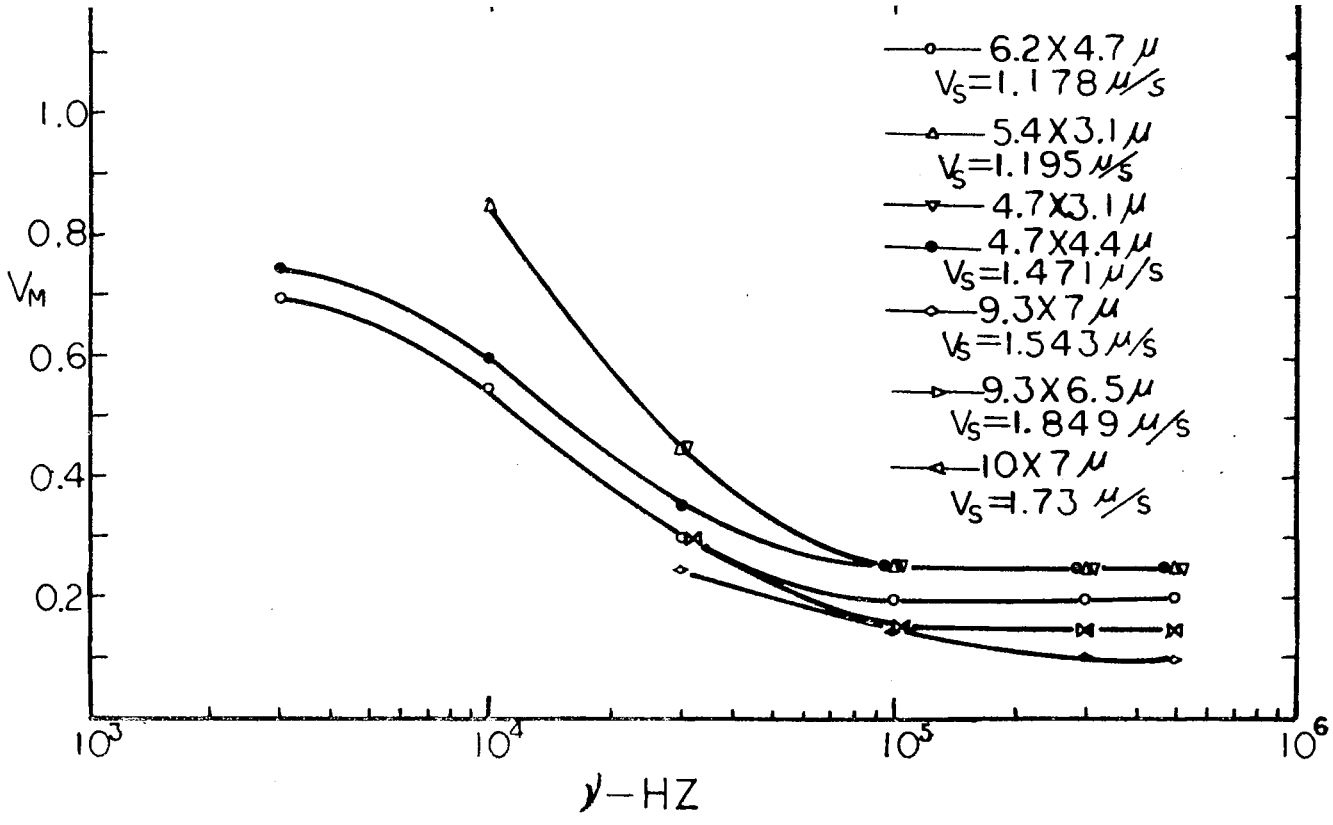

Figure 45. Single Cell Nonuniform Field Effect. w-w: 0.025 - 0.9 mm (2 Days and 6 Hr. Old Culture)

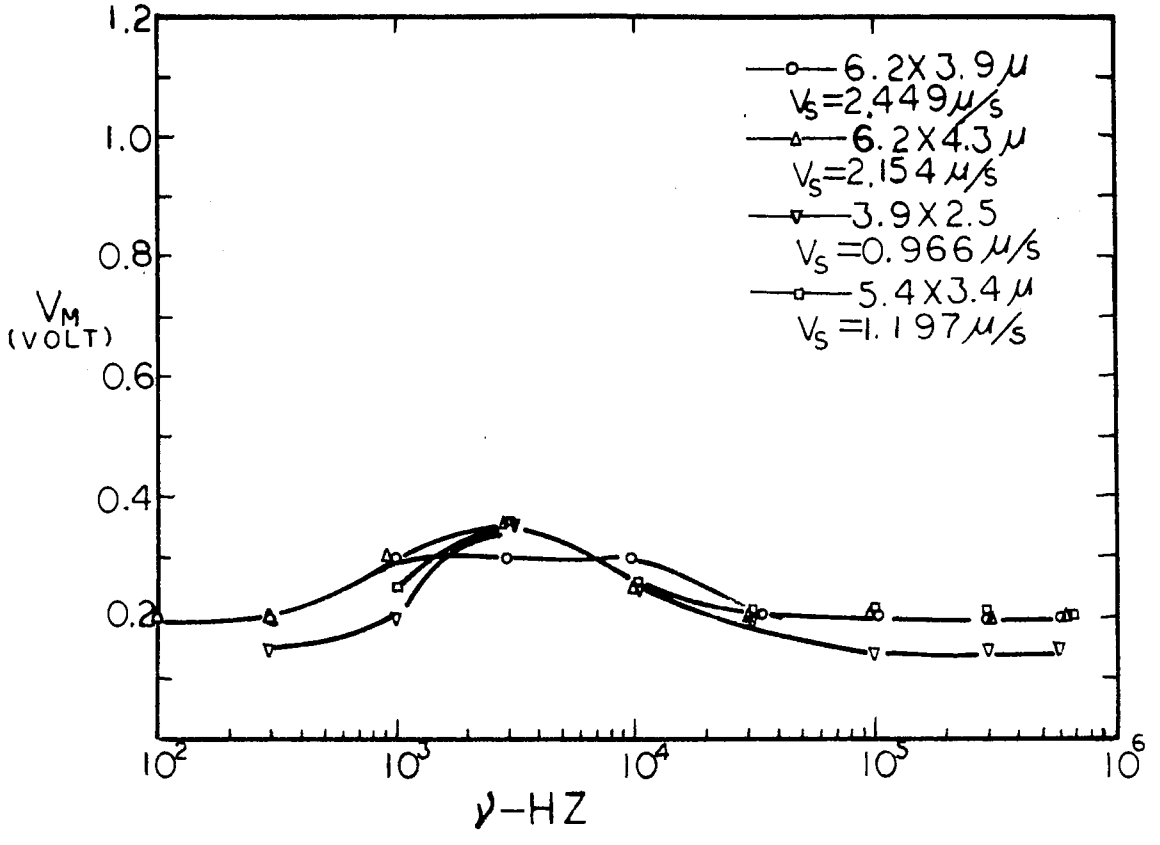

Figure 46. Single Cell Nonuniform Field Effect. w-w: 0.025 - 0.9 mm, ρ = 2.9 x 10^5 ohm-cm (5 Days Old Culture)

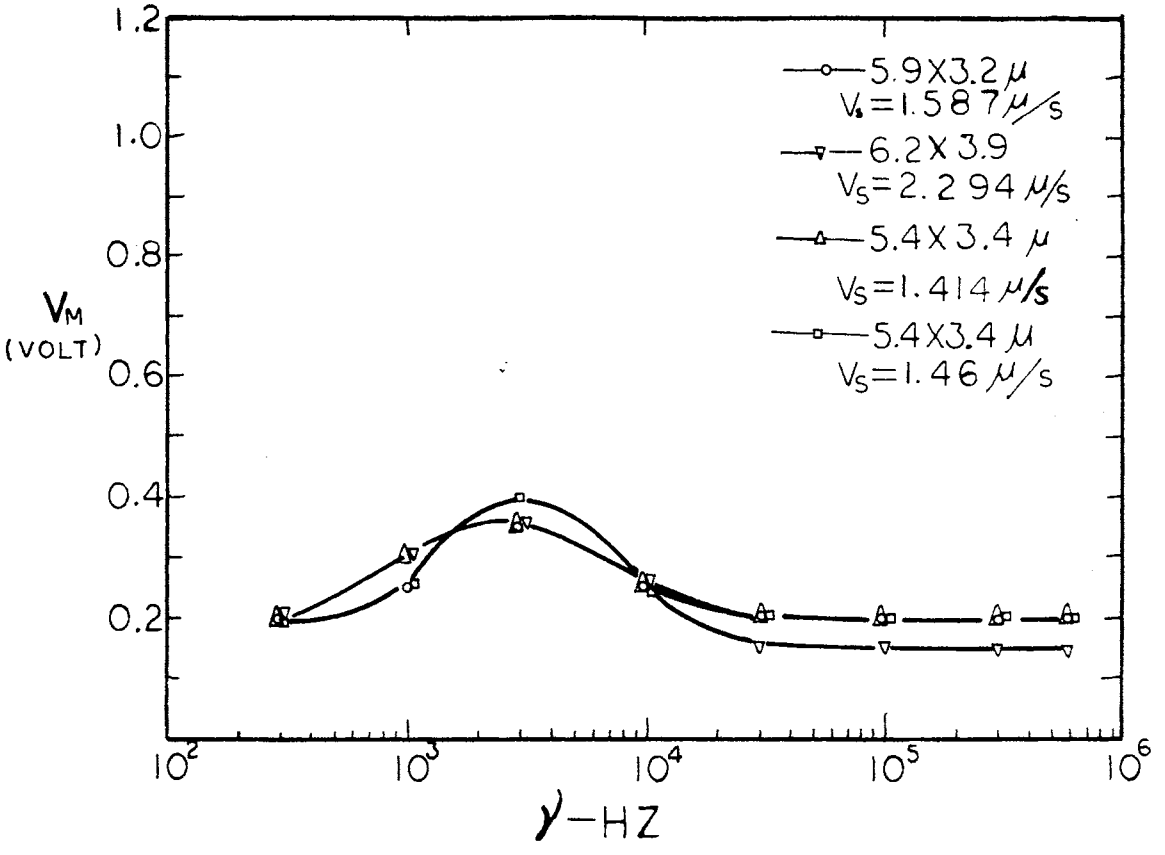

Figure 47. Single Cell Nonuniform Field Effect. w-w: 0.025 - 0.9 mm, ρ = 2.9 x 10^5 Ohm-Cm (5 Days Old Culture)

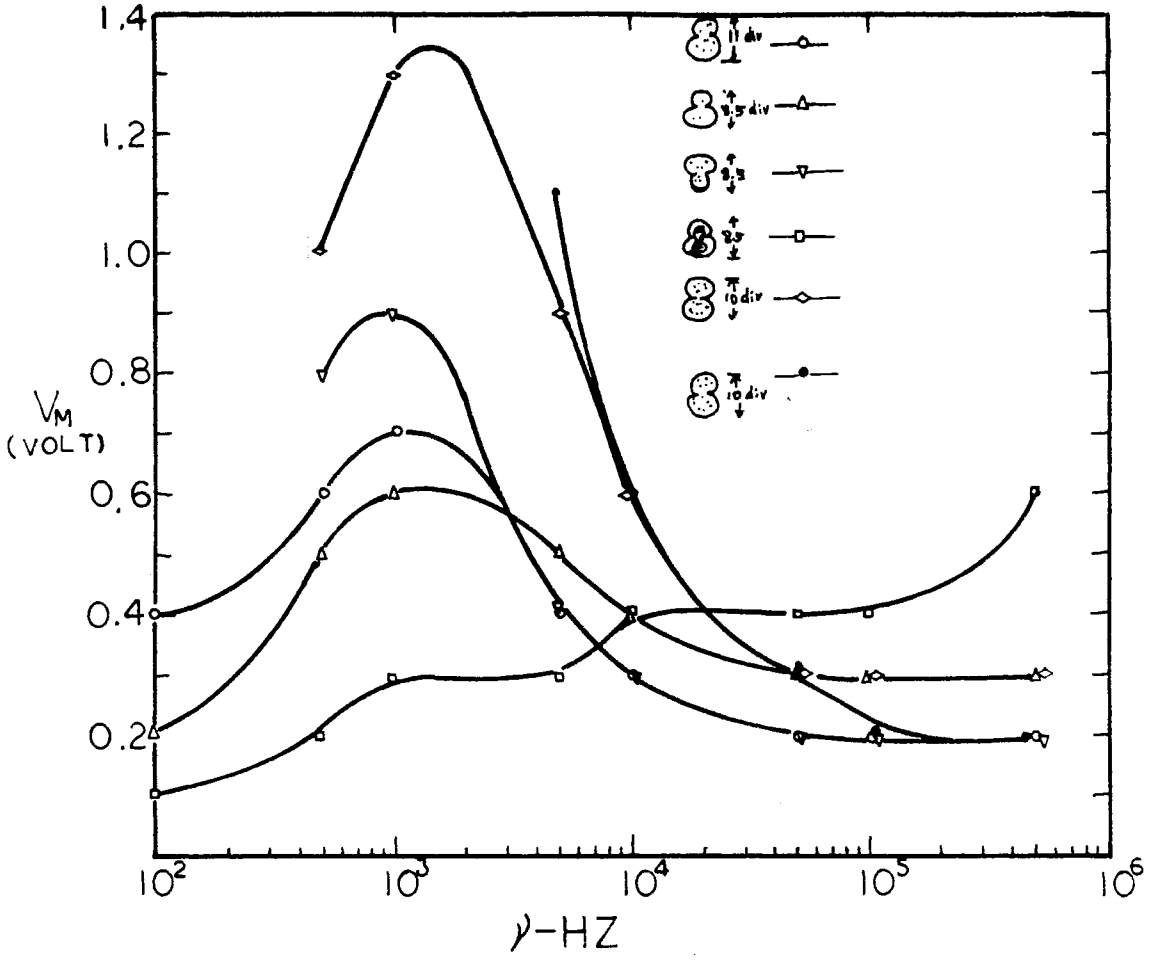

Figure 48. Single Cell Nonuniform Field Effect. w-w: 0.025 - 0.9 mm, ρ = 3.2 x 10^5 Ohm-Cm (10 Days Old Culture)

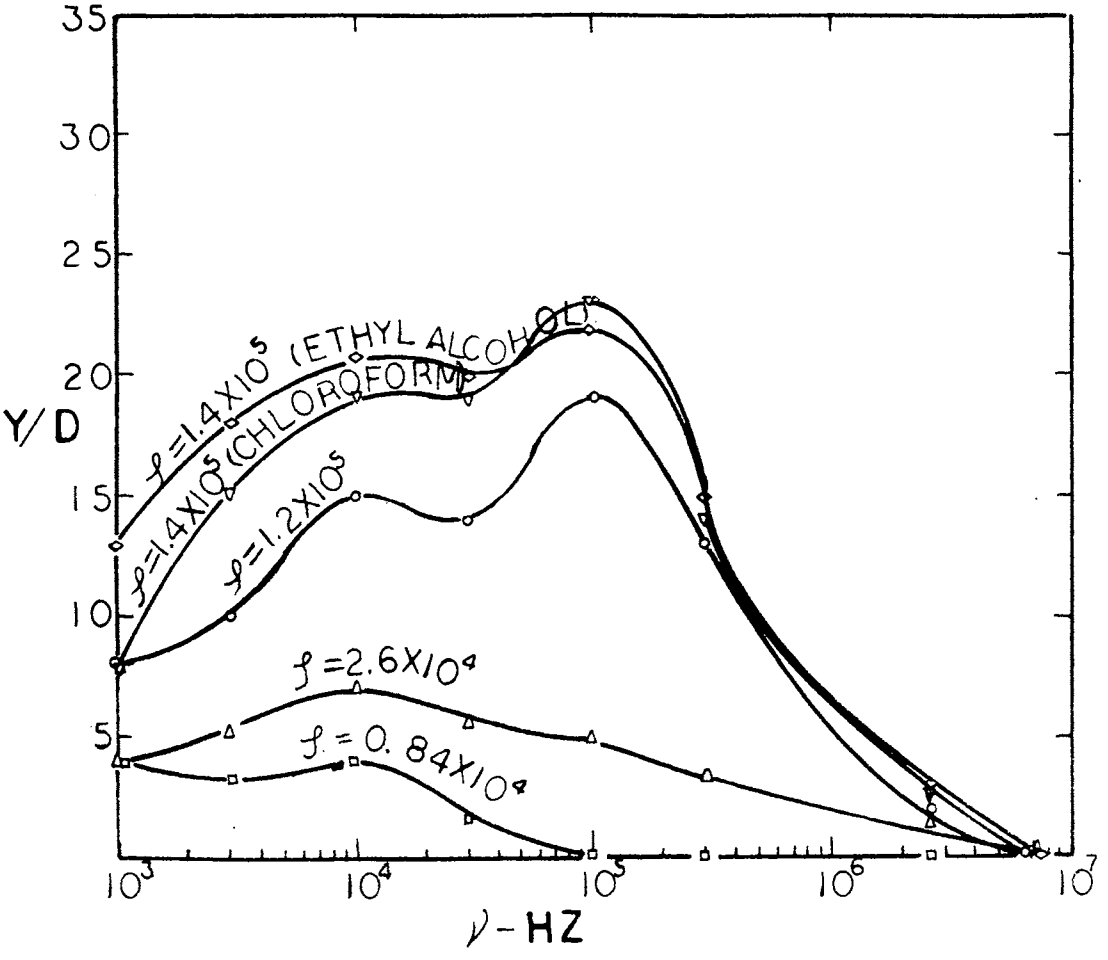

Figure 49. Yield Spectra of Zymcsan. w-w: 0.025 - 0.9 mm, 24 Volts, 210x, O.D. = 0.1

KNO_3) has also been shown. The zymosan was treated with chloroform for 4 minutes and treated with ethyl alcohol for 10 minutes.

CHAPTER V

MISCELLANEOUS EFFECTS

AC Electrophoretic Effect

In a uniform alternating electric field, a suspended, charged particle is subject to an alternating force. Motion is now resisted by viscous effects in the suspending medium and by inertia of the particle itself. So, for a sinusoidal field, the actual displacement, $\vec{r}$, of the particle is given by the differential equation

$$m\ddot{r} + h\dot{r} = qE \sin \omega t \qquad (9)$$

where m = mass of the particle, h = coefficient of viscous drag, q = effective net charge on the particle, and E = amplitude of the applied field.

The standard procedure for solving Equation (9) is first to consider the equation as being homogeneous, that is, first to set the right-hand side of the equation equal to zero and, secondly, to find a solution that will satisfy the right-hand side in particular. The solution of the homogeneous equation yields a solution that is called the complementary solution; the solution satisfying the right-hand side, the particular solution. The sum of these solutions is the complete solution desired. Consider now the homogeneous equation:

$$m\ddot{r} + h\dot{r} = 0$$

ıe auxiliary equation: $mD^2 + hD = 0 \therefore D = 0$, or $-\frac{h}{m}$.

Thus the complementary solution may now be written as:

$$\gamma_c = C_1 + C_2 e^{-h/mt}$$

Only terms in cos (ωt) and sin (ωt) will be obtained when the forcng function is represented by qE sin ωt. We can, therefore, assume the articular solution to be

$$\gamma_p = D \sin \omega t + F \cos \omega t$$

here D and F are arbitrary constants to be evaluated by satisfying quation (9).

$$\dot{\gamma}_p = D\,\omega \cos \omega t - F\,\omega \sin \omega t$$

$$\ddot{\gamma}_p = D\,\omega^2 \sin \omega t - F\,\omega^2 \cos \omega t$$

These derivatives are substituted into Equation (9), yielding:

$$-m\omega^2 (D \sin \omega t + F \cos \omega t) + h\omega (D \cos \omega t - F \sin \omega t) = qE \sin \omega t$$

Now the coefficients of the sine and cosine terms of the left-hand side must equal the coefficients of the right-hand side, respectively; that is:

$$-m\omega^2 D - h\omega F = qE$$
$$-m\omega^2 F + h\omega D = 0$$

Then

$$D = \frac{-qEm}{m^2\omega^2 + h^2}$$

$$F = \frac{-qEh}{m^2\omega^3 + \omega h^2}$$

ıe particular solution then becomes:

$$\gamma_p = \frac{-qE}{m^2\omega^2 + h^2}\left(m \sin \omega t + \frac{h}{\omega} \cos \omega t\right)$$

r

$$\gamma_p = -\frac{qE}{m\omega\sqrt{\omega^2 + (h/m)^2}} \sin (\omega t + \theta)$$

'here

$$\tan \theta = \frac{h}{m\omega}$$

:he complete solution may now be written as

$$\gamma = \gamma_c + \gamma_p$$

$$\gamma = (C_1 + C_2 e^{-\frac{h}{m}t}) - \left(\frac{qE}{m\omega\sqrt{\omega^2 + (h/m)^2}} \sin (\omega t + \theta)\right) \qquad (10)$$

This solution consists of two terms, a transient state (complementary solution) and a steady state (particular solution). The transient state vanishes with time. The time required for the transient very nearly to vanish is dependent upon h/m. The larger the value of h/m, the sooner will the transient state damp out (see Figure 50). The steady state is so called because if given a sufficient period of time, it represents the motion of a forced vibratory system.

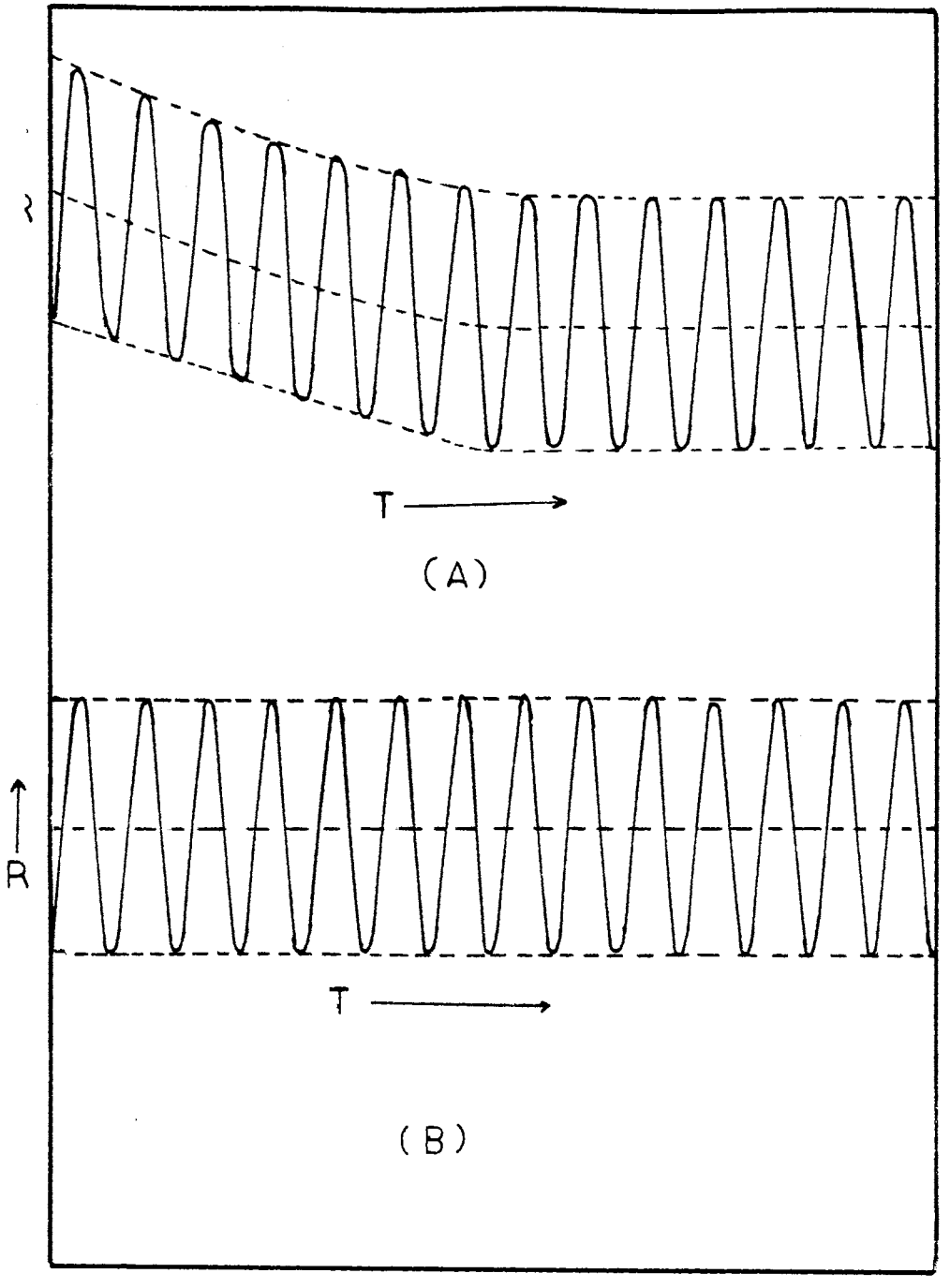

Figure 50. The Plot of Equation (11). (a) Small h/m; (b) Large h/m

Since there are two constants to be evaluated in Equation (10), two ındary conditions are required for their evaluation. Let us assume ıt the initial condition is

$$r = r_o \text{ when } t = 0$$

$$\dot{r} = 0 \text{ when } t = 0$$

at is, we have an initial displacement r_o and the mass is at rest itially. Substituting the initial conditions, we get:

$$C_1 = r_o + \frac{qE}{h\omega}$$

$$C_2 = -\frac{\omega m^2 qE}{h^3 + m^2\omega^2 h}$$

hus,

$$= (r_o + qE/h\omega - \frac{\omega m^2 qE}{h^3 + m^2\omega^2 h} e^{-\frac{h}{m}t}) - (\frac{qE}{m\omega\sqrt{\omega^2 + (h/m)^2}} \sin(\omega t+\theta)) \quad (11)$$

The drift velocity of the transient state is

$$V_d = \frac{\omega m^2 qE}{h^2 + m^2\omega^2} e^{-\frac{h}{m}t}$$

and the total drift distance

$$d = \frac{\omega m^2 qE}{h^3 + m^2\omega^2 h}(1-e^{-\frac{h}{m}t})$$

It is found that V_d and d are largest when $W_m = h/m$. Table I shows the values of V_d and d of different frequency and different time. We

TABLE I

THE VALUES OF DRIFT VELOCITY AND DRIFT DISTANCE AT VARIOUS FREQUENCIES

Frequency (Hz)	Time (Sec)	V_d (Cm/Sec)	d (Cm)
10	1×10^{-9}	0.1215618×10^{-2}	$0.1236271 \times 10^{-11}$
	1×10^{-7}	0.4366772×10^{-4}	$0.3611574 \times 10^{-10}$
	1×10^{-5}	0.0000000	$0.7341538 \times 10^{-10}$
100	1×10^{-9}	$0.12141618 \times 10^{-1}$	$0.1236271 \times 10^{-10}$
	1×10^{-7}	0.4366771×10^{-3}	0.3611573×10^{-9}
	1×10^{-5}	0.0000000	0.3741536×10^{-9}
10^3	1×10^{-9}	0.1215618	0.1236270×10^{-9}
	1×10^{-7}	0.4366770×10^{-2}	0.3611573×10^{-8}
	1×10^{-5}	0.0000000	0.3741533×10^{-8}
10^4	1×10^{-9}	0.1215614×10^{1}	0.1236267×10^{-8}
	1×10^{-7}	0.4366757×10^{-1}	0.3611562×10^{-7}
	1×10^{-5}	0.0000000	0.3741525×10^{-7}
10^5	1×10^{-9}	0.1215194×10^{2}	0.1235839×10^{-7}
	1×10^{-7}	0.4365247	0.3610314×10^{-6}
	1×10^{-5}	0.0000000	0.3740232×10^{-6}
10^6	1×10^{-9}	0.1174586×10^{3}	0.1194541×10^{-6}
	1×10^{-7}	0.4219375×10^{1}	0.3489668×10^{-5}
	1×10^{-5}	0.0000000	0.3615245×10^{-5}
10^7	1×10^{-9}	0.2705379×10^{3}	0.2751342×10^{-6}
	1×10^{-7}	0.9718326×10^{1}	0.8037621×10^{-5}
	1×10^{-5}	0.0000000	0.8326857×10^{-5}
3×10^7	1×10^{-9}	0.1124183×10^{3}	0.1143282×10^{-6}
	1×10^{-7}	0.4038316×10^{1}	0.3339923×10^{-5}
	1×10^{-5}	0.0000000	0.3460111×10^{-5}

use $Q = 5.652 \times 10^{-5}$ esu, a (particle radius) = 0.5N; $m = 0.5 \times 10^{-12}$ gm, E = 200 v/cm, $\eta = 0.01$ poise. These values are closely approximated by biological cells and colloids. From this table we see the time for the transient state nearly vanishes to less than 10^{-5} sec. The total drift distance is less than 1×10^{-5} cm, which could be neglected. Thus, the drift due to AC electrophoretic has a negligible effect on dielectrophoresis.

The steady state may also have an effect on dielectrophoresis. This can be explored by dielectric measurements (90). By writing the electric field as $E = E_o e^{i\omega t}$, the differential equation of motion is:

$$m\ddot{r} + h\dot{r} = qE \tag{12}$$

Under alternating current, the steady state conditions $\dot{r} = \dot{r}_o e^{i\omega t}$. Then Equation (12) reduces to $\dot{r}_o = \frac{qE_o}{h(1 + i\omega t)}$ where $T = m/h$. The electrophoretic current which results from the movement of charge particles with the field is given by the equation

$$I = Nq\dot{r}; \; I_o = Nq\dot{r}_o \tag{13}$$

where I_o is the peak value of I and N is the number of particles per volume unit (cm^3). Since the complex conductivity $K = \sigma + i\omega\varepsilon\varepsilon_r$ ($\varepsilon_r = 8.85 \times 10^{-14}$ farad/cm is the dielectric constant of vacuum) is related to I_o and E_o

$$I_o = KE_o \tag{14}$$

We can combine Equations (13) and (14).

$$K = \frac{Nq^2}{h(1 + i\omega T)}$$

This separates into

$$\sigma = \sigma_\infty - Nq^2/h * \frac{1}{1 + (\omega T)^2}$$

$$\varepsilon = \varepsilon_\infty - Nq/h\varepsilon_r * \frac{T}{1 + (\omega T)^2}$$

where σ_∞ and ε_∞ have been added to account for contributions due to mechanisms other than those discussed here. Schwan et. al. (90) estimated the numerical value for polystyrene particles. They found $\varepsilon_\infty - \varepsilon_o$ is smaller than 4 for volume fraction p = 0.3 taken by the particles, but they mix MkS and CGS units. The actual value was much smaller than they expected. Table II shows some values of $\varepsilon_\infty - \varepsilon_o$ at various frequencies. Using the same value as on the last page, $N = 10^7/cm^3$. The maximum value of $\varepsilon_\infty - \varepsilon_o$ is less than 10^{-8}. This means that the vibrational effect can be neglected. In conclusion, the AC electrophoretic movement does not affect the dielectrophoresis.

Orientation of Non-Spherical Particles

If a sufficiently strong ac field is impressed on a single, non-spherical, micron-sized particle polarizable in its suspending fluid, the particle may show a preferred orientation in the field. When the field is removed, the orientation will become random again. Thus, the phenomenon of orientation may be described as a competition between electrical orienting forces and thermal randomizing forces.

Changes in orientation of biological particles with changes in

TABLE II

THE VALUE OF $\varepsilon_\infty - \varepsilon_o$ OF THE ELECTROPHORETIC DISPERSION EFFECT AT VARIOUS FREQUENCIES

$\varepsilon_\infty - \varepsilon$	Frequency (Hz)
0.2934122×10^{-8}	0
0.2834560×10^{-8}	10
0.2834560×10^{-8}	30
0.2834560×10^{-8}	100
0.2834560×10^{-8}	300
0.2834560×10^{-8}	1000
0.2834557×10^{-8}	3000
0.2834522×10^{-8}	10000
0.2834206×10^{-8}	30000
0.2830624×10^{-8}	100000
0.2799521×10^{-8}	300000
0.2488487×10^{-8}	1000000
0.1258893×10^{-8}	3000000
0.1901489×10^{-8}	10000000
0.2246735×10^{-8}	30000000

frequency of radio-frequency fields were first reported by Teixeira-Pinto et al. (91), and the relationship of frequency and conductivity of the medium to the orientation of Euglena was determined experimentally by Griffin and Stowell (92), followed by a theoretical formulation and experimental test by Ferris and Griffin (93). Furedi (94, 95) studied the effects of audio and high radio frequency fields and also of a direct field on conducting and non-conducting particles suspended in various fluids, and the behavior of erythrocyles exposed to rf fields at a single frequdncy of 120 MHz. Griffin (95) also points out that the direction of orientation of erythrocytes is determined by the interaction of (a) the frequency of the applied electromagnetic field, (b) the conductivity of the suspending medium, and (c) the cell volume and hemoglobin concentration. Saito, Schwan and Schwarz (96) attempt to explain this orientation phenomenon simply as a result of the electrostatic forces acting on nonspherical particles of dielectric properties different from those of the suspending material. They show that as the frequency of the electric field changes, there may be sudden jumps in the stable direction as well as gradual changes.

Using dielectrophoresis, we found that B. cereous changes in orientation with frequency in the region of greater than 1 MHz. Since an accepted measure of the dielectrophoretic effect is the "yield", or linear extent of growth perpendicular to an electrode surface of a layer of percipitating particles the "Orientation effects" can't be neglected in the dielectrophoresis. For instance, in Figure 34 the collection of B. cereus at 14.6 MHz was parallel to the electrodes; the size of B. cereus is 1.1 by 4μ (average). If the cells at 14.6 MHz were collected perpendicularly, it would be 7.3 or fewer divisions long instead of 2 divi-

sions as we saw in the parallel collection. At 7.3 MHz or 2.55 MHz, the cells are not all parallel or all perpendicular. This makes the correction difficult. But by knowing the precise points in the parallel region and the perpendicular region, we can estimate the curve on a mixed region by extending the curve on both the parallel and perpendicular regions (dotted line in Figure 45). An optical instrument which tells the "yield" by the number of cells would give us a more correct answer.

Pearl-Chain Formation

That chains of living or non-living particles (pearl-chains) form along the lines of force of electromagnetic fields has been known for many years (91, 95, 98-104), and detailed experimental and theoretical analyses of the phenomenon have been carried out (98, 105).

Elongated particles participated in either conventional pearl-chains (particles form parallel to the lines of flux; that is, perpendicular to the wire-wire electrodes) or transverse chains (particles form perpendicular to the lines of flux; that is, parallel to the wire-wire electrodes), whether the particles themselves oriented across or with the field. Transverse chains formed even in field conditions that caused biological particles to rotate and exhibit dynamic instability (91, 94, 97).

Out of the papers devoted to the formation of oriented aggregates (pearl-chains) with the application of an alternating electric field to suspensions or emulsions, only in the work of Stauff (101) has an attempt been made to subject the experimental data to a statistical analysis. Using this information an evaluation was made of the energy effect of the formation of pearl-chains. Recently, Vorob'eva et. al (106)

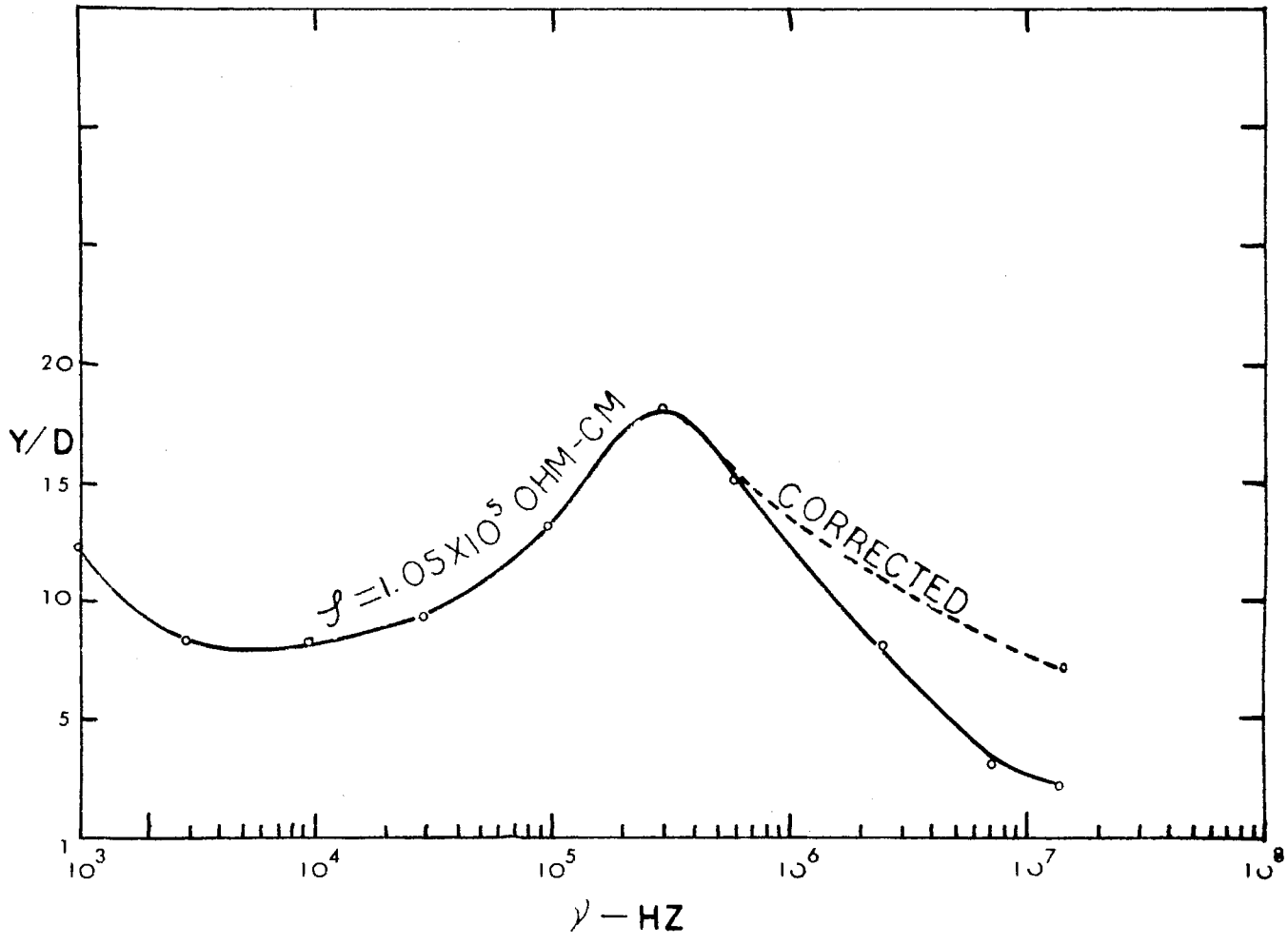

Figure 51. The Effect of Orientation on Yield Spectrum

undertook an experimental study of the aggregation of suspensions in an alternating electric field, characterizing this process also from the quantitative side, in particular, considering the size distribution of the aggregates developing. They show that the rate of formation of oriented aggregates increases with an increase in the initial concentration of the suspensions, as well as with an increase in the amplitude of the strength of the electric field; the rate decreases somewhat with an increase in the frequency of the field.

Because of lack of sufficient experimental data, it is difficult to discuss the effects of "the pearl-chain formation" on dielectrophoresis. Nevertheless, we still could indicate two points which may be important. First, the form of the low frequency collection (strongly aggregated) was qualitatively different from that of high frequency collection (more in chain formation). This causes a deviation in the "yield". The cells tend to form pearl-chains strongly at 100 KHz, but at low frequency such tendency is low. This result is similar to that of Vorob'eva et al.; that is, the rate of formation of pearl-chain decreases somewhat with an increases in the frequency (up to several hundred KHz) of the field. Secondly, since the rate of formation of pearl-chains increases with an increase in the initial concentration of the suspensions as indicated by Vorob'eva et al., and since the rate is also different in different frequencies, then we should expect the change in "yield" by different concentrations will be quite different at various frequencies, which is exactly what we have obtained (see Figures 13 and 39).

Stirring, Repulsion, and Rotation

These three phenomena that are associated with dielectrophoresis

still have no satisfactory explanation. The stirring (or interelectrode circulation in wire-wire electrodes) and repulsion phenomena have been observed under the action of strong, constant electric fields on hydrocarbon dispersions of soap (107). Shilov and Deinega (108) give a theory on the basis of a hypothesis as to the breaking down at the electrodes of the balance of the charges of the disperse phase. Thus, theory explained a number of effects arising in nonaqueous disperse systems in constant electrical fields (interelectrode compression of the structure, interelectrode circulation of the particles of the disperse phase, etc.). They also obtained criteria to determine the possibility of the deposition of particles on the electrodes, into which enter the intensity of the electrical field and parameters characterizing the particle. Their hypothesis may also be applied in an ac field with low frequency. Thus, it is likely that the major cause of the interelectrode circulation and repulsion was due to the breaking down of the balance of the charges of the disperse phase. In other words, the nonuniform field increases with a decrease of the distance from the electrode. Thus, near the negative electrode a stronger field will act on the positive charge of a particle than on a negative charge, while near the positive electrode, the contrary is true. In this connection, at the negative electrode, the positive charges will be torn away from a particle at a higher rate than the negative charges. As a result, a particle located in a nonuniform field near an electrode will take on the same sign as the electrode. When a sufficient negative charge has been obtained at the negative electrode, the particle will be ejected into the depths of the interelectrode space. Far from the electrode, the nonuniform field is less significant, and the charge of the particle will gradually return to its steady-state

value, the dielectrophoretic force bringing it back to the electrode again. Thus, the particle will circulate. The theory by Pohl (109) shows that in a real dielectric, the initial attraction to the central electrode felt by all particles because of the nonuniform field and its polarizing induction is gradually overcome by the repulsive effects of charge accumulated on the particles because of ionic conduction in the liquid. This theory could also be used to explain the circulatory motion. In our experiments, the circulatory motion happens prominently under 1 KHz. This should cause a great effect in the "yield" for the frequency below 1 KHz. One should be able to distinguish the unsymmetrical stirring that is due to the contamination from that discussed above.

Heating Effects

There are many accounts of lethal effects of high-frequency voltage fields on microorganisms (120, 121) in the absence of a lethally high temperature. There are also contrary reports (122, 123), and the matter is still not settled satisfactorily. But this does indicate that the heating effects may be important in the study of dielectrophoresis.

Pohl and Crane (29) investigated the Joule heating effects associated with aqueous dielectrophoresis. But in a lossy dielectric medium, the total heat developed is not only Joule heat but also dielectric loss. The heat developed in a dielectric by polarization current is called dielectric loss and is analogous to the Joule heat developed by free electrons or ions in a conductor; however, it is a property of neutral aggregates of particles, such as polar molecules, rather than of free ions. In the case of a polarization due to polar molecules, for example, the equilibrium distribution of the orientations of the molecules is

lightly changed by the application of an electric field. The dielectric constant depends upon the difference between the distribution of orientations with and without the applied field, while the dielectric oss represents the part of the energy of the applied field which is issipated as heat because of the "friction" (i.e., the molecular equivalent of macroscopic friction) which the molecules experience as they hange from the one equilibrium distribution of orientations to the ther.

For a dielectric which has a dielectric constant ε' and a loss-factor ε'' (or in other words which has a complex dielectric constant $\varepsilon' - i\varepsilon''$) contained in a parallel plate, if a potential different $V = V_o e^{i\omega t}$ is maintained between the plates, then the mean power, or heat developed per second: (124)

$$\bar{w} \text{ per second} = \sigma' \frac{E_o^2}{2} = \frac{\varepsilon'' \omega}{4\pi} \frac{E_o^2}{2} \text{ erg per sec.}$$

$$\bar{w} \text{ per cycle} = \frac{\varepsilon'' E_o^2}{4} \text{ ergs per cycle.}$$

These equations show that real conductivity $\sigma'(\sigma^* = \sigma' + i\sigma'')$ is proportional to the heat developed per second and ε'' to that developed per cycle.

When the dielectric with which we are dealing possesses the property of anomalous dispersion, according to Maxwell and Wagner, the expression for the loss factor ε'' as a function of frequency is

$$\varepsilon'' = \frac{(\varepsilon_1' N)\omega\tau}{1 + \omega^2\tau^2}$$

Thus:

$$\sigma' = \frac{\varepsilon'\omega}{4\pi} = \frac{1}{4\pi} \frac{\varepsilon_1' N\omega^2\tau}{1 + \omega^2\tau^2} \text{ (esu)}$$

$$= \frac{1}{4\pi \times 0.9 \times 10^{12}} = \frac{\varepsilon_1' N\omega^2\tau}{1 + \omega^2\tau}$$

$$\text{ohm}^{-1}\ \text{cm}^{-1}$$

where

$$N = q \left\{ \frac{n^2 \varepsilon_1^{\ 1}}{[\varepsilon_1^{\ 1}(n-1) + \varepsilon_2^{\ 1}]} \right\},$$

n is a form factor, which is determined by the proportion of the axis of the conductive particles that are considered to be ellipsoidal, q is the volume concentration of the particles in the medium.

Differentiation of (15) with respect to frequency shows that σ' has no maximum when plotted against frequency; the conductivity of any dielectric to which Equation (15) applies should always increase with frequency, where it changes at all. Hence, high frequency produces more heat than low frequency for the same electric field.

Pauly et al. (125) show that the conductivity increases twice for the frequency change from 1 MHz to 50 MHz on rat liver mitochondria suspension. The experiments by Pauly et al. (126) and Carstensen (53, 54) all show the increasing of conductivity with higher frequency of cell suspension. From 1 MHz to 50 MHz the conductivity changes about twice as much. Thus, we expect higher frequency would cause more damage to the cells. In the reports by NyRop (120) and Seaman (121) about the cell killed, it was above 10 MHz. Most of our work was below 10 MHz. The cells should thus have less chance for being damaged. Mason and

Townsley (31) and Hawk and Pohl (28) tested the viability of yeast cell after dielectrophoresis from 1 KHz to 1 MHz by standard plate counts using a wort agar medium. They found the cells still viable up to 1 MHz. Our frequency range is about the same as his. Thus, it is likely that the heating effect does not cause any serious effect on dielectrophoresis. If the high field and high frequency are used, the heating effects may be serious.

CHAPTER VI

DIELECTROPHORETIC PROPERTIES OF INANIMATE SUSPENSIONS

Heterogeneous Effects

The salient experimental fact revealed by this work is that a positive dielectrophoretic force, leading to collection, acts upon particles of AgBr, SiO_2 and ion exchange resin immersed in an aqueous media. The magnitude of the force depends upon the frequency, displaying a pronounced maximum in the kilohertz range. [Two to three dispersion regions existed: low-frequency range (LFD, several hundreds of Hz to several KHz), high frequency range (HFD, several ten KHz to MHz), and upper high frequency range (UHFD, upper MHz)]. In the early stage of the present experiments, low-frequency dispersion (~ 1 KHz) was not clearly observed, since in the same frequency range it was overlapped by large electrode polarization; and as the frequency was lowered, the interelectrode circulation was serious. This made the measurement become difficult. However, after several experimental verifications, the presence of low-frequency dispersion is now certain. In considering this result, we first note that the static or low-frequency dielectric constant of pure water, 78.54 at 25°C (126), is more than six times the corresponding value of 12.5 at 290°K, reported for AgBr by Lowndes (127). The measured dielectric constant at room temperature for SiO_2 films, prepared in a variety of ways, approaches the value of 3.8 - 3.9 (128). Since, as

seen from Equation (1), these values alone would predict a negative force, we must look to some form of dispersion in the dielectric properties of the system to explain the observations.

It should next be determined whether a dispersion occurring in either bulk water or bulk AgBr, SiO_2 or ion exchange resin alone could be important. Again, however, theory states that dispersion as a bulk property of the suspending medium would favor a negative dielectrophoretic force. In any case, it is well known that no dielectric dispersion occurs in pure water until the dipolar relaxation region is reached at microwave frequencies (129). Data on the room temperature dielectric constant of AgBr at a microwave frequency of 22 GHz, obtained by Smith (130), are in excellent agreement with the low-frequency value reported by Lowndes. Thus, available experimental evidence demonstrates the absence of dielectric dispersion in pure bulk AgBr in the frequency range important for this work. In fact, according to Lowndes and Martin (131), no dispersion would be expected until the infrared frequency range is reached, at which point resonant dispersion associated with lattice polarization would occur. Sedgwick (128) measured the dielectric constant of SiO_2 films at 150 KHz (room temperature). The value 3.8 - 3.9 was found. Frommer et al. (132) found the value of the dielectric constants of the suspensions of SiO_2 in paradioxane and benzene are 2-8. The values are independent of frequency in the range of 10-100 KHz. These data infer the absence of dielectric dispersion in pure bulk SiO_2 in the frequency range important for this work. Thus, it is evident that the dielectric dispersion responsible for the positive dielectrophoretic force must arise from the heterogeneous nature of the suspensions.

Molecular Interpretation of the Dispersion

The precise nature of the dielectric dispersion has been the subject of some disagreement. Rotation as a basis of polarization phenomena was first suggested by Debye (133, 134, 135). Other mechanisms that have been proposed are proton fluctuation (136), the Maxwell-Wagner effect (137, 138), the ion mobility model (139), the surface conductivity theory (140), the ion atmosphere interpretation (141), and the suggestion of Jacobson (142) that the water of hydration is responsible for the dispersion. These alternative interpretations are summarized in Table III, and their dependence on the various measured dielectric parameters are indicated. The various models will be discussed in turn, beginning at the top of the table and working down.

Debye Rotation

The most obvious test of the Debye theory for dielectric dispersion is made by examining the relaxation time τ according to the equation

$$\tau = 4\pi x^3 \eta/kT$$

where x is the effective radius of the rotating particles, assumed to be spherical, η is the viscosity, and k is the Boltzmann constant. The rotation may be due to the whole cell or its constituents. For the whole cell, let $x = 0.5 \times 10^{-3}$ cm, and $\eta = 0.008937$ poise at $T = 298^{\circ}K$. The value of τ is 0.34/sec. Thus, the rotation of the whole cell is not relevant to the present case since the characteristic frequency ($f_o = 1/2\pi T$) of the dispersion decreases with increase in molecular size. For as small a molecule as water, its value is near 20 GHz; for protein

TABLE III

POSSIBLE MECHANISMS OF DIELECTRIC DISPERSION

Mechanism	Dielectric Increment	Relaxation Time
	(Symbols are Defined in the Text)	
Debye rotation	Const. $x\ \mu^2/MT$	$4\pi x^3\ \eta/kT$
Proton fluctuation	Const. $\Sigma \dfrac{V_i^2}{2 + \dfrac{[H^+]}{K_i} + \dfrac{K_i}{[H^+]}}$	No available quantitative treatment
Maxwell-Wagner	$9\ \zeta \dfrac{(\varepsilon_1\sigma_2 - \varepsilon_2\sigma_1)^2}{(\varepsilon_2 + 2\varepsilon_1)(\sigma_2 + 2\sigma_1)^2}$	$\dfrac{\varepsilon_2 + 2\varepsilon_1}{\sigma_2 + 2\sigma_1}$
Surface conductivity	as Maxwell-Wagner with K_p replaced by $\sigma_2 + 2\lambda/a$	
Schwarz ion mobility	$\dfrac{9}{4} \dfrac{\rho}{(1 + \frac{1}{2}\rho)^2} \dfrac{e_o^2 R\sigma_o}{\varepsilon_o kT}$	$\dfrac{R^2}{2UkT}$
Ion atmosphere	$\dfrac{\text{Const.}}{C^{\frac{1}{2}}}$ - Const.	$\dfrac{\text{Const.}}{C_{ions} \times \sigma_1}$
Water structure	No quantitative treatment available	

molecules near 1 MHz (143-146). Thus, it is seen that the Debye model would be able to account for the dispersion over MHz.

Proton Fluctuation

The properties of this model are not so amenable to simple mathematics as were those of the previous mechanisms. This is due to the kinetic nature of the problem. This theory is not yet fully developed as far as the relaxation time is concerned and, therefore, it is not possible to decide whether the data can be explained by it. Scheider (147) has shown that this model must be considered in close conjunction with that of molecular rotation.

Maxwell-Wagner

In considering the Maxwell-Wagner theory, the difficulty is encountered that it requires high internal volume conductivities which seem unreasonable for substances with compact structures. The work by Hall (148) and Muller (149) on AgBr gives $\sigma_2 = 2 \times 10^{-8}$ mho-cm^{-1} which would make the characteristic frequency too low. But an internal protein conductance of about 0.1m Mho-cm^{-1} is possible. In this case τ reduces because of the negligible contribution of σ, involved in most published protein work to:

$$\tau = \varepsilon_o [\varepsilon_2 + 2\varepsilon_1]/\sigma_2$$

i.e., the characteristic frequency $f_o \approx 1$ Mc. Hence, the Maxwell-Wagner model deserves consideration.

Surface Conductivity (O'Konski)

O'Konski's theory, which is essentially the same as that of Maxwell-Wagner but with different boundary conditions, appears to account for a number of known dielectric properties of aqueous proteins, nucleic acids, nucleoproteins, and charged colloids. From Table III,

$$\tau = \varepsilon_o \frac{\varepsilon_2 + 2\varepsilon_1}{\sigma_2 + 2\lambda_s/a + 2\sigma_1} .$$

In this equation, ε_2 is the relative permittivity of the particles and σ_2 its conductivity. The surface conductance is λ_s, and the radius of the particle is a. All the parameters in the equation are independent of frequency in the range of measurement. Assuming negligible conductance inside and outside the particle:

$$\tau = (\varepsilon_2 + 2\varepsilon_1)\ \varepsilon_o \frac{a}{2\sigma_s d} \approx \varepsilon_o \left(\frac{\varepsilon_1 a}{\sigma_s d}\right)$$

where σ_2 and d are the conductivity and thickness of the electric double layer respectively. (The product, $\sigma_s d$, is identical with the surface conductance λ_s) this is just equal to Equation (4). If independent and accurate data of surface conductance were available for particles, we could find the τ of those particles. According to Cole (150), Fricke and Curtis (151), and Schwan, et al. (152), the surface conductance of a colloidal particle is composed of two parts; one is frequency independent while the other one depends upon the frequency. With regard to the investigation by Schwan et al. (152), λ_s has to be interpreted as the high frequency limit of the frequency-dependent part of the surface conductance. It always has been found in the order of magnitude of 10^{-9}

mho (151, 152). Moreover, we can estimate λ_s by means of Equation (73) $\lambda_s = e_o^2 \sigma_o U$; here, σ_o is surface density of charge, U is mechanical mobility, using a result of Sieglaff and Mazur (153). From electrophoretic measurements these authors determined the density of charge units on the surface of polystyrene spheres in a comparable system to be 1.9×10^{13} cm^{-2}. Thus, we may reasonably assume a σ_o in the order of magnitude of 10^{13} cm^{-2}. With potassium ions as the counterions, the calculation likewise yields a λ_s around 10^{-9} mho. Thus, for typical σ_1 values in the 0.1m mho/cm. range and for particle size in the μ-range, the characteristic frequency is in the MHz range. The result of Honig and Hengst (154) gives σ_o in the order of 10^{11} cm^{-2} for AgBr. Using $u = 5.01 \times 10^{15}$ $cm^2/(CVsec)$, the mobility for Ag^+ in an almost free solution, the calculation yields a λ_s around 10^{-10} mho. Thus, the characteristic frequency is in the upper Mc range.

Hence, it seems that the O'Knoski theory is able to account for the high frequency dispersion (about MHz range).

Schwarz Ion Mobility

The Schwarz model was specificially developed for colloidal particles, which is what we are interested in. Schwarz developed his model for $\sigma_1 >> e^2 \sigma_o U a^{-1}$ where e_o is the charge of each ion, σ_o is the surface ion density, U is the surface ion mobility, a is the radius of the solute particles, and σ_1 is the solvent conductivity. The relaxation time

$$\tau = \frac{a^2}{2UkT}$$

or the characteristic frequency

$$f = \frac{1}{2\pi T} = \frac{UkT}{\pi a^2}$$

Using $U = 3.4 \times 10^{11}$ $m^2/(CVsec)$, the mobility for the sodium ion in free solution for particle sizes in the μ-range, the predicted value of f is 1.3 KHz. Thus, the Schwarz model is able to account for the low frequency (~ 1 KHz) dispersion.

Ion Atmosphere

The ion atmosphere model (Debye and Falkenhagen) was not specifically developed for colloidal particles but is worth considering for completeness. Debye and Falkenhagen showed that the conductance of simple electrolytes exhibits a dispersion at frequencies corresponding to the time of relaxation of the ion atmosphere. Such effects would presumably be enhanced in our case because of the high effective charge density of the particles. A dispersion in conductance means that σ, the specific conductance, is a complex quantity, and the imaginary term of $\sigma = (\sigma' - i\sigma'')$ represents an effective increment in dielectric constant. Unfortunately, the Debye and Falkenhagen treatments of the dielectric constant and conductivity of simple electrolyte solutions are not adequate for colloidal electrolytes, where particle shape and size are important parameters of the system. Thus, this model is not relevant to the present case.

Water Structure

For aqueous solutions of macromolecules Jacobson has put forward a qualitative theory for dielectric dispersion and high values of low-frequency dielectric increments by suggesting that these effects are caused partly, or mainly, by a structural change in the water lattice

because of the macromolecules. He uses the conception of Forslind (155) for a water lattice. The latter considers that in the ideal ice lattice each water molecule is surrounded tetrahedrally by four other molecules, but in turning to water the lattice acquires a number of vacant points with lone interstitial water molecules situated in the open spaces of the lattice. Jacobson attributes the structural change to the stabilization of the lattice by hydrogen bonding between the water lattice and the hydrogen bonding atoms on the surface of the macromolecules so that a "lattice-ordered" hydration shell is formed with properties intermediate between those of ice and water. The degree of ordering depends on the amount of structural similarity between the water lattice and the macromolecule. Thus, if the latter has many oxygen and nitrogen atoms on the surface in such positions that they fit into the ideal water lattice, a very pronounced ordering effect is obtained. On the other hand, the hydrogen bonding atoms can be in such a position that little or no ordering occurs. Since ice with a higher lattice order has a higher dielectric constant than water, the increased order should account for the high low-frequency increments of aqueous solutions. Also, since dispersion effects are shown by water in the region 10^{10} Hz and by ice in the region 10^{2} to 10^{4} Hz, depending on its temperature, then a lattice-ordered shell might be expected to give dispersion effects between 10^{2} and 10^{10} Hz according to the degree of order in the shell. This is the region in which macromolecular solutions show these effects.

From the considerations of this section it is seen that the high-frequency dispersion (10^{4} - 10^{6} Hz) could be recognized as the Maxwell-Wagner-type dispersion, to which O'Konski's theory is applicable. The Debye rotation explains dispersions at frequencies higher than 10^{6} Hz.

The low-frequency one (several hundreds of Hz to several KHz) is due to counterion fluctuation along the particles under the external field. Schwarz's theory correspoinds to the mechanism of this low frequency dispersion and essentially is different from the Maxwell-Wagner type mechanism. The water structure model with response with 10^2 - 10^{10} Hz should also be considered. In our cases, all these mechanisms are present, although sometimes one of them is dominant to approximate the whole dispersion curve.

In conclusion, it appears to the author that dipolar rotation, ionic double layer polarization, the Maxwell-Wagner type mechanism (O'Konski's theory), and the water structure in various cases seem equally acceptable qualitatively, and so in general the possibility of a contribution from all and even from as yet unsuspected mechanisms must be considered.

The Yield Equation

Yield is the accepted measure of the dielectrophoretic effect (the linear extent of growth perpendicular to an electrode surface of a precipitating layer). The yield is measured directly under the microscope as the total growth observed at a prescribed time or time intervals after the onset of precipitation. For a uniform suspension with concentration C (particles/m^3), the average distance d between adjacent particles in a suspension is $1/d^3 = C$ or $d = (C)^{-1/3}$. t_1, the time required for the first particle (nearest to electrode) to move to electrode, is

$$t_1 = \int_{d=(c)^{-\frac{1}{3}}}^{a} \frac{dr}{V}$$

where:

r = distance

V = velocity

if it is initially at a distance $d = (C)^{-1/3}$ from the electrode, where a is the radius of particle. Since the particle moves to the electrode, we would get a negative sign for V, so

$$t_1 = \int_a^{(C)^{-\frac{1}{3}}} \frac{dr}{V}$$

For the second nearest particle, the time t_2 for moves to the end of first particle is

$$t_2 = \int_{2a+a}^{2(C)^{-\frac{1}{3}}} \frac{dr}{V}$$

Similarly,

$$t_3 = \int_{2(2a)+a}^{3(C)^{-\frac{1}{3}}} \frac{dr}{V}$$

$$t_n = \int_{(n-1)(2a)+a}^{n(C)^{-\frac{1}{3}}} \frac{dr}{V}$$

n is the last particle being collected in certain time interval $t_n = t$. Pohl (13), equating the magnitudes of the dielectrophoretic and viscous drag forces and solving for the velocity, gives for the cylindrical electrode case

$$V_{(mks)} = \frac{2a^2 \varepsilon_o \varepsilon_1 V_1^2}{3\eta r^3 [\ell_n (r_1/r_2)]^2} \left(\frac{\varepsilon_2 - \varepsilon_1}{\varepsilon_2 + 2\varepsilon_1}\right)$$

r_1 is the radius of the inner cylinder at potential V_1, and r_2 is the radius of grounded outer cylinder. Thus,

$$t = \int_{(n+1)(2a)+a}^{h(C)^{-\frac{1}{3}}} \frac{3\pi r^3[\ell_n(r_1/r_2)]^2}{2a^2\varepsilon_o\varepsilon_1 V_1^2}\left(\frac{\varepsilon_2 + 2\varepsilon_1}{\varepsilon_2 - \varepsilon_1}\right) dr$$

$$t = H\int_{(n-1)(2a)+a}^{n(C)^{-\frac{1}{3}}} r^3 dr = \frac{H}{4}\left[r^4\right]_{(n-1)2a+a}^{n(C)^{-\frac{1}{3}}}$$

where $$= \frac{H}{4}\{n^4(C)^{-4/3} - a(2n-1)^4\} \qquad (15)$$

$$H = \frac{3\pi[\ell_n(r_1/r_2)]^2}{2a^2\varepsilon_o\varepsilon_1 V_1^2}\left(\frac{\varepsilon_2 + 2\varepsilon_1}{\varepsilon_2 - \varepsilon_1}\right)$$

Since Yield = Y = 2an or n = y/2a.

$$\frac{4tC^{4/3}}{H} = (y/2a) - (aC^{1/3})^4\,(y/a-1)^4$$

After rearranging, we obtained the equation

$$(1-K)y^4 + 4aKy^3 - 6a^2Ky^2 + 4a^3Ky - a^4K = 4tK/H \qquad (16)$$

where

$$K = (2aC^{1/3})^4$$

This equation represents the curve of yield spectrum with various physical parameters.

$$F(y,w,\sigma,\varepsilon,C,t,V,a,\eta) = (1-K)y^4 +$$

$$4aKy^3 - 6a^2Ky^2 + 4a^3Ky - a^4K - \frac{4tK}{H} = 0$$

Thus, we could find the relation between the yield and those parameters by Equation (15). For instance, in keeping constant H and K, we could find the relation between the yield and the time. Figure 52 shows the curve for the experimental data of yield vs. time and the curve by Equation (15), (the value $H = 3.22 \times 10^{-3}\ a^{-4}$ and $K = 1.23$ being used). These two curves fit very well. From the theory of dielectrophoresis (156, 89) one expects the amount of collection to vary directly with the square root of the time that the field is applied. This means that we should have a straight line when we plotted yield vs. $(\text{time})^{1/2}$. But experimental results for yeast (29, 89) only show a straight line for the time less than one minute. Beyond this, the yield does not increase substantially. Crane (89) explains this by saying the cells are settling. In looking at Equation (15) for larger t, n is large; then we might use $2n-1 \approx 2n$ in Equation (15). Thus,

$$n = \sqrt{2}\ C^{1/3}\ [\frac{t}{H(1-16a^4C^{4/3})}]^{1/4}$$

Hence, the yield y for large n

$$y = 2\sqrt{2}\ t^{1/4}\ \frac{C^{1/3}}{(1-16a^4C^{4/3})1/4}\ [\frac{2a^6\varepsilon_o\varepsilon_1V_1^2}{3\eta(\ell_n(r_1/r_2)]^2}\ (\frac{\varepsilon_2 - \varepsilon_1}{\varepsilon_2 + 2\varepsilon_1})]^{1/4} \qquad (17)$$

This indicated that the yield is dependent on $t^{1/4}$ instead of on $t^{1/2}$ for large t.

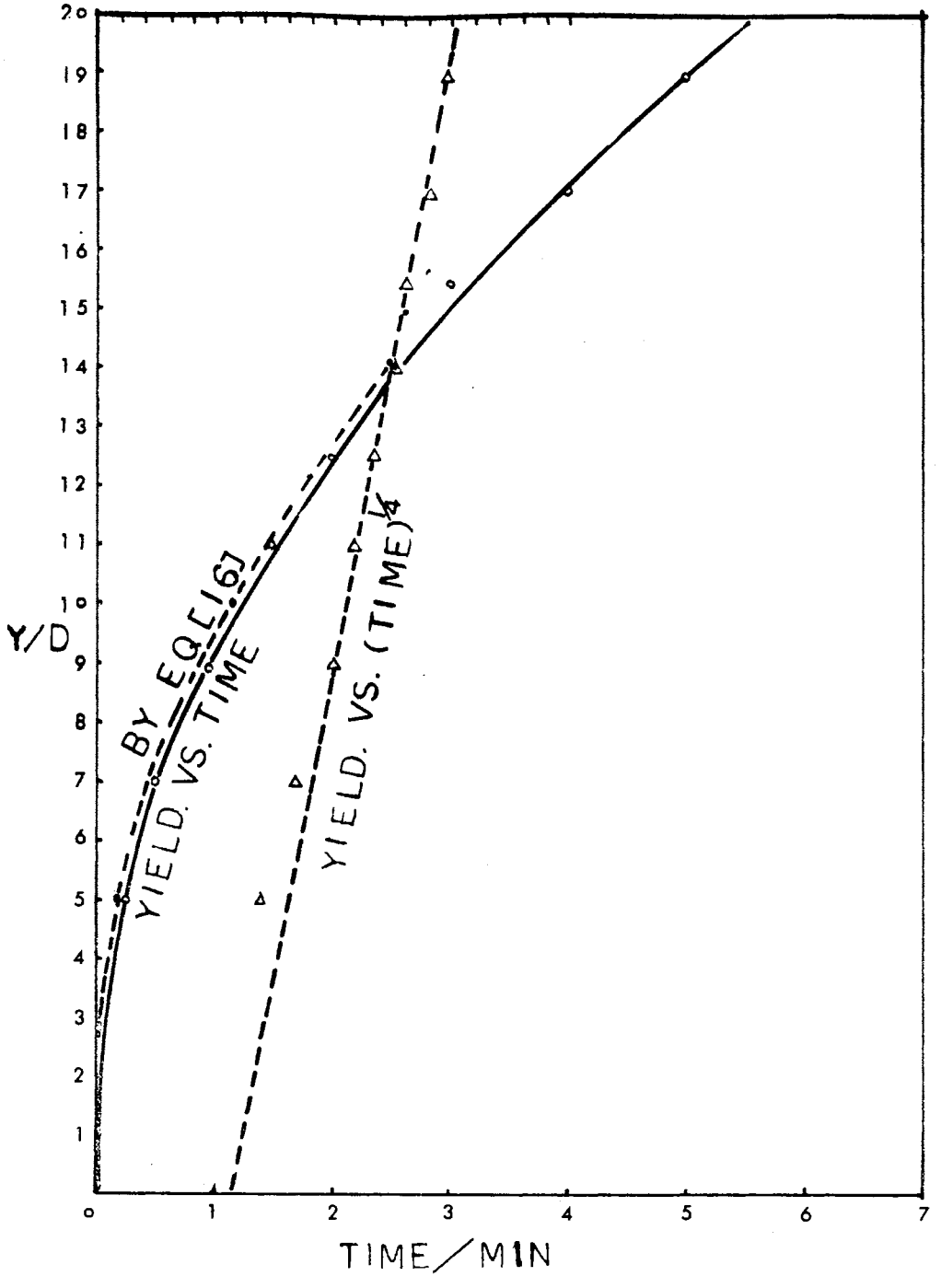

Figure 52. The Curves of Yield Vs. Time By Experiments and Equation (16). 20 Volts at 2.55 MHz, w-w: 0.025 - 0.3 mm, 820x

In connection with the frequency dependence, we have difficulty because the permittivities, ε_2 and ε_1, of the particle and the medium are frequency and conductivity dependent. So far, we still do not have a satisfying theory, even though some of the theory could explain part of them. But from the present experimental data, we found that the empirical equation for the yield spectrum could be written as:

$$y = \sum_{i=1}^{3} y_i \tag{18}$$

Thus, from Equation (16) and (18), we could predict the yield under other different conditions, where

$$Y_i = \frac{A_i \rho^{n_i+1} \nu}{B_i + (\nu^{mi} \rho)^2} \tag{19}$$

Since we lack information on the low frequency range (> 1 KHz), it is difficult to make the empirical equation perfect. But using the following constants for AgBr in Equation (18); $A_1 = 5.5267 \times 10^4$, $B_1 = 2.9584 \times 10^{14}$, $A_2 = 1.19 \times 10^3$, $B_2 = 2.69 \times 10^{12}$, $A_3 = 4.25 \times 10^7$, $B_3 = 2.9584 \times 10^{20}$, $n_1 = n_2 = n_3 = 0.6936$, $m_1 = m_3 = 1$, $m_2 = 1/3$, we have good curves (compare Figure 53 and 10). Figure 54 shows the yield spectra of SiO_2 by Equation (18); we used the constants: $A_1 = 1.66 \times 10^4$, $B_1 = 2.271 \times 10^{12}$, $A_2 = 1.32 \times 10^4$, $B_2 = 3.61 \times 10^{12}$, $A_3 = 3.114 \times 10^8$, $B_3 = 4.41 \times 10^{20}$, $n_1 = n_2 = n_3 = 0.6936$, $m_1 = 2/3$, $m_2 = 1/3$, $m_3 = 1$. This could be compared to Figure 11. Thus, Equation (16) and Equation (18) could give the information under different conditions. In other words, from one set of data we are able to predict the data under different physical parameters. This would save much experimental work.

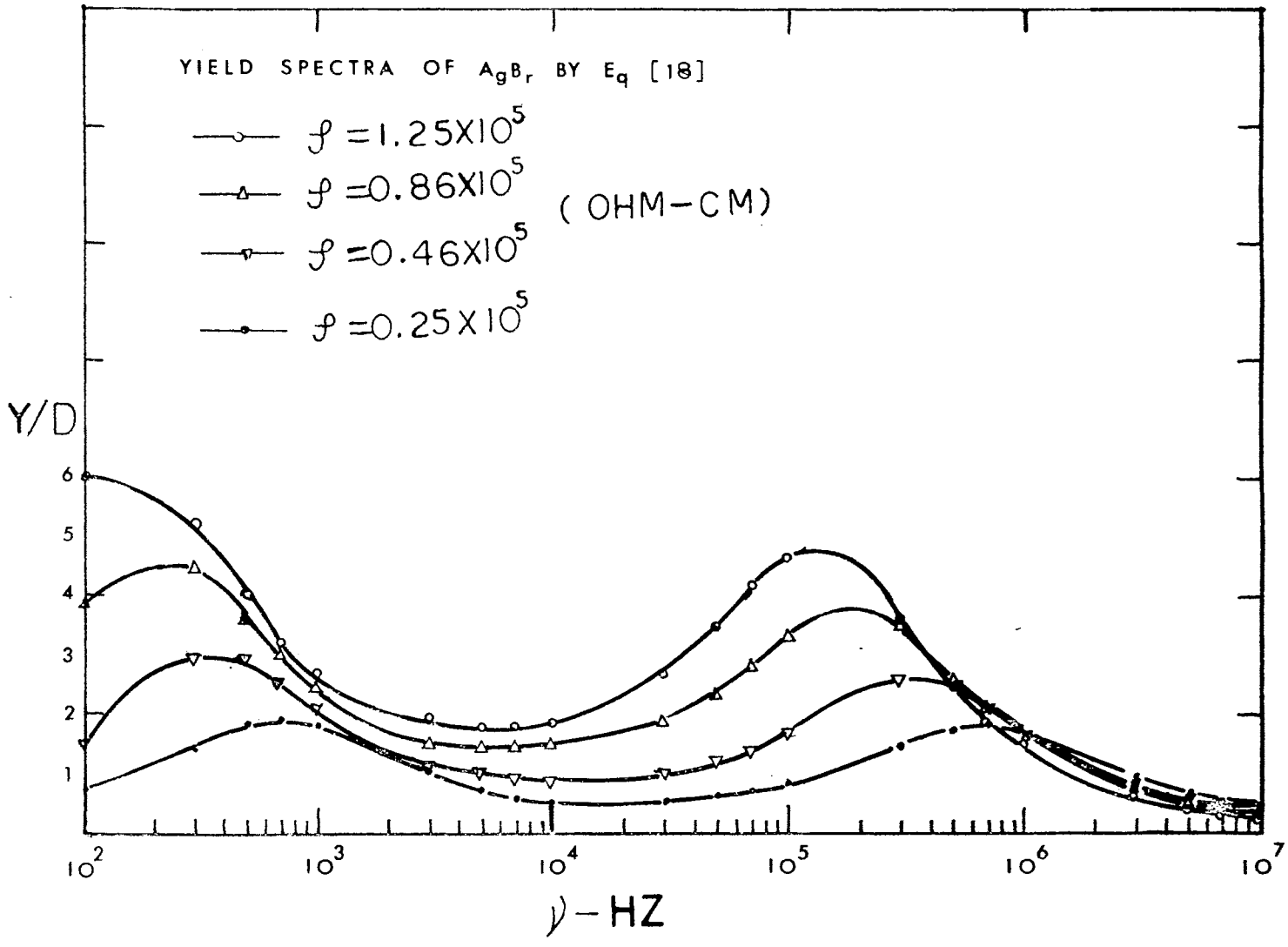

Figure 53. Yield Spectra of AgBr by Equation (18)

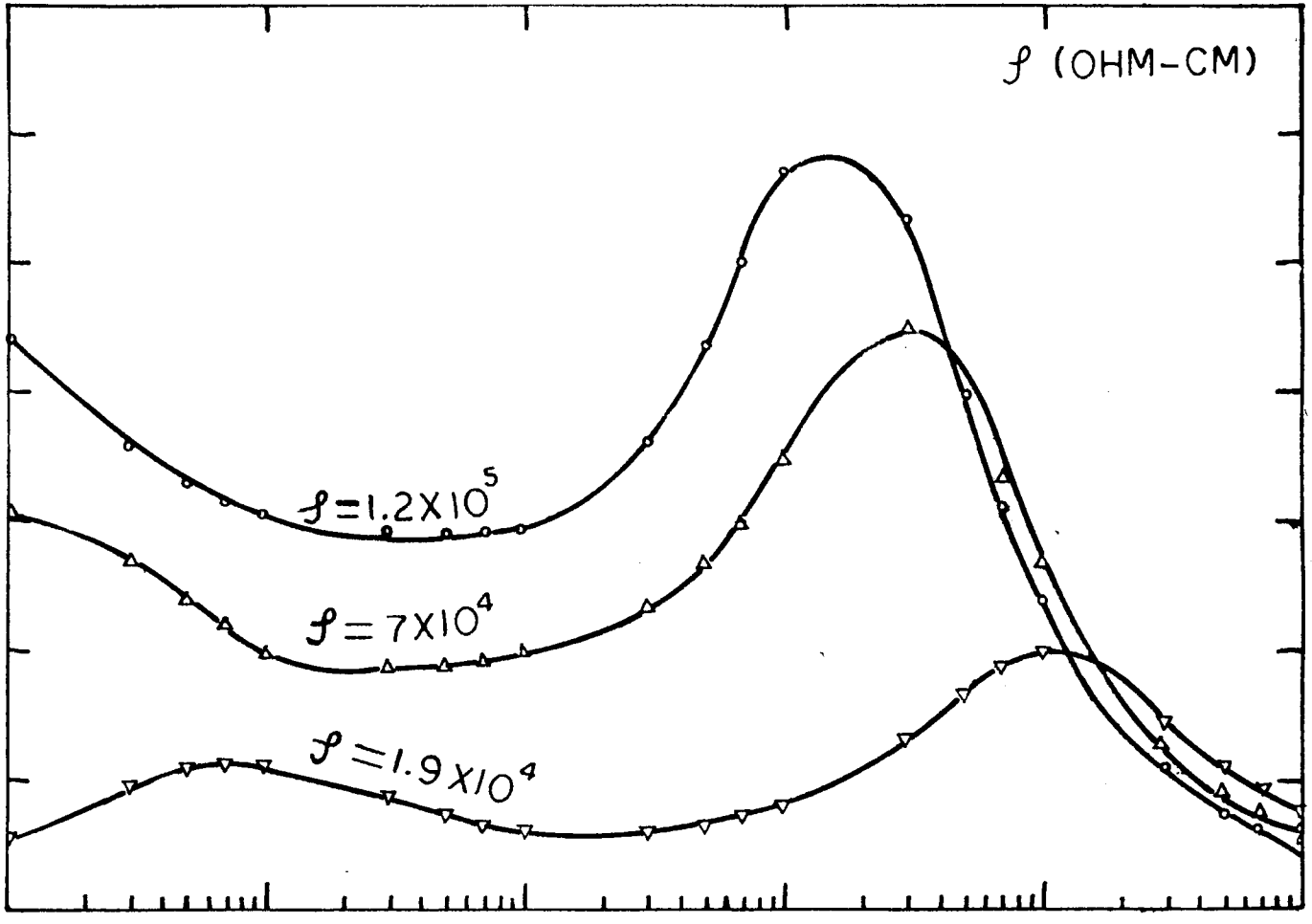

Figure 54. Yield Spectra of SiO_2 By Equation (18)

However, more data are needed in order to confirm these equations.

Summary

A positive dielectrophoretic force leading to collection has been observed to act upon AgBr, SiO_2 and ion exchange resin particles in aqueous suspension. This observation has been related to dielectric dispersion originating in the heterogeneous nature of the suspensions. Various possible mechanisms exist to explain this behavior. From these, three deserve major consideration: Modified Maxwell-Wagner effect--surface conductance, ion mobility in double layers and water structure. The high frequency dispersion has been attributed to a modified Maxwell-Wagner effect. The other, low-frequency one, corresponds to ionic double layer polarization. Water structure variation accounts for both dispersions. In general, the possibility of a contribution from as yet unsuspected mechanisms must be considered.

The yield equation [Equation (16) and Equation (18)] predicted all the information under different conditions. Thus, from one of yield spectrum, we could predict the information under different conditions. This would simplify the future work of dielectrophoresis.

CHAPTER VII

DIELECTROPHORETIC PROPERTIES OF CELLULAR SUSPENSIONS

Rat Liver Mitochondria

Rubenstroth-Bauer and Zeininger (157) reported that mitochondria are surrounded by a membrane of relatively high electricla resistance as shown by measurements of the frequency dependence of the conductivity of a mitochondrial suspension, but were unable to state actual electrical membrane properties. Pauly et al. (158) studied the rat liver mitochondrial membranes from 5×10^5 Hz to 2.5×10^8 Hz. They suggested that the similarity in membrane capacity between isolated mitochondria and intact cells is indicative of a structural similarity. According to their report, characteristic frequencies are 2.8 MHz for the suspension in 0.012 MKCl solution ($\rho \simeq 2 \times 10^3$ ohm-cm) and 27 MHz for the suspension in 0.13 MKCl solution ($\rho \simeq 15$ ohm-cm). In our experiment we use the resistivity at $10^5 \sim 10^4$ which gives the yield peak around 100K ~ 5 MHz which is consistent with their data. It is difficult to get a direct comparison of our observed yield spectra with dielectric dispersion data. Because of experimental difficulties associated with the high conductivity of these systems, such data are lacking.

The data (Figure 20 and 21) at high frequencies (0.1m ~ 10 MHz) indicate two large yield peaks. Measurement with another rat liver mitochondria (Figure 22), however, shows low yield peaks. The peaks at high

frequencies strong effect by the length of time after isolation (Figure 23). It is therefore concluded that variations of preparation and of the length of time after isolation have a strong influence on the yield.

From the yield spectra of solid particles (AgBr, SiO_2, and ion exchange resins), we found the figures compare well with the data given for rat liver mitochondria. The similarity with the yield spectra of mitochondria suggests the common mechanisms between them. As indicated by Schwan (26), the β-dispersion (around 1 MHz) of tissue and biological cell suspensions is caused by the Maxwell-Wagner effect between the cell membrane and the suspending medium. Because of the similarity of the electrical properties of mitochondria and intact cells, it suggested that the high frequency, dispersion (around 1 MHz) is caused by mitochondrial membranes and the associated Maxwell-Wagner effect of outer and inner conductivity differences.

The effect of a small amount of Na^+ succinate (the mitochondria close to resting but having some oxidation) or Na^+ succinate and DNP (rapid oxidation) is hard to differentiate, because of its closeness to the ionic effects. The experimental difficulties associated with the high conductivity of these systems make the investigation of such effects more difficult.

Bacteria

To relate the dielectric properties of bacterial cells to their cytological structure, a model has been proposed by Carstensen (50, 52) in which the typical bacterial cell is a three-phase structure consisting of a conducting core (the cytoplasm), contained within a thin insulating membrane (the plasma membrane), which in turn is surrounded by

a porous, conducting cell wall. The concentration of mobile ions in the cell wall needed to account for the low-frequency conductivity of whole cells was calculated to be almost as great as the cytoplasmic concentration, even though the cell wall is porous and poses no mechanical barrier to diffusion of small ions out into the suspending medium. In fact, the apparent concentration of mobile ions within the wall exceeded the medium concentration in some instances by as much as a factor of ten. This retention of mobile ions within the wall structure suggests that they are serving as counterions for fixed charges there. At frequencies below 500 KHz, the effective, homogeneous conductivities and dielectric constants of bacterial cells depend upon the properties of the cell wall. This is supported by three recent studies. The first has shown that the resistance of the bacterial membrane is too great to account for the high conductivities at frequencies below 500 KHz (52). The second has shown that the conductivity of isolated bacterial cell walls is nearly high enough to explain the conductivities observed for the intact cell (53). The third has shown that the conductivity of the bacterial cell is very low if its cell wall is removed. Furthermore, removal of the cell wall from M. lysodeikticus reduces its low-frequency, effective, homogeneous, dielectric constant by more than two orders of magnitude over most of the frequency range below 100 KHz (54). In this way the use of protoplasts shows that the intact cell wall is responsible not only for the high conductivities, but also for the high dielectric constants of bacteria at low frequencies. Our data supported such a theory. We observed high dielectrophoretic force in bacteria cells at frequency below 500 KHz, which indicated the existence of high dielectric constants at low frequencies. The frequency range of the dielec-

tric dispersion is very broad. From the characteristics of the conductivity of bacterial cells it has been suggested that the cell wall may be similar to an ion exchange resin in the sense that both are porous materials with fixed charges and mobile counterions (50). For this reason, ion exchange resins have been chosen as a model system in studies of the dielectric properties of bacteria.

Ion exchange particles of a size equivalent to that of the bacterial cell have dielectric constants as high as 10^6 (159, 160). The relaxation frequency for the broad low frequency dielectric dispersion of ion exchange particles is comparable to that of bacteria (1 - 10 KHz). The magnitude of the effective, homogeneous dielectric constant and conductivity of the ion exchange particle is related to the fixed charge (or mobile counterion) concentration of the resin. Our yield spectra of E. coli are very similar to those of basic ion exchange resin as we can compare in Figures 18, 19, 32, and 33. Thus, our data offer strong support for the model proposed by Carstensen.

Figures 27 and 28 show the yield spectra of the whole cell (P. aeruginosa) and cell debris. The only difference is the magnitude which was due to the difference in size. Thus, the similarity in yield spectra of the whole cell and cell debris suggested that internal subcellular components give no effective contribution for frequencies under 10 MHz. This agrees with Schwan (26). Thus, the major effect on our study of the dielectrophoresis of the cell is due to the cell membrane and cell wall.

Sud and Schaechter (161) measured the amount of cell-wall and cell membrane material in Bacillus megaterium growing at different steady-state rates. On a dry weight basis, the content of wall hexosamine and

diaminopimelic acid and of membrane lipid phosphorus was found to be inversely proportional to the growth rate of the culture. And this inverse dependence of the content of cell membrane on the growth rate for Bacillus megaterium is also reflected in the major phospholipids of E. coli (162). Thus, when the bacteria grow on culture, their cell walls would be different for different ages of the culture. Such an effect has been observed in Figures 35 and 38.

Because of the similarity of the yield spectra and its effect by ions of the particles and cells, the same mechanism should exist in both of them. Schwarz's theory for in double layer polarization again predicts the characteristic frequency at ≈ 1 KHz. In the case of bacteria, the fixed charges and counterions are distributed throughout a shell of finite thickness (the cell wall).

Yeasts and Zymosan

The observed high values of the apparent dielectric constant of yeasts (163) have been explained in accordance with Maxwell-Wagner's theory on the assumption that a thin layer of high conductivity is located in the cell envelope (164). The thin layer thereby assumed has been suggested to be a plasma membrane which consists of lipids and proteins, making a transport barrier to ions and molecules. Sugiura and Koga (165) destroyed the transport barrier of yeast cells (Saccharomyces cerevisiae) by treatment with $HgCl_2$ and cetyltrimethylammonium bromide (CTAB) to watch ε change over the range 1 KHz to 2 MHz. Both ε values and initial frequencies decreased versus the intact cell. They suggested that the electrically assumed thin layer might correspond to the lipid part in the plasma membrane of the microbe. Our experiments support

such views. Lipids are soluble in many organic solvents. By merely shaking living cells with chloroform, ribose-nucleic acid is released into the suspending fluid without any evidence of the cell's loss of capacity to take the Gram stain (166). Thus, the chloroform treatment might be viewed as destroying the lipid part in the plasma membrane as well as in the cell wall. Figure 40 shows the marked loss of yield spectra above 100 KHz after the cell is treated by chloroform, but there is no change at high frequency of Zymosan (cell wall) by chloroform (see Figure 49). This suggested upper high frequency dispersion (> 100 KHz) could be attributed mostly to the membrane.

Figure 42 shows the different yield spectra of congo-red stained and non-stained-yeast (both had been killed under the same condition); the difference is between 3 KHz and 300 KHz. Since the congo-red stained on the cell wall (166), this experiment also supports the attribution of dielectric dispersion under 100 KHz by the cell wall.

Shakin (167) reported that a number of generations must occur in the presence of glucose before daughter cells of stationary or old cultures become amenable to protoplast formation by the action of snail enzyme. Lieblova and Beran (169) indicated that the youngest cells differed from the other cell in the presence of proteins, RNA and DNA. This infers that the cell wall may change from one generation to another, since the size of the cell is correlated with the cell cycle age (the age of cells during the cell cycle) (169). Thus, we should expect the cells different in size to have a different dielectrophoretic force (beside the different dielectrophoretic force owing to the size) below 100 KHz. This is exactly what we observed in the single-cell-dielectrophoresis. Hartwell (170) has found that in yeasts there are density

fluctuations during the cell cycle with a minimum density at the time of cell division and a maximum after DNA replication. A diagram of the cell cycle including the ordering of various events as determined in the study by Hartwell is shown in Figure 55. The cells about the same size but different in sedimentation velocity (under gravitational force only) or different in density show a pronounced difference in dielectrophoretic force below 100 KHz (see Figures 43 and 44 for particle size about 8.2 by 5.8μ). This indicates the possible variation of the cell wall within one cell cycle. Experiments to test this point further are needed. Measurements of single-cell dielectrophoretic yield spectra should be made using a high power microscope which could give better differentiation in slight variations of sizes. It seems likely that the single-cell dielectrophoresis could be a useful tool in the study of the development of the cell envelope in the cell cycle or ages (the age of cells during the cell cycle).

Summary

The dielectrophoretic properties of mitochondria, bacteria, yeast, and zymosan are determined at frequencies from 1 K to 10 MHz. They are quite similar to AgBr, SiO_2 and ion exchange resin particles. This suggested that a common mechanism existed between them. The dispersion at the high frequency range has been attributed to a modified Maxwell-Wagner effect (O'Konski theory is applicable) which takes account of the double layer existing at the interface between the membrane and the suspending medium. The counterions, which explain the dispersion at low frequency (Schwarz's theory is applicable), are confined to the very thin layer just outside the charged surface of the particle. In the

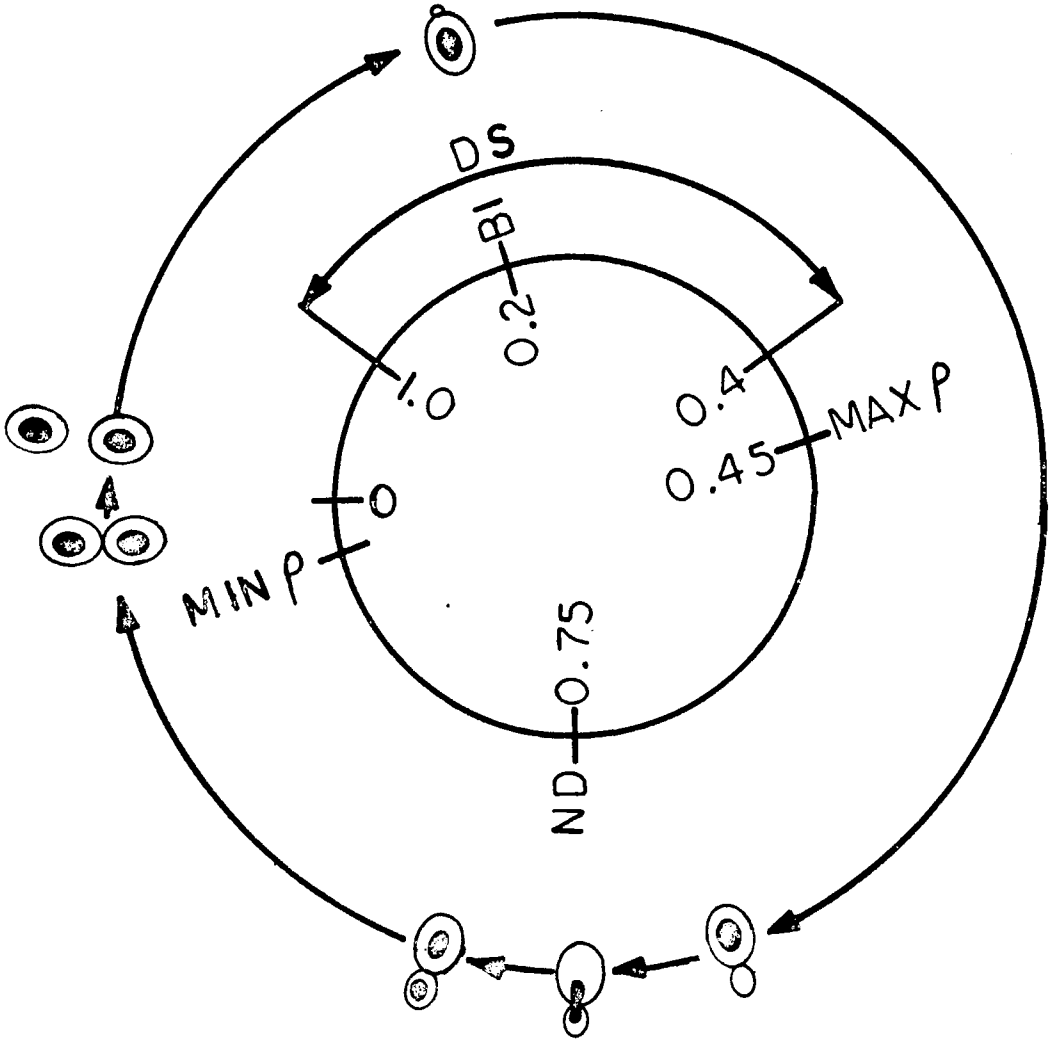

Figure 55. Ordering of Events Within the Cell Cycle of Saccharomyces cerevisiae. The Approximate Times of Cell Separation (CS), Bud Initiation (BI), DNA Synthesis (DS), Density Minimum (Min ρ), Nuclear Division (ND), and Density Maximum (Max ρ) are Indicated in Fractions of a Cell Cycle With Cell Separation Defined as the Beginning and End of a Cycle

case of bacteria, the fixed charges and counterions are distributed throughout a shell of finite thickness (the cell wall), which gives a broader dispersion range.

Single-cell dielectrophoresis offers the opportunity to study dielectric behavior of the yeasts at different ages (the age of cells during the cell cycle) and during the development of the cell envelope in the cell cycle. It appears to be a useful tool for the cell studies in the future.

CHAPTER VIII

SUMMARY AND SUGGESTIONS FOR FUTURE STUDY

Summary

A positive dielectrophoretic force leading to collection has been observed to act upon AgBr, SiO_2 and ion exchange resin particles (the models for cells) in aqueous suspension. This observation has been related to dielectric dispersion originating in the heterogeneous nature of the suspensions. Various possible mecha-isms exist to explain this behavior. From these, three deserve major consideration: Modified Maxwell-Wagner effect--surface conductance, double-layer ion mobility, and water structure. The high frequency dispersion has been attributed to a modified Maxwell-Wagner effect. The other, low-frequency one, corresponds to ionic double layer polarization. Water structure variation accounts for both dispersions. In general, the possibility of a contribution from all and even from as yet unsuspected mechanisms must be considered.

The new semi-empirical yield equation [Equation (16) and Equation (18)] predicted all the information under different conditions. Thus, from one of yield spectrum, we could predict the information under different conditions. This would simplify the future work of dielectrophoresis.

The dielectrophoretic properties of mitochondria, bacteria, yeast, and zymosans are determined at frequencies from 1K to 10 MHz. They are

quite similar to AgBr, SiO_2 and ion exchange resin particles. This suggested that a common mechanism existed between them. The dispersion at the high frequency range has been attributed to a modified Maxwell-Wagner effect (O'Konski theory is applicable) which takes account of the double layer existing at the interface between the membrane and the suspending medium. The counterions, which explain the dispersion at low-frequency (Schwarz's theory is applicable), are confined to the very thin layer just outside the charged surface of the particles. In the case of bacteria, the fixed charges and counterions are distributed throughout a shell of finite thickness (the cell wall), which gives a broader dispersion range.

The new technique of single-cell-dielectrophoresis offers the opportunity to study dielectric behavior of the yeasts at different ages (the age of cells during the cell cycle) and during the development of the cell envelope in the cell cycle.

Investigation of the electrical parameters of biological specimens has recently gained growing attention because of their close dependence on the molecular structural features of the structure. On the basis of dielectric measurement it is possible to judge the electrical symmetry, the geometric dimensions and the form of the molecules, the amount of bound water, the structural changes in the cells and tissues exposed to radiation, chemical agents, etc. On the other hand, experimental determination of the contribution made by the individual cells to the measured effect often presents great difficulties because of the closeness of the electric characteristics of the cell and the intercellular medium and also because of the smallness of the volumetric fraction occupied by the cells in the suspension. There is no doubt that the

development of precise and sensitive dielectrophoresis for determining the dielectric constants will help to solve these problems more successfully. It is hoped that more investigators will become interested in the utilization of the merits of the dielectrophoresis.

Suggestions for Future Study

1. Develope an optical detection system to counting the yield.
2. Study the cell (yeast) age and cell cycle by single-cell-dielectrophoresis.
3. Use the method by Sebastian (171) to separate the cells by size to study the size effect on dielectrophoresis (should consider the same life stage in cell cycle).
4. Study the porous effects on low frequency by using ion exchange resins with different cross linkages. (There is very little literature on the physics of electric conductivity and polarization phenomena manifested by salt-filled porous materials. But Wagner (172) found the dielectric constant was larger than 10^7 at room temperature for porous materials with larger amounts of a proper solvent present. The cause of a high dielectric constant by pores is possible). Such a study would be a great help in the cell wall study.
5. Since a modified Maxwell-Wagner mechanism is favored, experiments to test this point further are needed. Measurements of dielectrophoretic yield spectra should be made using cells which are modified chemically, enzymatically, and physically on their surface.
6. Test the viability of the cells on the non-uniform field effect

[The work by Mason (31) is not enough, because he used the mixed (live-dead) cells].

7. Conduct more experiments for various parameters to test Equation (18).
8. Investigate the electrode polarization effect and find the method for a perfect clean electrode surface in order that low frequency (below 1 K) can be studied.
9. Study the difference in bacteria, protoplasts, ghosts, and cell wall. This could be used to interpret the role and character of the various polarization mechanisms present in the cells and organelles.

BIBLIOGRAPHY

(1) Pohl, H. A., J. Appl. Phys. 22, 869 (1951).

(2) Gilbert, W., De Magnete, Peter Short, London (1600).

(3) Quincke, G., Ann. Phys., Lpz., 62, 1 (1883).

(4) Clark, A. L., Physiol. Rev., 6, 120 (1898).

(5) Pellat, H., C. R. Acad. Sci., 123, 691 (1896).

(6) Fortin, C., C. R. Acad. Sci., 140, 576 (1905).

(7) Gyemant, A., Wiss. Veroff. Siem. Konz., 5, No. 2, 55 (1926).

(8) Greinacher, H., Helv. Phys., 21, 261 (1948).

(9) Pickard, W. F., J. Appl. Phys., 32, 1888 (1961).

(10) Soyenoff, B. C., J. Phys. Chem., 35, 2993 (1931).

(11) Winslow, W. M., J. Appl. Phys., 20, 1137 (1949).

(12) Pohl, H. A. and J. P. Schwar, J. Appl. Phys., 30, 69 (1959).

(13) Pohl, H. A., J. Appl. Phys., 29, 1182 (1958).

(14) Pohl, H. A., Sci. American, 203, 107 (1960).

(15) Pohl, H. A. and C. E. Plymale, J. Electrochem. Soc., 107, 390 (1960).

(16) Verschure, R. H. and L. Ijlst, Nature, 619 (1966).

(17) Black, B. C. and E. G. Hammond, J. Amer. Oil Chemists. Soc., 42, 932 (1965); 42, 936 (1965).

(18) Hawk, I. L., "Effects of Non-uniform Electric Fields on Real Dielectrics in Water" (unpub. M. S. Thesis, Oklahoma State University, 1967).

(19) Feeley, C., "Dielectrophoresis of Solids in Liquids of Differing Dielectric Constant and Conductivity" (unpub. M. S. Thesis, Oklahoma State University, 1969).

(20) Chen, K. W. L., "Dielectrophoresis of Solids in Aqueous Solutions" (unpub. M. S. Thesis, Oklahoma State University, 1969).

(21) Muth, E., Kolloid Z. 41, 97 (1927).

(22) Liebesny, P., Arch. Phys. Therapy, 19, 736 (1939).

(23) Heller, J. H., et al., Exp. Cell. Res., 20, 548 (1960).

(24) Saito, M. and H. P. Schwan, Proc. Conf. Biol. Effects of Microwave Radiation, I, 85 (1960).

(25) Saito, M., H. P. Schwan, and G. Schwarz, Biophys. J., 6, 313 (1966).

(26) Schwan, H. P., Advan. Biol. Med. Phys., 5, 147 (1957).

(27) Schwan, H. P., J. Electrochem. Soc. 116, 22c (1969).

(28) Pohl, H. A. and I. Hawk, Science 152, 647 (1966).

(29) Pohl, H. A. and J. S. Crane, Biophysical J., 11, 711 (1971).

(30) Ting, I. P., K. Jolley, C. A. Beasley and H. A. Pohl, Biochemica and Biophysical Acta 234, 324 (1971).

(31) Mason, B. D. and P. M. Townsley, Can. J. Microbiol. 17, 879 (1971).

(32) Maxwell, J. C., "A Treatise of Electricity and Magnetism", Oxford Univ. Press, London and New York (1873).

(33) Wagner, K. W., Am. Physik 40, 817 (1913).

(34) Wagner, K. W. Arch. Electrotech 2, 371 and 3, 83.

(35) Debye, P., Physic. Z., 13, 97 (1912).

(36) Debye, P., "Polar Molecules", The Chemical Catalog Co., New York.

(37) Cole, K. S., "Membranes, Ions and Impulses", University of Calif. at Berkeley Press, Berkeley, Calif. (1968).

(38) Schwan, H., "Determination of Biological Impedances", pp. 323-407 in W. L. Nastuk, ed., Physical Techniques in Biological Res., Vol. 6, Academic Press, Inc., New York (1963).

(39) Schwan, H. P. and Cole, K. S., "Bioelectricity: Alternating Current Admittance of Cells and Tissues" in O. Glasser, ed., Medical Physics, Vol. 3, Yearbook Publishing Co., Chicago (1960).

(40) Edsall, J. T. and J. Wyman, Biophysical Chemistry. Thermodynamics Electrostatics, and the Biological Significance of the Properties of Matter, Vol. 1, Academic Press Inc., New York (1958).

(41) Wyard, S. J., "Solid State Biophysics", McGraw-Hill Co., New York (1969).

(42) Papers Honoring K. S. Cole, J. Cell Co., Physiol 66, (Suppl. 2) II (1965).

(43) Protides of The Biological Fluids, Proceedings of the Thirteenth Colloquium: Proteins and Related Subjects., Bruges, Belgium, Elsevier Publishing Co., Amsterdam (1966).

(44) Digest of Literature on Dielectrics, Vol. 32, Published by National Academy of Sciences, Washington, D.C., 1970.

(45) Brooks, S. C., J. Gen. Physiol. 5, 365 (1922).

(46) Zoond, A. J., Bacteriol. 14, 279 (1927).

(47) Fricke, H., H. P. Schwan, K. Li, and V. Bryson., Nature. 177, 134 (1956).

(48) Schwan, H. P. and Carstensen, E. L. Science 125, 985 (1957).

(49) Pauly, H., IRE (inst. Radio Engrs.) Bio-Med. Electron 9, 93 (1962).

(50) Carstensen, E. L., H. A. Cox, Jr., W. B. Mercer, and L. A. Natale., Biophys. J. 5, 289 (1965).

(51) Einolf, C. W., Jr. and E. L. Carstensen, Biochim. Biophys. Acta. 148, 506 (1967).

(52) Carstensen, E. L., Biophys. J. 7, 493 (1967).

(53) Carstensen, E. L. and R. E. Marquis Biophysical J. 8, 536 (1968).

(54) Einolf, Jr., C. W. and E. L. Carstensen, Biophysical J. 9, 634 (1969).

(55) Schwarz, G., J. Phys. Chem. 66, 2636 (1962).

(56) Javid, M., and P. M. Brown, "Field Analysis and Electromagnetics", p. 145, McGraw-Hill Book Co., New York (1963).

(57) Jones, D. F., "Theory of Electricity and Magnetism", p. 52, Pergamon Press, New York (1964).

(58) Neufeld, J., Phys. Rev., 152, 708 (1966).

(59) Sher, L. D., Ph.D. Thesis, University of Pennsylvania, "Mechanical Effects of AC Fields on Particles Dispersed in a Liquid, Biological Implications", (1963).

(60) Sher, L. D., Nature, 220, 695-696 (1968).

(61) Pohl, H. A., J. Electrochem. Soc. 107, 386 (1960).

(62) Kruyt, H. R., in "Colloid Science", H. R. Kruyt, Ed., Vol. 1, p. 5, Elsevier, Amsterdam, 1952.

(63) Pohl, H. A. and Crane, J. S., "Dielectrophoretic Force", J. Theoretical Biology, in Press.

(64) Von Hippel, A. H., Dielectrics and Waves, John Wiley, N. Y., (1954).

(65) Maxwell, J. C., Electricity and Magnetism, Vol. I, 452 (Clarendon, Oxford, 1892).

(66) Wagner, K. W., Ann Physick 40, 817 (1913); Arch. Electrotech., 2, 37 (1914).

(67) Van Beek, L. K. H., in "Progress in Dielectric", J. B. Birks, Ed., Vol. 7, p. 69, Heywood, London 1967.

(68) Miles, J. B., Jr., and Robertson, H. P., Phys. Rev. 40, 583 (1932).

(69) O'Konski, C. T., J. Phys. Chem. 64, 605 (1960).

(70) Debye, P., and H. Falkenhagen, Physik Z., 29, 121, 401 (1928).

(71) Polder, D. and J. H. VanSanten, Physica, 12, 257 (1946).

(72) Fricke, H., J. Phys. Chem. 57, 934 (1953).

(73) Schwarz, G., J. Phys. Chem. 66, 2636 (1962).

(74) Jost, W., "Diffusion in Solids, Liquids, Gases", (Third Printing) p. 25, 139, Academic Press, New York, 1960.

(75) Schurr, J. M., J. Phys. Chem., 68, 2407 (1964).

(76) Dukhin, S. S., T. S. Sorokina, and T. L. Chelicdze, Colloid, J. 31, 564 (1969).

(77) Dukhin, S. S., T. S. Sorokina, and T. L. Chelidze, Colloid, J. 31, 658 (1969).

(78) Shilov, V. N., and S. S. Dukhin, Colloid. J. 32, 90 (1970).

(79) Shilov, V. N., and S. S. Dukhin, Colloid. J. 32, 245 (1970).

(80) Stoilov, S. P., and S. S. Dukhin, Colloid. J. 32, 631 (1970).

(81) Mandel, M., Mol. Phys. 4, 489 (1961).

(82) Oosawa, F., Biopolymers, 9, 677 (1970).

(83) Oosawa, Polyelectrolytes, Marcel Dekker, New York 1970.

(84) Minakata, A., N. Imai, and F. Oosawa, Biopolymers 11, 347 (1972).

(85) Gouy, G., J. Physique, 9, 457 (1910).

(86) Chapman, D. L., Phil. Mag. 25, 475 (1913).

(87) Stern, O., Z. Electrochem. 30, 508 (1924).

(88) Grahame, D. C., Chem. Rev., 41, 441 (1947).

(89) Crane, J. S., "The Dielectrophoresis of Cells" (Ph.D. Thesis, Oklahoma State University, 1967).

(90) Schwan, H. P., G. Schwarz, J. Maczuk, and H. Pauly, J. Phys. Chem., 66, 2626 (1962).

(91) Teixeira-Pinto, A. A., Nejelski, L. L. Jr., Cutler, J. L., and Heller, J. H., Exp. Cell. Res. 20, 548 (1960).

(92) Griffin, J. L. and R. H. Stowell, Exptl. Cell. Res. 44, 684 (1966).

(93) Ferris, C. D. and J. L. Griffin, Proc. 21st Ann. Conf. Electrical Techniques in Medicine and Biology Apr. 19, Houstin (1964).

(94) Furedi, A. A. and I. Ohad, Biochem. Biophys. A. 79, 1 (1964).

(95) Furedi, A. A. and R. C. Valentine, Bioch. Biophys. A. 56, 33 (1962).

(96) Griffin, J. L., Exptl. Cell. Res. 61, 113-120 (1970).

(97) Saito, M., H. P. Schwan, and G. Schwarz, Biophys. J. 6, 313 (1966).

(98) Schwan, H. P. and L. D. Sher, J. Electro. Soc. 116, 22c (1969).

(99) Muth, E., Kolloid-Z., 41m 2 (1927).

(100) Krust, H. R. and J. G. Vogel, Kolloid-Z., 95, 2 (1941).

(101) Stauff, J., Kolloid-Z., 54, 152 (1941).

(102) Krasny-Ergen, W., Hochfrequenztechn. Und Elektroakust., 48, 126 (1936).

(103) Winkel, Z. Angew. Chem., 143, 162 (1955).

(104) Us'Yarov, O. G., I. S. Lavrov, and I. F. Efremov, Kolloidn-Zh. 28, 596 (1966).

(105) Saito, M., and Schwan, H. P., in Biological Effects of Microwave Radiation 1(edit. by Peyton, M. F.) 85 (Plenum Press, New York, 1961).

(106) Vorob'eva, T. A., I. N. Vlodavets, and P. I. Zubov, Colloid. J. 31, 533 (1969).

(107) Deinega, Yu. F. and G. V. Vinogradov, Dokl. Akad. Nauk SSS R 174, 398 (1967).

(108) Shilov, N. N. and Yu, F. Deinega, colloid. J. 31, 731 (1969).

(109) Pohl, H. A., J. Electrochem. Soc. 107, 386 (1960).

(110) NyRop, J. E., Nature, Lond., 157, 51 (1946).

(111) Seaman, W. L., Can. J. Plant. 47, 39 (1967).

(112) Ingram, M. and L. J. Page, J. Appl. Bact. 16, 69 (1953).

(113) Burton, H. Nature, 166, 434 (1950).

(114) Murphy, E. J. and S. O. Morgan, Bell System Tech., J., 18, 502 (1939).

(115) Pauly, H., L. Packer and H. P. Schwan., J. Bioph. Bioch. Cytol. 7, 589 (1960).

(116) Harned, H. S., and Owen, B. B., "The Physical Chemistry of Electrolyte Solutions," 2nd ed., p. 118, Reinhold, New York, 1950.

(117) Lowndes, R. P., Phys. Lett. 21, 26 (1966).

(118) Sedwick, T. O., J. Elechm. Soc. 118, 349 (1971).

(119) Hasted, J. B., in "Progress in Dielectrics," J. B. Birks, Ed., Vol. 3, p. 101, Wiley, New York, 1961.

(120) Smith, G. C., Thesis, Cornell University, Ithaca, New York, 1962.

(121) Lowndes, R. P., and Martin, D. H., Proc. Roy. Soc. Ser. A308, 473 (1969).

(122) Frommer, M. A. and M. Ish-Shalom, J. Colloid. I. Sci. 21, 170 (1966).

(123) Debye, P., Physik. Z., 13, 97 (1912).

(124) Debye, P., Collected papers, Interscience Publishers Inc., New York, 1954.

(125) Debye, P., Polar Molecules, Chem. Catalog Co., Inc., New York, 1929, Dover Publication, Inc.

(126) Kirkwood, J. G. and Shumaker, J. B. Proc. Natn. Acad. Sci. U.S.A. 38, 855 (1952).

(127) Maxwell, J. C., A Treatise on Electricity and Magnetism, Oxford University Press (1892).

(128) Wagner, K., Ann. Phys. 40, 817 (1913).

(129) Schwarz, G., Phy-Chem. 66, 2636 (1962).

(130) O'Konski, C. T., J. Phys. Chem. 64, 605 (1960).

(131) Debye, P. and H. Falkenhagen, Phys. Z. 29, 121, 401 (1928).

(132) Jacobson, B. J. Am. Chem. Soc. 77, 2919 (1955).

(133) Schwan, H. P., "Determination of Biological Impedances", pp. 326-407 in W. L. Nastuk, ed., Physical Techniques in Biological Research, Vol. 6, Academic Press, Inc., New York (1963).

(134) Schwan, H. P., Advan. Biol. Med. Phys. 5, 147-209 (1957).

(135) Takashima, S., Protides Biol. Fluids 13, 393-402 (1966).

(136) Oncley, J. L., "The Electric Moments and the Relaxation Times of Proteins as Measured From Their Influence Upon the Dielectric Constants of Solutions", p. 543 in E. J. Cohn and J. T. Edsall, ed., Proteins, Amino Acids and Peptides, Reinhold Publishing Corp., New York (1943).

(137) Scheider, W., Biophys. J. 5, 617 (1965).

(138) Hall, J. E. "The Electrical Conductivity of Silver Bromide Membranes and Diffuse Double Layer Theory", Ph.D. Thesis, Univ. of Calif. Riverside, Calif. (1968).

(139) Müller, P. Phys. Stat. Solidi, 12, 775 (1965).

(140) Cole, K. S., Cold Spring Harbor Symp. Quant. Biol., 1, 1 (1933).

(141) Fricke, H. and H. J. Curtis, J. Phys. Chem., 41, 729 (1937). Further reference of older papers will be found here.

(142) Schwan, H. P., G. Schwarz, J. Maczuk, and H. Pauly, J. Phys. Chem., 66, 2626 (1962).

(143) Sieglaff, C. L., and J. Maxur, J. Colloid Sci., 15, 437 (1960).

(144) Honig, E. P., and J. H. Th. Hengst, J. Colloid. Interf. Sci. 31, 545 (1969).

(145) Forslind, E. Acta Polytech., 3, no. 5 (1952).

(146) Pohl, H. A., J. Appl. Phys. 22, 869 (1951).

(147) Ruhenstroth-Bauer, G., and Zeininger, K., Naturwissenschaften 43, 426 (1956).

(148) Pauly, H., L. Packer, and H. P. Schwan, J. Biophy. Biophy. Biochem. Cytol. 7, 589 (1960).

(149) Einolf, C. W., Jr., and E. L. Carstensen, Biophysical Society, Twelfth Annual Meeting A 47, 1968.

(150) Einolf, C. W., and E. L. Carstensen, J. Phys. Chem. 75, 1091 (1971).

(151) Sud, I. J., and M. Schaechter, J. Bact. 88, 1912 (1964).

(152) Ballesta, J. P. G., and M. Schaechter, J. Bact. 110, 452 (1972).

(153) Fricke, H., and H. F. Curtis, Nature, 134, 102 (1934).

(154) Sugiura, Y., S. Koga, and J. H. Akabori, J. Gen. Appl. Microbiol 10, 163 (1964).

(155) Sugiura, Y., and S. Koga, Biophy. J. 5, 439 (1965).

(156) Lamanna, C., and M. F. Mallette, J. Bact. 60, 499 (1950).

(157) Shahin, M. M., J. Bact. 110, 769 (1972).

(158) "Yeasts" —— The Proceedings of the 2nd Symposium of Yeasts Held in Bratislava 16-21, July 1966, ed. by A. Kockova-Kratochivilova, Vydavatelstvo Slovenskej Akademie Vied, Bratislava, 1969, p. 365.

(159) Ibid., p. 353.

(160) Hartwell, L. H., P. J. Bact. 104, 1280 (1970).

(161) Sebastian, J., B. L. A. Carter, and H. O. Halvorson, J. Bact. 108, 1045 (1971).

(162) Wagner, O. E., J. Phys. Chem. 74, 288 (1970).

APPENDIX

DIELECTROPHORETIC PRECIPITATION OF SILVER BROMIDE SUSPENSIONS

Dielectrophoretic Precipitation of Silver Bromide Suspensions

CHI-SHIH CHEN AND HERBERT A. POHL

Department of Physics, Oklahoma State University, Stillwater, Oklahoma 74074

AND

J. S. HUEBNER* AND L. J. BRUNER

Department of Physics, University of California, Riverside, California 92502

Received December 11, 1970; accepted March 1, 1971

Spatially nonuniform ac electric fields will exert a unidirectional force upon either charged or neutral polarizable bodies suspended in liquid dielectric media. The motion resulting from this force, called dielectrophoresis, has been studied in aqueous suspensions of silver bromide particles. The rate of dielectrophoretic precipitation of the particles onto parallel wire electrodes was measured as a function of frequency at various fixed values of solution pAg. Additional measurements were made using dioxane and water/dioxane mixtures as the suspending medium. The observed frequency dependence of the precipitation rate or "yield" shows a maximum at frequencies between 10^5 and 10^6 Hz, which correlates well with published data on the frequency dependence of the dielectric dispersion of silver bromide emulsions. The results imply that the major contribution to polarization in the system studied is provided by the migration of point defects in a diffuse space charge layer located in the subsurface of the silver bromide particles. The type and density of defects is dependent upon the solution pAg, as evidenced by observed shifts of the frequency of peak yield with pAg. This frequency is, however, insensitive to variation of the macroscopic dielectric constant of the suspending medium. These observations are attributed to a modified Maxwell-Wagner effect.

I. INTRODUCTION

In this paper we describe an experimental investigation of the response of aqueous suspensions of silver bromide (AgBr) particles to spatially nonuniform ac electric fields. The objective of this study has been to ascertain whether this response could be correlated with known properties of the double layer existing at the AgBr/aqueous solution interface. An adequate introduction to this subject requires consideration of three more or less distinct but interrelated topics. These are dielectrophoresis, dielectric dispersion in heterogeneous systems, and the double layer structure of the AgBr/aqueous electrolyte interface. We proceed to each topic in turn.

a. *Dielectrophoresis.* A polarizable neutral particle will experience a unidirectional force of electrical origin if placed in an inhomogenous dc or ac electric field. Motion resulting from this force has been designated as "dielectrophoresis" by Pohl (1), since it depends upon the polarizability or dielectric constant of the particle, as well as the dielectric constant of the medium in which it is suspended. For a perfectly insulating sphere of radius a, having dielectric constant or relative permittivity ϵ_2, and immersed in a perfectly insulating medium of dielectric constant ϵ_1, the dielectrophoretic force has been shown (2) to be given by

$$\vec{F} = 2\pi a^3 \epsilon_o \left[\frac{\epsilon_1(\epsilon_2 - \epsilon_1)}{\epsilon_2 + 2\epsilon_1}\right] (\Delta|\vec{E}|^2) \qquad [1]$$

* Present address: Biophysics Department, Michigan State University, East Lansing, Michigan 48823.

where $|\mathbf{E}|$ is the magnitude of the dc or root mean square ac electric field at any point in the suspending medium, and ϵ_0 is the permittivity of free space. Though this result must be generalized to describe real systems accurately, it nevertheless illustrates the following essential points:

1) The force is proportional to the gradient of the mean electrical energy density or to the product of the electric field gradient and the field itself. Thus the force does not change sign upon reversal of the field direction, and will therefore maintain a time averaged unidirectional value different from zero when a nonuniform ac field is present. The same force will act when the polarizable particle carries a net charge. In this case an additional periodic electrophoretic displacement of the particle will occur, but any time averaged displacement different from zero will be due solely to the dielectrophoretic effect, *i.e.*, to the polarizability of the particle rather than to its excess charge.

2) The magnitude of the dielectrophoretic force acting upon a suspended particle is proportional to its volume. Therefore, if the particles are too small, the operation of diffusional forces will overshadow the dielectrophoretic force so that effects due to the latter will not be observed (3). These considerations set a lower limit on particle size for dielectrophoretic studies in the range 0.1--1.0μ. This same size range generally delineates the boundary between suspensions and colloidal dispersions (4) as well.

3) Dielectrophoretic deposition or precipitation of particles at convex electrode surfaces, in the regions of highest mean electrical energy density, requires that the dielectric constant of the particle exceed that of the suspending medium. This is the case of greatest practical interest. At this point, however, it is necessary to consider generalizations of the dielectrophoretic force expression which are appropriate when both the medium and the particle are composed of lossy dielectrics (5). Such considerations show that a comparison of static dielectric constants does not provide a reliable indication of whether dielectrophoretic precipitation will occur. They show that a high dielectric dispersion associated with the particle will generally facilitate its precipitation. Precipitation may in fact occur in a frequency range of high dispersion associated with the particle, even though the static dielectric constant of the particle material is lower than that of the suspending medium.

In practice the accepted measure of the dielectrophoretic effect is the "yield," or linear extent of growth perpendicular to an electrode surface of a layer of precipitating particles. The yield is measured directly under the microscope as the total growth observed at a prescribed time or time intervals after the onset of precipitation. Theoretical yield expressions have been developed for the cases of coaxial cylindrical (3), and concentric spherical (6), electrode geometries.

b. *Dielectric Dispersion in Heterogeneous Systems.* In the preceding subsection the relevance of dielectric properties to dielectrophoresis was considered entirely within the context of the bulk dielectric properties of the two substances involved. It assumed further that both substances had zero conductivity. When the conductivities of the substances are introduced explicitly it then becomes necessary to consider interfacial polarization effects of the Maxwell-Wagner type (7, 8). These effects introduce frequency-dependent dielectric dispersion in heterogeneous systems such as are under consideration here. This is so even though the dielectric constants and conductivities are assumed to be ideal (purely real constants) and independent of frequency. This is in fact usually assumed in developing the theory of the Maxwell-Wagner effect. The Maxwell-Wagner dispersion can also contribute to the dielectrophoretic force on suspended particles (5). The theory of the Maxwell-Wagner effect has been fully reviewed by Van Beek (9). He shows that a Debye type dielectric dispersion with a characteristic relaxation time

$$\tau = \epsilon_o \left(\frac{2\epsilon_1 + \epsilon_2}{2\sigma_1 + \sigma_2} \right) \qquad [2]$$

will occur. Here σ_1 and σ_2 are the bulk conductivities of the suspending medium and of the particle, respectively. This result is

valid for spherical particles in the limit of zero volume fraction of particles.

Another source of dielectric dispersion in heterogeneous systems will arise when the suspended particles are surrounded by electric double layers (9). Two different theoretical approaches to the problem have been taken. In the first approach the high surface conductance of the double layer is represented by a thin conducting shell which surrounds the suspended particle. This model is simply a generalization of those normally considered in the analysis of the Maxwell-Wagner effect. An estimate of the characteristic relaxation time is readily made by noting that the self-capacitance C of a conducting sphere in an insulating medium is of the order

$$C \sim \epsilon_0 \epsilon_1 a, \qquad [3]$$

whereas the effective resistance R_s of the surface layer is

$$R_s \sim (\sigma_s d)^{-1}, \qquad [4]$$

where σ_s is the conductivity of the material which comprises the surface layer and d is its thickness. The time constant which controls the redistribution of charge over the surface of the particle is then

$$\tau \sim R_s C, \sim \epsilon_0 \left(\frac{\epsilon_1 a}{\sigma_s d}\right). \qquad [5]$$

This argument applies equally well to the case of volume conduction through the particle. In this case, $d \to a$, and $\sigma_s \to \sigma_2$. Then τ no longer depends upon a, and a result corresponding to Eq. [2] in the limiting case, $\epsilon_1 \gg \epsilon_2$, $\sigma_2 \gg \sigma_1$, is obtained. The "conducting shell" model was first analyzed by Miles and Robertson (10). Later and more detailed developments have been given (11, 12).

In the second theoretical approach to the problem of double layer dispersion, exemplified by the work of Schwarz (13), the migration of charge in the double layer is presumed to be diffusion controlled. Under this condition the relaxation time should be of the order

$$\tau \sim a^2/D \sim a^2/(ukT), \qquad [6]$$

where D is the microscopic diffusion coefficient of the mobile charge carriers in the double layer, u is the mechanical mobility, equal to velocity per unit force, k is the Boltzmann constant, and T is the absolute temperature. Note that the mechanical mobility u is equal to μ/q, where μ is the electrical mobility and q is the magnitude of the charge on the migrating entity, *e.g.*, ion or crystal lattice defect. Equation [6] follows directly from the solution of the one-dimensional random walk problem, and the Nernst-Einstein relation (14). Schwarz considered the polarization to be caused by field-induced migration of counterions over the surface of a charged particle to which they were strongly bound. Recently Shilov and Dukhin (15) have taken account of diffusion in treating the polarization of a diffuse counterion atmosphere. They obtained for the relaxation time a result equivalent to that given by Eq. [6]. Viewed in this way the problem may be regarded as an extension of the theory of dielectric dispersion in electrolyte solutions which was developed by Debye and Falkenhagen (16). In that case the characteristic distance over which counterions must diffuse to relax a polarized state is the Debye length rather than the particle radius.

In this enumeration of dielectric dispersion mechanisms in heterogeneous systems, which is not exhaustive (5), we have sought only to expose the underlying physical basis of those mechanisms which are most likely to be operative in the AgBr/aqueous electrolyte system. The cited literature should be consulted for more rigorous treatments.

c. *Double Layer Structure of the AgBr/Aqueous Electrolyte Interface.* Our understanding of the structure of the AgBr/aqueous electrolyte interface has been strongly influenced by the work of Grimley and Mott (17) and of Grimley (18). They argued on the basis of known solid state properties of AgBr that a double diffuse double layer, extending into both the solid and liquid phases, should be present. Solid AgBr contains thermally generated, electrically charged, mobile point defects which determine its electrical properties in bulk. These defects are interstitial Ag^+ ions, and negatively charged vacancies on the silver

sublattice. Thus solid AgBr is electrochemically equivalent to a liquid electrolyte. The interface between it and water should be similar to that between two immiscible liquids containing electrolytes. The liquid/liquid interface was first described by Verwey and Niessen (19). They introduced the double diffuse double layer as an extension of the Gouy-Chapman concept of a diffuse charge layer adjacent to a geometric surface charge layer of opposite sign. The comprehensive review by Lidiard (20) surveys known properties of electrically active defects in AgBr and other ionic crystals.

It is clear that the portion of the double layer charge distribution located within the solid, together with any charge adsorbed on its surface, will give the solid a net charge. This net charge is counterbalanced by the adjacent diffuse charge layer in the liquid. Hence AgBr particles in aqueous suspension will generally carry a net charge and will be surrounded by counterion atmospheres. It is well known that the sign and magnitude of the net charge on AgBr is sensitive to the Ag^+ ion concentration (pAg) in the surrounding solution. At a pAg of 5.4, the point of zero charge (p.z.c.) of AgBr, its net charge is zero. Honig and Hengst (21) have summarized the various experimental methods for measuring the p.z.c. of AgBr and of other inorganic precipitates, and have tabulated the results obtained. The value quoted for the pAg at the p.z.c. of AgBr is for classical polydisperse sols freshly prepared by precipitation upon mixing relatively concentrated aqueous solutions of reagent grade $AgNO_3$ and KBr. Sols prepared under other conditions may or may not display the same p.z.c.

This introduction has established that we have at hand an experimental technique, dielectrophoresis, which should be selectively sensitive to double layer structure in heterogeneous systems. In addition we have the AgBr/aqueous electrolyte system in which the double layer structure can be modified in a known fashion by changing solution pAg, a readily accessible experimental variable.

II. EXPERIMENTAL METHODS

Cells for dielectrophoresis were constructed by mounting two parallel platinum wires directly above the surface of a glass microscope slide. The wire diameter was 25 μ and the spacing between them was approximately ten wire diameters. The wires were placed about 0.1 mm above the surface of the slide. This arrangement was secured by anchoring the wire pair in drops of epoxy cement placed about 1 cm apart on the slide and allowed to dry. Copper wires were soldered to one free end of each platinum wire, then cemented to the slide to provide durable electrical connections to the platinum electrodes.

For measurements an assembled cell was placed on the horizontal stage of a binocular microscope and illuminated from below. The electrodes were bathed with a few drops of the suspension to be studied, and then a thin glass cover slip was floated on the liquid just above the wires. This retarded evaporation and provided a planar interface for viewing the wires and the intervening liquid through the microscope.

Electrical excitation from low frequencies to 600 kHz was provided by a Hewlett-Packard Model 200 CD audio oscillator. Its output level was increased to 120 volts peak to peak by a simple triode amplifier, then applied to the electrodes. All measurements were made at this voltage level. Frequencies below 1 kHz were not investigated because, at this level, formation of gas bubbles due to electrolysis of water occurred. A Heathkit Model DX-100 transmitter provided excitation at various fixed frequencies between 1.7 MHz and 27 MHz, also at 120 volts peak to peak. Voltage amplitude and waveform were monitored at all frequencies on a Tektronix Model 547 oscilloscope and a Hewlett-Packard Model 410C voltmeter.

Solution pAg was measured potentiometrically using a silver wire electrode. A Beckman reference electrode (calomel in saturated KCl solution) was used. The reference electrode was connected to the Ag^+ ion bearing solution via a Beckman salt bridge containing 0.1 M KNO_3. Electrode emf was measured with a Beckman Model SS-2 pH meter. The system was standardized by using a 10^{-4} M $AgNO_3$ solution prepared volumetrically.

Suspensions were prepared by addition of 100 ml of 0.1 M reagent grade $AgNO_3$ to a

slightly larger volume of 0.1 *M* reagent grade KBr. The suspension was immediately diluted to less than 0.01 *M* with respect to the residual KNO_3. This reduction of ionicity was sufficient to prevent agglomeration of the AgBr particles. The suspension was permitted to stand overnight for precipitation in shallow Pyrex containers. The supernatant solution was then carefully removed by aspiration and replaced by distilled water. The precipitated AgBr particles were readily resuspended. This procedure was repeated twice, with the final addition of distilled water being of smaller quantity to obtain a more concentrated suspension. This "master suspension" served as the starting material for all experiments. Since the measurements to be made necessitated exposure of the suspensions to intense illumination, no effort was made to protect them from ambient light. By evaporating a known volume of the suspension and weighing the residue it was established that the particle concentration was about 1% by weight. Droplets of the suspension were dried on Formvar grids, and the AgBr particles were examined under the electron microscope. A particle size in the range 0.1–0.5 μ was observed. The particles were irregular in shape. No development of crystallographic faces was evident.

Direct measurement of the pAg of the suspensions by immersion of the electrodes described above was found to be unsatisfactory because of persistent variation with time of the recorded potential. This is thought to have been caused by an accumulation of particles at the electrodes. This difficulty was encountered both in the precipitated and fully dispersed suspensions, indicating that colloidal particles remained in suspension in the former case. This difficulty was circumvented by preparing a series of dilute colloid-free solutions of $AgNO_3$ with pAg values between 4 and 5, and of KBr with pAg values between 7.4 and 8.4. In both cases the corresponding concentrations lie between 10^{-5} and 10^{-4} *M*. The pAg range between 5 and 7.4 was covered by mixing appropriate ratios of the two solutions at 10^{-5} *M*, thereby maintaining approximately constant ionicity over the range. Solutions so prepared in this pAg range were also found to be sufficiently free of colloidal particles to permit potentiometric pAg determinations without difficulty. Suspensions used for measurements were prepared by allowing 15 ml of the fully dispersed master suspension to precipitate in a Pyrex beaker. The supernatant was then removed and the precipitate was resuspended in an equal volume of colloid-free solution having the desired pAg. The procedure was repeated, after which the pAg of the suspension was taken to be equal to that of the colloid-free solution used in its preparation. It was found that suspensions of the concentration required could not be prepared in the pAg range from 4.8 to 5.6. In this range the particles coagulated and could not be resuspended, undoubtedly because of the close proximity to the point of zero charge at a pAg of 5.4.

Suspension of AgBr particles in dioxane and in water/dioxane mixtures was also accomplished by replacement of the supernatant above the precipitated suspension. Solution pAg in this case was determined solely by equilibration with the AgBr present. It was not measured or otherwise controlled. Redispersion of the suspension was accomplished readily in pure dioxane and in the mixtures.

Dielectrophoretic yield was measured by direct observation of the linear extent of growth of precipitate perpendicular to the electrodes. Measurement was made at the end of a 20-sec interval during which the ac potential was applied. Typical conditions of collection are illustrated by the photomicrographs shown in Fig. 1. It is evident that collection is not homogeneous so that the yield measurements must be considered semiquantitative. An average of several measurements was made at each frequency studied. Though its measurement is not precise the yield nevertheless varied sufficiently widely as a function of frequency so that meaningful results could be obtained.

EXPERIMENTAL RESULTS

All experimental results to be presented here have been obtained under the conditions described in the preceding section. Measured

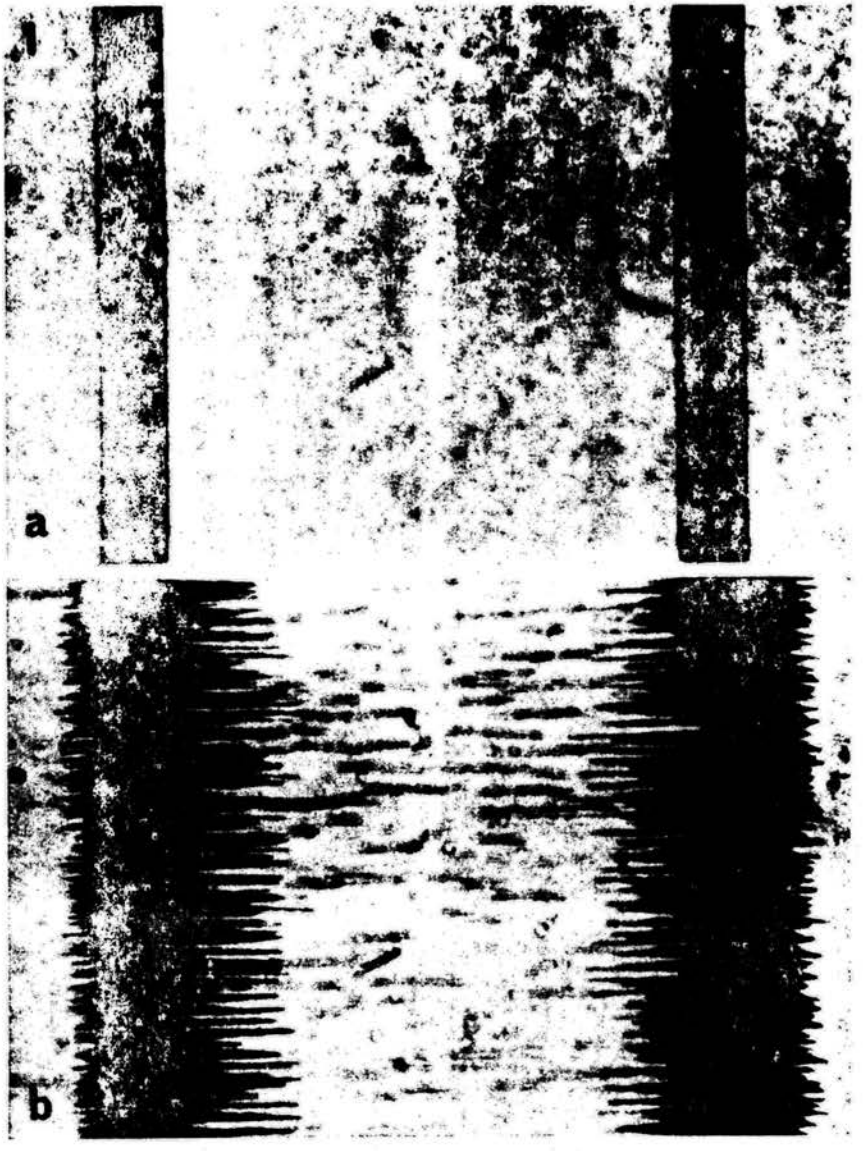

FIG. 1. (*a*) A photomicrograph showing the parallel wire electrodes prior to dielectrophoretic collection. (*b*) The collection of AgBr particles occurring upon application of an ac potential for approximately 1 min. The ac frequency is 100 kHz and the amplitude is 120 volts peak to peak. The solution pAg is 6.2.

yield values are presented as a ratio of y, the observed linear extent of yield, to D, the wire diameter. Figure 2 illustrates, for aqueous suspensions at three different pAg values, the dependence of the yield upon the frequency of the applied ac potential. The most striking feature of these results is the yield peak, which occurs at frequencies ranging from 250 to 600 kHz, depending upon solution pAg. The variation with pAg of ν_p, the frequency at which the peak occurs, is illustrated in Fig. 3.

The enhanced yield occurring at low frequencies and low pAg could not be studied extensively because of the low frequency limit imposed upon the measurements by

the onset of electrolysis at the voltage levels required. In addition the form of the low-frequency collection was qualitatively different, with aggregation of the particles in solution and subsequent motion of the aggregates to the electrodes being observed.

The dependence of yield upon frequency in suspending media consisting of dioxane and dioxane/water mixtures is illustrated in Fig. 4. These measurements suggest that the macroscopic dielectric constant of the suspending medium has little effect upon the dielectrophoretic yield. In particular relatively little shift of ν_p, the frequency of the high-frequency peak, is observed. The dioxane/water system permits continuous variation of the macroscopic dielectric constant between that of pure dioxane, 2.101 at 25°C, to that of pure water, 78.54 at 25°C. A tabulation of dielectric constant versus wt % dioxane is provided by Harned and Owen (22).

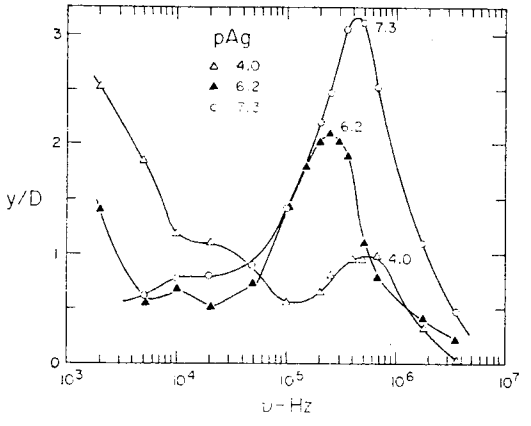

FIG. 2. The dielectrophoretic yield is shown as a function of frequency for aqueous suspensions at three different values of pAg.

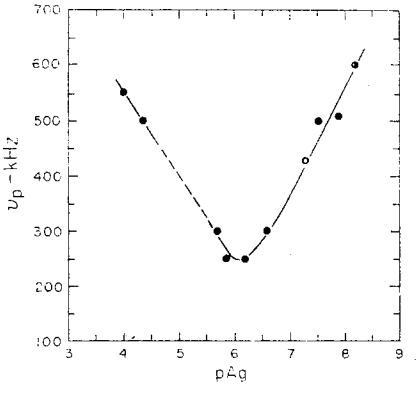

FIG. 3. The variation of ν_p, the frequency of peak yield, with pAg is illustrated for aqueous suspensions. The dashed line shows the pAg range over which stable concentrated suspensions could not be formed.

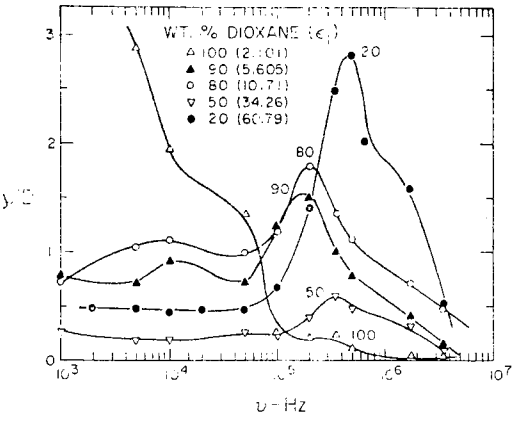

FIG. 4. Dielectrophoretic yield spectra are shown for suspending media consisting of dioxane and four different dioxane/water mixtures. The macroscopic dielectric constant of the medium, ϵ_1, is shown for each case.

Inspection of Fig. 4 indicates that the amplitude of the high-frequency peak is low in pure dioxane but increases markedly upon addition of water. At 50 wt % water, however, a striking minimum in peak amplitude is observed. This minimum could not be correlated with any charge reversal phenomenon. Qualitative observations of electrophoretic motion under the influence of a small applied dc potential indicated that the particles were negatively charged throughout the entire range of dioxane/water composition.

DISCUSSION

The salient experimental fact revealed by this work is that a positive dielectrophoretic force, leading to collection, acts upon particles of AgBr immersed in aqueous media. The magnitude of the force depends upon the frequency, displaying a pronounced maximum in the kilohertz range. In considering this result we first note that the static or low-frequency dielectric constant of pure water, 78.54 at 25°C (22), is more

than six times the corresponding value of of 12.5 at 290°K, reported for AgBr by Lowndes (23). Since, as seen from Eq. [1], these values alone would predict a negative force, we must look to some form of dispersion in the dielectric properties of the system to explain the observations.

It should next be determined whether a dispersion occurring in either bulk water or bulk AgBr alone could be important. Again, however, theory states that dispersion as a bulk property of the suspending medium would favor a negative dielectrophoretic force. In any case it is well known that no dielectric dispersion occurs in pure water until the dipolar relaxation region is reached at microwave frequencies (24). Data on the room temperature dielectric constant of AgBr at a microwave frequency of 22 GHz, obtained by Smith (25), are in excellent agreement with the low-frequency value reported by Lowndes. Thus available experimental evidence demonstrates the absence of dielectric dispersion in pure bulk AgBr in the frequency range important for this work. In fact, according to Lowndes and Martin (26), no dispersion would be expected until the infrared frequency range is reached, at which point resonant dispersion associated with lattice polarization would occur. Thus it is evident that the dielectric dispersion responsible for the positive dielectrophoretic force must arise from the heterogeneous nature of the suspensions.

With this point established, a direct comparison of our observed yield spectra with dielectric dispersion data for aqueous AgBr suspensions, or sols, would logically follow. Such data are lacking, however, presumably because of experimental difficulties associated with the high conductivity of these systems. Kruyt and Kunst (27) have measured the real part of the dielectric constant of AgBr sols at frequencies between 150 kHz and 2 MHz. They reported a monotonic decrease of dielectric constant with increasing frequency. The decrease is about 5%, which is consistent with the dispersion in this frequency range implied by our data. The dielectric dispersion of AgBr emulsions in insulating gelatin has been measured by Van Biesen (28). His plots of dielectric dispersion versus frequency bear a striking resemblence to the yield spectra which we observe, particularly with regard to the occurrence of dispersion maxima at frequencies between 10^5 and 10^6 Hz. Though this resemblance alone does not suffice to prove the point, it does suggest that the same dispersion mechanism is operative in both the suspensions and the emulsions.

Van Biesen has interpreted his data in terms of the classical Maxwell-Wagner theory, without modification to take account of double layer structure at the particle surfaces. He observed a shift in the frequency of peak dispersion to lower values with increasing grain size, and attributed the effect to a transition from high surface conductivity towards lower bulk conductivity with increasing size. It would appear, however, that the modified Maxwell-Wagner theory, with the relaxation time given by Eq. [5], can account more explicitly for his observation. This follows since the frequency of peak dispersion is related to the relaxation time by

$$\nu_p = 1/(2\pi\tau). \qquad [7]$$

Additional support for this interpretation is provided by our data on the variation of ν_p with solution pAg, shown in Fig. 3. We attribute the observed minimum in the plot of ν_p versus pAg to a corresponding minimum in σ_s, the surface conductance introduced in Eq. [5]. This interpretation would be entirely consistent with the observation by Matejec (29), of conductance minima for pure and doped AgBr membranes exposed to aqueous solutions of varying pAg. In the pAg range above the minimum, silver ion vacancies are presumed to be the majority defect in the surface layer, their concentration increasing with pAg. At low pAg Ag^+ interstitials predominate, increasing in concentration with decreasing pAg. The conductance minimum occurs in the transition region. Similar observations of surface conductance minima have been made for pure and illuminated sulfur-doped AgBr membranes in this laboratory (30).

On the other hand, our findings for dioxane and water/dioxane mixtures indicate

that the dispersion mechanism is insensitive to the macroscopic dielectric constant of the suspending medium. For a Maxwell-Wagner mechanism, based upon either Eq. [2] or [5], a peak shift to higher frequency with decreasing ϵ_1 should have been observed. The shift should have been of the same order as the change in ϵ_1, which amounted to more than an order of magnitude in our experiment. The frequency of peak dispersion (yield) in the mixed liquids and in pure dioxane, however, remained within the range of the data for the pure aqueous medium. The small shifts that were observed were generally in the sense opposite to that expected on the basis of Maxwell-Wagner theory. The insensitivity of ν_p to ϵ_1 may also be inferred by the close resemblance of our yield spectra in aqueous suspensions to Van Biesen's dispersion data. The dielectric constant of gelatin is known to depend strongly upon its water content (31), which depends in turn upon the relative humidity of the ambient atmosphere (32). Since the emulsions studied by Van Biesen were placed in an evacuated chamber we presume that in his experiment $\epsilon_1 \sim 2.8$, an appropriate value for dry gelatin.

Dispersion by a diffusion-controlled mechanism, with a relaxation time given by Eq. [6], could account for the insensitivity of ν_p to ϵ_1. It could not, however, account for the variation of ν_p with pAg observed for aqueous suspensions of AgBr. In view of the independent experimental evidence supporting the validity of the latter observation, we favor a description of the dielectric dispersion in terms of the modified Maxwell-Wagner mechanism for which the relaxation time is given by Eq. [5]. Perhaps the water in the vicinity of the AgBr particles is bound to such an extent that an effective value of ϵ_1 which is much lower than that of pure water should be considered appropriate.

Though dispersion by a Maxwell-Wagner mechanism is favored, experiments to test this point further are needed. Measurements of dielectrophoretic yield spectra, or of dielectric dispersion in emulsions, should be made using AgBr particles which are doped with $CdBr_2$. A variation of conductivity with cadmium content has been reported by Brady and Hamilton (33) for AgBr grains, and by Teltow (34) for bulk AgBr. Corresponding shifts in the frequency of peak yield or of peak dispersion can be expected if the Maxwell-Wagner mechanism is operative.

SUMMARY

A positive dielectrophoretic force, leading to collection, has been observed to act upon AgBr particles in aqueous suspension. This observation has been related to dielectric dispersion originating in the heterogeneous nature of the suspensions. Specifically, a peak in the dielectrophoretic yield occurring at frequencies between 10^5 and 10^6 Hz has been correlated with a reported maximum in the dielectric dispersion of AgBr emulsions which lies in the same frequency range. The dielectric dispersion has, for both cases, been attributed to a modified Maxwell-Wagner effect which takes account of the double layer existing at the interface between AgBr and the suspending medium. Further experiments to test this interpretation are suggested.

ACKNOWLEDGMENTS

We are indebted to Professor Thomas A. Mille. and to Dr. John Crowe of the College of Biological and Agricultural Sciences, University of California, Riverside, for electron micrographs of the suspensions used in these experiments. This work was supported by the U.S. Public Health Service through Grant GM-13687.

REFERENCES

1. POHL, H. A., *J. Appl. Phys.* **22**, 869 (1951).
2. POHL, H. A., *J. Appl. Phys.* **29**, 1182 (1958).
3. POHL, H. A., *J. Electrochem. Soc.* **107**, 386 (1960).
4. KRUYT, H. R., *in* "Colloid Science" H. R. KRUYT, Ed., Vol. 1, p 5. Elsevier, Amsterdam, 1952.
5. POHL, H. A., AND CRANE, J. S., "Dielectrophoretic Force," to be published.
6. CRANE, J. S., AND POHL, H. A., "Theoretical Models of Cellular Dielectrophoresis," to be published.
7. MAXWELL, J. C., "Electricity and Magnetism," Vol. 1, p 452. Clarendon, Oxford, 1891.
8. WAGNER, K. W., *Arch. Elektrotech.* **2**, 371 (1914).
9. VAN BEEK, L. K. H., *in* "Progress in Dielec-

trics," J. B. Birks, Ed., Vol. 7, p 69. Heywood, London, 1967.
10. MILES, J. B., JR., AND ROBERTSON, H. P., *Phys. Rev.* **40**, 583 (1932).
11. O'KONSKI, C. T., *J. Phys. Chem.* **64**, 605 (1960).
12. SCHWAN, H. P., SCHWARZ, G., MACZUK, J., AND PAULY, H., *J. Phys. Chem.* **66**, 2626 (1962).
13. SCHWARZ, G., *J. Phys. Chem.* **66**, 2636 (1962).
14. JOST, W., "Diffusion in Solids, Liquids, Gases," (Third printing) pp 25, 139. Academic Press, New York, 1960.
15. SHILOV, V. N., AND DUKHIN, S. S., *Kolloid. Zh.* **32**, 117 (1970).
16. DEBYE, P., AND FALKENHAGEN, H., *Physik. Z.* **29**, 401 (1928).
17. GRIMLEY, T. B., AND MOTT, N. F., *Discussions Faraday Soc.* **1**, 3 (1947).
18. GRIMLEY, T. B., *Proc. Roy. Soc. Ser. A* **201**, 40 (1950).
19. VERWEY, E. J. W., AND NIESSEN, K. F., *Phil. Mag.* **28**, 435 (1939).
20. LIDIARD, A. B., *in* "Handbuch der Physik," S. Flugge, Ed., Vol. 20, p 246. Springer, Berlin, 1957.
21. HONIG, E. P., AND HENGST, J. H. TH., *J. Colloid Interface Sci.* **29**, 510 (1969).
22. HARNED, H. S., AND OWEN, B. B., "The Physical Chemistry of Electrolyte Solutions," 2nd ed., p 118. Reinhold, New York, 1950.
23. LOWNDES, R. P., *Phys. Lett.* **21**, 26 (1966).
24. HASTED, J. B., *in* "Progress in Dielectrics," J. B. Birks, Ed., Vol. 3, p 101. Wiley, New York, 1961.
25. SMITH, G. C., Thesis, Cornell University, Ithaca, New York, 1962.
26. LOWNDES, R. P., AND MARTIN, D. H., *Proc. Roy. Soc. Ser. A* **308**, 473 (1969).
27. KRUYT, H. R., AND KUNST, H., *Kolloid-Z.* **91**, 1 (1940).
28. VAN BIESEN, J., *J. Appl. Phys.* **41**, 1910 (1970).
29. MATEJEC, R., *Z. Elektrochem.* **66**, 326 (1962).
30. HUEBNER, J. S., AND BRUNER, L. J., "The Electrical Conductance of Pure and Doped Silver Bromide Membranes in Aqueous Solutions," to be published.
31. FRICKE, H., AND PARKER, E., *J. Phys. Chem.* **44**, 716 (1940).
32. CURME, H. G., *in* "The Theory of the Photographic Process," T. H. James, Ed., 3rd ed., p 54. Macmillan, New York, 1966.
33. BRADY, L. E., AND HAMILTON, J. F., *J. Appl. Phys.* **35**, 1565 (1964).
34. TELTOW, J., *Ann. Physik* **5**, 63 (1949).

VITA

Chi-Shih Chen

Candidate for the Degree of

Doctor of Philosophy

Thesis: ON THE NATURE AND ORIGINS OF BIOLOGICAL DIELECTROPHORESIS

Major Field: Physics

Biographical:

Personal Data: Born in Taiwan, Rep. of China, February 8, 1939, the son of Chau-Chin and Suny-Yi Chen.

Education: Graduated from Chiang Jion High School, Taiwan, in 1959; received the Bachelor of Science degree from Chung-Yuan College in May 1964, with a major in physics; received the Master of Science degree from University of Oregon in May, 1968, with a major in physics; completed the requirements for the Doctor of Philosophy degree at Oklahoma State University in May, 1973.

Professional Experience: Assistant specialist on study of air pollutants at Sanitary Engineering Research Laboratory, University of California, Berkeley, in summer, 1966; held Teaching Assistantship with University of Oregon, Eugene, Oregon, 1966-1968, with Oklahoma State University, Stillwater, Oklahoma 1969-1972.

Other: Coauthors with H. A. Pohl, J. S. Huebner and L. J. Bruner of "Dielectrophoretic Precipitation of Silver Bromide Suspensions", J. Colloid. Interface Sci. 37, 354 (1971).